UNIVERSITY OF BELGRADE

FACULTY OF MEDICINE

Jadžić S. Jelena

# THE BONE TISSUE CHANGES IN INDIVIDUALS WITH ALCOHOLIC AND NON-ALCOHOLIC CHRONIC LIVER DISEASE

Doctoral dissertation

Belgrade, 2021

УНИВЕЗИТЕТ У БЕОГРАДУ

МЕДИЦИНСКИ ФАКУЛТЕТ

Јаџић С. Јелена

# ПРОМЕНЕ У КОШТАНОМ ТКИВУ КОД ОСОБА СА ХРОНИЧНИМ ОБОЉЕЊИМА ЈЕТРЕ АЛКОХОЛНЕ И НЕАЛКОХОЛНЕ ЕТИОЛОГИЈЕ

докторска дисертација

Београд, 2021

**PhD Advisor:**

Associate professor Danijela Đonić

University of Belgrade - Faculty of Medicine

**Members of evaluation committee:**

1. Prof. Marija Đurić, University of Belgrade - Faculty of Medicine
2. Prof. Đorđe Ćulafić, University of Belgrade - Faculty of Medicine
3. Ass. Prof. Željka Savić, University of Novi Sad - Faculty of Medicine

**Date of Public presentation: _____**

**Ментор:**

проф. др Данијела Ђонић

Унивезитет у Београду- Медицински факултет

**Чланови комисије за оцену и одбрану докторске дисертације:**

1. проф. др Марија Ђурић, Унивезитет у Београду - Медицински факултет
2. проф. др Ђорђе Ћулафић, Унивезитет у Београду - Медицински факултет
3. доц. др Жељка Савић, Унивезитет у Новом Саду - Медицински факултет

**Датум јавне одбране докторске дисертације: _____**

*This way, I would like to thank all individuals who, each one in their unique way, helped me through my PhD studies and inspired me in my professional and personal development.*

*First, I would like to express my greatest gratitude to associate professor Danijela Đonić, my PhD advisor, for her continuous support, time, and effort invested in every segment of this PhD thesis. Her constant constructive guidance, enormous patience, and motivation have inspired and encouraged me to express my best potentials and creativity, not only in the field of science. Mainly, I'm thankful that we continuously worked as a team in overcoming every obstacle and problem during these years.*

*I owe special gratitude to professor Marija Djurić and assistant professor Petar Milovanović for their exceptional enthusiasm for research, their wisdom, and advice that helped me both personally and professionally. Above all, I am grateful for the given opportunity to become part of this outstanding research team.*

*I am thankful to my colleagues from the Laboratory of Bone biology and Bioanthropology and team members from the Institute of forensic medicine for collaboration, help, and immeasurable support they have provided during my research. It was a pleasure to work with all of you.*

*I want to thank associate professor Nada Tomanović for performing pathohistological evaluation and assistant professor Miomira Ivović for conducting osteodensitometry during our study. I owe particular gratitude to Vesna Petronijević for her help in the bone sample preparation for immunohistochemistry analysis. I am grateful to the members of the PhD Advisory board for constructive suggestions regarding this thesis. Additionally, I am thankful to Uroš, who did the final proofreading without any hesitation.*

*Finally, I would like to express my deepest gratitude to my family and friends, who have believed in me all these years and encouraged me to follow my dreams. Especially, I am grateful to my mother for her endless love and for showing much understanding in times when this dissertation was my only preoccupation. I owe special gratitude to my brother Marko, who provided me with all support I needed from the moment I stepped onto my academic path. I'm thankful to my students for making our windmill battle worth fighting for. To my dear Bane – a big thank you for being by my side when I needed it the most.*

***Title of the doctoral dissertation**:*

THE BONE TISSUE CHANGES IN INDIVIDUALS WITH ALCOHOLIC AND NON-ALCOHOLIC CHRONIC LIVER DISEASE


***Summary***

*Background:* Although experts agree that increased femoral and vertebral fracture risk is present in patients suffering from various forms of alcoholic and non-alcoholic chronic liver diseases (CLD), previous osteodensitometry studies reported inconsistent findings. Namely, some authors showed reduced bone mineral density (BMD) values of the lumbar spine and femoral neck in patients with different forms of CLD. In contrast, other researchers failed to demonstrate significant BMD differences in patients with alcoholic and non-alcoholic liver disorders, when compare to healthy control individuals. Additionally, the association of bone changes with the severity of clinical manifestations in individuals with different types of end-stage CLD was previously analyzed and inconsistent results were yielded. Considering that BMD decrease cannot fully explain increased bone fragility in CLD patients, the analysis of the bone microstructure, mechanical properties and cellular indices in proximal femora and lumbar vertebrae is required to fulfill the puzzle of CLD-induced compromised bone strength. Complex pathophysiology of bone changes in CLD patients is still insufficiently clarified, considering that liver disease can induce bone turnover disorder, while chronic alcohol abuse present in alcohol-induced liver disorders has an additional negative influence on bone. Some authors argue that the dominant mechanism of CLD-induced bone loss is decreased bone formation, while other results suggest enhanced bone resorption as a more dominant mechanism in the etiopathogenesis of bone loss in CLD of alcoholic and non-alcoholic origin.

*Hypotheses and aims:* We hypothesized that impaired integrity of lumbar spine microstructure is present in persons with alcoholic and non-alcoholic (cardiac) end-stage CLD and that it could be associated with the severity of liver tissue disturbances (given by pathohistological score of liver damage) observed in the same individuals. Moreover, we hypothesized that region-dependent worsening in femoral osteodensitometry and geometry

parameters, cortical or trabecular micro-architecture and micro-hardness leads to increased susceptibility to femoral fracture in persons with various stages of alcoholic liver disease (ALD). Finally, we hypothesized that disruption of osteocytic lacunar network and altered expression of osteocyte-specific molecules (connexin 43 /Cx43/ and sclerostin) is present in persons with alcoholic and non-alcoholic (cardiac) end-stage CLD. To test these hypotheses, we conducted clinical assessment of fracture risk (using DXA and HSA measurement), analyses of the cortical and trabecular bone micro-architecture of lumbar vertebrae and proximal femora (using micro-computed tomography, micro-CT), Vickers micro-hardness assessment of femoral bone mechanical competence, as well as immunohistochemistry assessment of the two osteocyte-specific molecules (Cx43 and sclerostin) in lumbar vertebrae and femoral bone samples obtained from individuals with alcoholic and non-alcoholic CLD and healthy control individuals.

*Material and Methods:* Following pathohistological analysis of liver tissue samples, micro-CT was performed to assess the micro-architectural difference in lumbar vertebrae sampled from men with end-stage alcoholic CLD (ALC group, n=20), with end-stage non-alcoholic (cardiac) CLD (non-ALC group, n=15) and healthy sex-matched individuals without any sign of liver disorder (control group, n=20). After pathohistological confirmation of various ALD stages, DXA and HSA measurement, micro-CT and Vickers micro-indentation testing were performed on proximal femora sampled postmortem from adult men with various stages of alcoholic liver disease (ALD group, n=13) and healthy age-matched controls (n=20). To estimate potential effect of ALD stage on femoral bone impairment, ALD individuals were subdivided into individuals with initial ALD stage (fatty liver disease, FLD group, n=6) and individuals with end-stage ALD (ALC group, n=7). Finally, the comparison of the Cx43 and sclerostin osteocytic expression was evaluated by immunohistochemistry assessment of vertebral and femoral bone samples obtained from persons with alcoholic and non-alcoholic (cardiac) end-stage CLD and healthy controls.

*Results and conclusions:* Our data demonstrated impaired integrity of cancellous bone microstructure in lumbar vertebrae body collected from individuals with alcoholic and non-alcoholic end-stage CLD. On the other side, in same individuals, the vertebral cortical shell remained without significant micro-architectural disruption. Our data indicated an

important role of the severity of liver tissue disturbances in the lumbar trabecular bone impairment, while in our study, alcoholic origin of CLD was not a crucial factor for negative effect on bone. Additionally, our findings suggest that significant changes in femoral bone densitometry, geometry, microstructure and Vickers micro-hardness could shed light on the micro-architectural and compositional basis for increased femoral fracture risk in ALD patients. In particular, micro-architectural properties of inter-trochanteric region showed the most prominent alterations between ALD men and healthy individuals that may result in increased susceptibility to inter-trochanteric femoral fracture in ALD men. Even though femoral mechano-structural deterioration could not be neglected in individuals with the initial ALD stage, more severe bone alterations were observed in individuals suffering from end-stage ALD. This study suggested that decreased Cx43 expression in bone samples may elucidate CLD-induced deterioration of intercellular communication in osteocytic network of individuals with end-stage CLD. Additionally, our data demonstrate that increased sclerostin expression in bone samples of alcoholic and non-alcoholic (cardiac) end-stage CLD individuals, may reveal its potential role in mediating low bone formation associated with CLD. Hence, it could be hypothesized that sclerostin-targeting medicaments may provide a beneficial effect in attenuating bone changes among CLD patients. Finally, our data indicate that individual vertebral and femoral fracture risk assessment should be recommended for all CLD patients, with particular accent on liver cirrhosis patients. Adequate and timely treatment of liver disease may decelerate the progression of bone impairment in patients with CLD of alcoholic and non-alcoholic origin.

**Keywords:** Chronic liver disease, Alcoholic liver disease, Lumbar vertebrae, Femoral fracture, Osteoporosis, Bone microstructure, Bone mechanical properties, Connexin 43, Sclerostin, SOST, Men

*Scientific field:* **Medicine**

*Specific scientific field:* **Skeletal biology**

UDK number: _____

***Наслов докторске дисертације:***

ПРОМЕНЕ У КОШТАНОМ ТКИВУ КОД ОСОБА СА ХРОНИЧНИМ ОБОЉЕЊИМА ЈЕТРЕ АЛКОХОЛНЕ И НЕАЛКОХОЛНЕ ЕТИОЛОГИЈЕ


***Резиме***

*Увод:* Иако се стручњаци слажу да је повећани ризик од прелома бутне кости и слабинског дела кичменог стуба присутан код пацијената са различитим облицима алкохолне и неалкохолне хроничне болести јетре, резултати претходних остеодензитометријских (клиничких) истраживања нису у потпуности сагласни. Наиме, одређени аутори су показали значајно ниже вредности минералне густине костију које указују на остеопенију и/или остеопоротске промене слабинског дела кичменог стуба и врата бутне кости код болесника са различитим хроничним обољењима јетре. Насупрот томе, други истраживачки тимови нису доказали статистички значајну разлику између вредности минералне коштане густине код болесника са хроничним болестима јетре алкохолне и неалкохолне етиологије. Такође, претходне студије у којима је анализирана повезаност између коштаних промена и озбиљности клиничких манифестација код особа са цирозом јетре различите етиологије су показале неконзистентне резултате. Узимајући у обзир да смањење минералне густине костију не може у потпуности објаснити повећану склоност ка коштаним преломима код пацијената са хроничним обољењима јетре, анализа микроструктурних, механичких и ћелијских својстава коштаног ткива је потребна како би се разјаснила морфолошка основа повећане склоности ка настанку коштаних прелома код ових особа. Комплексни патофизиолошки механизми настанка коштаних промена код пацијената са хроничним обољењима јетре још увек нису довољно разјашњени, јер болест јетре сама по себи може узроковати поремећај коштаног метаболизма са једне стране, док дужевременска злоупотреба алкохола код пацијената са хроничним обољењима јетре узрокованим алкохолом има додатни негативан ефекат на скелетни систем. Одређени аутори тврде да је смањено стварање кости, доминантан механизам губитка коштане масе у хроничним обољењима јетре.

С друге стране, остали резултати сугеришу појачану разградњу коштаног матрикса као доминантнији етиопатогенетски механизам губитка кости изазваног хроничним обољењем јетре.

*Хипотезе и циљеви:* Претпостављамо да је измењена микроструктура слабинског дела кичменог стуба присутна код особа са алкохолним и неалкохолним обољењем јетре и да би те микроструктурне промене могле бити повезане са патохистолошким стадијумом оштећења ткива јетре. Додатно, наша је претпоставка да регионално погоршање параметара остеоденситометрије, геометрије, кортикалне или трабекуларне микроструктуре и тврдоће кости, може бити основа за повећан ризик од настанка прелома бутне кости код особа са хроничном болести јетре алкохолне етиологије. Такође, претпостваљамо да је промењена експресија молекула специфичних за остеоците (конексин-43 и склеростин) присутна у коштаном ткиву слабинских кичмених пршљенова и бутне кости узркована иреверзибилним стадијумом хроничне болести јетре алкохолне и неалкохолне (кардијалне) етиологије. Да би тестирали претходно наведене хипотезе, спроведена је клиничка процена ризика од фрактуре (користећи остеоденситометријска мерења), анализа кортикалне и трабекуларне мироструктуре кичмених пршљенова и бутне кости (користећи методу микро-компјутеризоване томографије), анализа мехничких карактеристика кости (користећи методу Викерс микроиндентације), и процена експримираности молекула специфичних за остеоците (конексина-43 и склеростина) на узорцима кичмених пршљенова и бутне кости узоркованих од особа са хроничним обољењима јетре алкохоле и неалкохолне (кардијалне) етиологије.

*Материјал и методе:* Након патохистолошке анализе узорака ткива јетре, методом микро-компјутеризоване томографије је извршена процена параметара трабекуларне и кортикалне микро-архитектуре тела слабинских кичмених пршљенова, узоркованих од одраслих мушкараца са алкохолном цирозом јетре (n=20), од одраслих мушкараца са хроничним обољењем јетре неалкохолне етиологије (кардијална фиброза, n=15) и здравих индивидуа истог пола (контролна група, n=20). Након патохистолошке потврде различитих стадијума алкохолне болести јетре, урађена је остеоденситометријска и структурна анализа кука. Затим је урађена микро-

компјутеризована томографија и Викерс микроиндентација спроведена на узорцима горњег окрајка бутне кости који су узети од кадаверичних донора са алкохолном болести јетре (n=13) и здравих контролних индивидуа истог пола и старости (± 5 година, n=20). Да би се проценио потенцијали утицај стадијума алкохолне болести јетре на коштано ткиво, те индивидуе су додатно подељене на особе са почетним стадијумом (масна болест јетре, n=6) и на особе са иреверзибилним стадијумом алкохолне болести јетре (n=7). Коначно, остеоцитна експресија конексина-43 и склеростина процењена је имунохистохемијском анализом узорака тела слабинских кичмених пршљенова и бутне кости особа са иреверзибилним стадијумом хроничног обољења јетре алкохолне и неалкохолне (кардијалне) етиологије.

*Резултати и закључци:* Ово истраживање је показало измењене параметре трабекуларне микро-архитектуре тела слабинских кичмених пршљенова узоркованих од особа са иреверзибилним стадијумом алкохолне и неалкохолне (кардијалне) хроничне болести јетре. Наиме, смањен удео трабекуларне кости у укупном волумену јер узрокован смањеним бојем и дебљином трабекула код испитиваних особа ($p<0.05$). Насупрот томе, код истих индивидуа, кортикална микроструктура слабинских кичмених пршљенова није била подложна значајном оштећењу ($p>0.05$). Резултати ове студије указују да је патохистолошки стадијум оштећења ткива јетре повезан са пропадањем трабекуларне микроструктуре тела слабинских кичмених пршљенова код особа са иреверзибилним стадијумом хроничног обољења јетре алкохолне и неалкохолне етиологије. С друге стране, алкохолна етиологија хроничног обољења јетре није била пресудан фактор у настанку негативних ефеката на коштано ткиво код истих индивидуа. Уз то, наши резултати сугеришу да би промене параметера остеоденситометрије, геометрије, коштане микроструктуре и микротврдоће на узорцима бутне кости могле да расветле морфолошку основу за настанак повећаног ризика од прелома бутне кости код пацијената са алкохолном болести јетре. Најизраженије разлике у микроструктури су показане у интер-трохантеричном региону бутне кости особа са алкохолном болести јетре, што може резултирати повећаним ризиком за настанак интер-трохантеричног прелома бутне кости. Иако

оштећење коштаног ткива није занемарљиво код особа са почетним стадијумом алкохолне болести јетре, озбиљније промене у микроструктури трабекуларног и кортикалног дела узорака бутне кости су уочене код особа са иреверзибилним стадијумом болести (алкохолна цироза јетре). Смањена експресија конексина-43 у узорцима кичмених пршљенова и бутне кости указује на погоршање интерцелуларне комуникације међу остеоцитима код особа са иреверзибилним стадијумом хроничне болести јетре алкохолне и неалкохолне (кардијалне) етиологије. Уз то, наши подаци показују да повећана експресија склеростина у узорцима кичмених пршљенова и бутних костију може расветлити потенцијалну улогу смањења коштане продукције у настанку скелетног оштећења узрокованог хроничним обољењем јетре. Стога, специфична терапија усмерена на склеростин може имати позитивне ефекте у лечењу промена на костима код особа са иревезибилним стадијумом хроничног обољења јетре. Коначно, наши подаци указују да је индивидуални клинички приступ у процени ризика од прелома слабинског дела кичменог стуба и бутне кости нужан код пацијената са хроничним обољењем јетре алкохолне и неалкохолне етиологије, с посебним нагласком на особе са цирозом јетре, као иреверзибилним стадијумом болести. Адекватно и правовремено лечење болести јетре може успорити пропадање коштаног ткива код пацијената са хроничним болестима јетре алкохолне и неалкохолне етиологије.

**Кључне речи:** Хронична болест јетре, Алкохолна болест јетре, Слабински кичмени пршљенови, Прелом бутне кости, Остеопороза, Микроструктура кости, Механичке особине кости, Конексин 43, Склеростин, Мушкарци

*Научна област:* **Медицина**

*Ужа научна област:* **Биологија скелета**

УДК број: _____

# 1. INTRODUCTION

## *1.1. Chronic liver disease (CLD)*

Chronic Liver Disease (CLD) is one of the most common health problems in European countries (Blachier et al. 2013). The etiological factors for CLD are numerous and ranging from viral, genetic, cholestatic, autoimmune, and metabolic disorders to liver damage due to the chronic consumption of various toxic substances (for instance liver-metabolized drugs and toxins; and products of metabolism, such as alcohol) (Blachier et al. 2013). It has been known that major causes of CLD are amenable to prevention and treatment. However, the socio-economic and health burden associated with CLD is growing each year across Europe, suggesting that prevention and treatment strategies are urgently required (Blachier et al. 2013; Pimpin et al. 2018). The clinical epidemiology data of CLD patients varies between countries within Europe (Blachier et al. 2013; Pimpin et al. 2018). For instance, median age-standardized prevalence of CLD was nearly 1200/100.000 in Austria and Romania, while same reported prevalence was approximately two times lower in Iceland, Malta and Serbia (Pimpin et al. 2018). Still, significantly higher standardized mortality ratio among CLD patients in Serbia, is highlighting the necessity for the improvement and implementation of the effective nationwide disease control strategies (Popovic et al. 2013; Pimpin et al. 2018; Blachier et al. 2013).

Alcoholic liver disease (ALD) is the most frequent form of non-cholestatic liver disease caused by long-term alcohol abuse (consuming more than 50g of pure alcohol for men and 30g of pure alcohol for women in a period longer than five consecutive years), which can be manifested in three pathohistological forms: fatty liver disease (FLD), acute and chronic alcoholic steatohepatitis (ASH), and, finally, alcoholic liver cirrhosis (ALC) known as a solid ground for malignant alteration and progression to hepatocellular carcinoma (Seitz et al. 2018; Blachier et al. 2013). However, it is important to emphasize that amount of alcoholic drinks per day is not linearly correlated with the pathohistological staging of the liver disorder (O'Shea et al. 2010). Warningly, recent epidemiological studies emphasized that unexpectedly high level of alcohol consumption has been observed across different European

countries (Streba et al. 2014; Pimpin et al. 2018), including Serbia (Pimpin et al. 2018; Popovic et al. 2013). Previously stated represents a solid base leading to a substantial increase in the ALD occurrence (Richardson & Singal 2018; Streba et al. 2014; Seitz et al. 2018).

Other common form of non-cholestatic chronic liver disorder is congestive hepatopathy (Myers et al. 2003). This liver disorder is caused by long-term congestive heart insufficiency (right heart failure), leading to centrilobular congestion, sinusoidal dilatation and ischemic parenchymal necrosis, and finally, progressive hepatic fibrosis (Wells & Venkatesh 2018; Koehne de Gonzalez & Lefkowitch 2017; Giallourakis et al. 2002). The incidence of congestive hepatopathy is variable (15%-65%) among patients with severe chronic heart failure (Xanthopoulos et al. 2019). Still, exact determination of the occurrence probability of various congestive hepatopathy stages is not available in European countries, due to its often asymptomatic clinical presentation (Giallourakis et al. 2002; Xanthopoulos et al. 2019; Houghton et al. 2019).

### *1.2. The CLD-induced bone disruption*

It's known that individuals with CLD could suffer from osteoporosis and increased bone fragility (Crawford et al. 2003). Previously, these CLD-induced bone changes (osteopenia, osteoporosis and osteomalatia) were commonly known as “hepatic osteodystrophy” (López-Larramona et al. 2011). However, the “CLD-associated osteopenia/osteoporosis” is more commonly used term during recent years (Guañabens & Parés 2018; Guarino et al. 2016), due to the fact that osteomalatia could be present in primary biliary cholangitis and cirrhosis (Mounach et al. 2008; Parés & Guañabens 2018), while it is not so frequent among other CLD forms nowadays (Guañabens & Parés 2018; Guarino et al. 2016). Recent publications indicated that increased bone fragility in these patients depends on the etiology, duration, and stage of CLD (Crawford et al. 2003). Namely, osteoporosis was initially described exclusively as a complication of primary biliary cholangitis and primary biliary cirrhosis as the most common forms of cholestatic liver disease (Beck et al. 2018; Guarino et al. 2016). Still, the same bone changes were later observed in other (non-cholestatic) hepatic disorders (Guañabens & Parés 2018; Gokcan 2020; Ranjan et al. 2021; Bansal et al. 2016) as well. It has

been reported that between 20% and 53% of viral hepatitis patients, between 25% and 34% of hereditary hemochromatosis patients, and up to 55% of various end-stage CLD patients meet diagnostic criteria for osteoporosis (Guarino et al. 2016; Guañabens & Parés 2018; Crawford et al. 2003). Additionally, according to available data, between 11% and 22% of ALD and up to 50% of ALC patients suffer from osteoporotic bone changes (Bang et al. 2014; López-Larramona et al. 2011; López-Larramona et al. 2013). The variability of previously published data on the incidence of osteoporosis is caused primarily by differences in the applied diagnostic criteria, methodology, and design of the study. In addition, these studies varied in the principles and norms applied for the selection of study participants (both diseased individuals and healthy controls), as well as in the number of subjects included in the study (limited study sample size).

Epidemiological analysis of osteoporosis incidence among patients with cardiac liver fibrosis and congestive hepatopathy is absent in the current literature, but considering that heart failure (Lyons et al. 2011; Aluoch et al. 2012) and chronic liver disorders (Guañabens & Parés 2018; Guarino et al. 2016) are recognized as significant risk factors for osteoporosis development, we may assume increased osteoporosis incidence among these individuals. Furthermore, epidemiological studies suggested that all types of CLD, including alcohol-induced liver cirrhosis and congestive liver fibrosis, are more frequent in men (Houghton et al. 2019; Pimpin et al. 2018), in whom osteoporosis is less common when compared to aged (postmenopausal) women (Djonic et al. 2011).

### *1.3. The prevalence of fragility fracture in CLD patients*

Most research groups agree that fracture incidence is increased in patients suffering from various stages of non-alcoholic (Nakchbandi & van der Merwe 2009; Nakchbandi 2014; Guarino et al. 2016) and alcoholic CLD (Bang et al. 2015; Asoudeh et al. 2021). In previous publications, reported incidence of fragility fractures varied among 3% and 44% of patients with various forms of CLD (Nakchbandi 2014; López-Larramona et al. 2011; Otete et al. 2018). Most research groups agree that the incidence of fractures is two to three times higher in end-stage CLD patients compared to controls (Liang et al. 2018; Nakchbandi 2014). However,

certain studies have reported an eightfold increase in the risk of bone fractures in these patients (Otete et al. 2018). Taken together, it has been estimated that in the population of 100.000 persons there were at least 2000 patients with CLD, of whom 60-880 experienced at least one bone fracture (Nakchbandi 2014). Such a significant number of fractures is predicted because it has been reported that previous fracture further increase the risk for developing a new fracture (Nakchbandi 2014). Thus, one person may be prone to developing more than one non-traumatic (low-trauma) fracture during the life time.

Many authors also believe that the lumbar spine could be more severely affected when compared to other skeletal sites in patients with end-stage liver disorders (Wibaux et al. 2011; Ninkovic et al. 2001; Culafić et al. 2014; Chen et al. 2017; Liang et al. 2018). According to available literature, more than one-third of patients suffering from end-stage CLD has been diagnosed with at least one vertebral compression fracture during their lifetime (Peris et al. 1995; Guañabens & Parés 2018; Wibaux et al. 2011). Besides patients with alcohol-induced liver cirrhosis (Wibaux et al. 2011; Ninkovic et al. 2001; Culafić et al. 2014; Chen et al. 2017; Liang et al. 2018), significantly increased incidence of vertebral fracture has been shown in patients with congestive heart failure (Lyons et al. 2011; Frost et al. 2007; Van Diepen et al. 2008).

In recently published study on two European national cohorts of English and Danish patients, the femoral fracture risk was 2.9% and 6.4% in patients with end-stage ALD (Otete et al. 2018), which is significantly higher compared to the general population (Otete et al. 2018). In the contemporary literature, two morphological types of femoral fracture has been differentiated: intracapsular (femoral neck) femoral fracture and extracapsular (inter-trochanteric and subtrochanteric) femoral fracture (Tanner et al. 2010). Recent epidemiological studies have shown that inter-trochanteric femoral fractures are more likely osteoporotic (Michaëlsson et al. 1999; Crilly et al. 2016). Moreover, CLD and heavy alcohol consumption were associated with an increase in the cumulative risk of inter-trochanteric fractures (Cauley et al. 2009; Montomoli et al. 2018; Michaëlsson et al. 1999). Simultaneously, the incidence of femoral neck fractures increases during ageing, not only in men, but also in women of advance age (Milovanovic et al. 2017; Djonic et al. 2011; Jo et al. 2016). It is

important to emphasize that ALC patients diagnosed with fragility fractures are significantly younger than most osteoporotic patients (Otete et al. 2018). The most prominent increase in the cumulative risk of femoral fracture is present in patients with alcohol-induced end-stage CLD younger than 45 years and corresponds to the risk of healthy controls of the same sex older than 75 years (Otete et al. 2018). In addition, mortality after bone fracture in these patients is significantly less favorable than those without liver disease, with a threefold increase compared to healthy individuals of the same age (Otete et al. 2018). Therefore, increased fracture risk in patients with various forms of CLD represents a significant socio-economic burden on the health system (Asoudeh et al. 2021) that urgently requires the development of newel more effective measures of prevention, diagnosis, and treatment.

### *1.4. Alterations in bone mineral density and geometry observed in different CLD stages*

Although experts agree that increased fracture risk is present in CLD patients, numerous osteodensitometry studies reported opposite results in patients with different CLD stages. Namely, in some cross-sectional clinical studies, significantly lower bone mineral density (BMD) was noted in patients suffering from viral, autoimmune and primary biliary cirrhosis (Mounach et al. 2008; Gallego-Rojo et al. 1998; Wakolbinger et al. 2019), while other authors failed to show a significant BMD decrease induced by viral cirrhosis and primary sclerosing cholangitis (González-Calvin et al. 2009; Campbell et al. 2005). On the other side, multiple authors showed reduced BMD values, suggesting osteopenia and/or osteoporotic changes of the lumbar spine and femoral neck in patients with ALD (Berg et al. 2008; Carey et al. 2003) and ALC (Díez-Ruiz et al. 2010; Mahmoudi et al. 2011; Culafić et al. 2014). Yet, others failed to show significant deterioration trend in BMD values of lumbar spine and proximal femora in individuals prone to chronic alcohol abuse (Bang et al. 2015; Laitinen et al. 1992; Kanis et al. 2005). Interestingly, previously conducted research reported that alcohol intake was associated with increased BMD values in men of advanced age (Cawthon et al. 2006). In addition, other authors observed site specific BMD alteration among patients prone to heavy alcohol intake (Ulhøi et al. 2017). Moreover, some cross-sectional studies showed significantly lower BMD values in ALC patients compared with patients with end-stage CLD induced by

variety of other causes (González-Calvin et al. 2009). In contrast, other research teams failed to demonstrate significant differences between BMD values in patients with alcoholic and non-alcoholic liver cirrhosis (Bang et al. 2015).

However, DXA-assessed BMD is of limited informative value in the fracture risk assessment, so previous studies pointed out that changes in femoral geometry should be considered as additional bone strength determinant (Djonic et al. 2011). Hip structural analysis (HSA) performed on ALC patients has shown altered femoral neck cross-sectional area, buckling ratio and section modulus suggesting compromised bone strength in these individuals (Culafić et al. 2014). Still, due to small number of individuals included in previously mentioned study, the further research is required to confirm these observations. Moreover, particular research interest in BMD and HSA evaluation in patients with congestive hepatopathy and its irreversible stage (cardiac liver fibrosis) has been absent in the contemporary literature, indicating that more comprehensive research is required.

### *1.5. The CLD-induced deterioration in bone micro-architecture*

A BMD decrease cannot fully explain increased bone fragility since it has been shown that a significant number of CLD patients who have physiological values of BMD could experience at least one pathological fracture during their life (Bang et al. 2015; Kanis et al. 2005). Therefore, these data are indicating that it is necessary to assess the bone micro-architectural and compositional properties (Djonic et al. 2011) to understand the basis for increased bone fragility among alcoholic and non-alcoholic CLD patients. The methodology of bone microstructure assessment has evolved from static and dynamic two-dimensional histomorphometry analysis to three-dimensional microstructural analysis using computed tomography (micro-CT analysis and peripheral quantitative CT analysis, pQCT). Histomorphometry revealed that microstructural disruption in primary biliary cirrhosis patients was due to reduced trabecular number and thickness (Guichelaar et al. 2002). The same trabecular deterioration was confirmed by bone histomorphometry in patients with ALC and chronic alcoholic pancreatitis (Schnitzler et al. 2010; Jorge-Hernandez et al. 1988). Similarly, a recently published pQCT analysis showed trabecular damage and significant

deterioration of the cortical bone microstructure of the distal tibia and distal radius (Figure 01) in patients with end-stage CLD of various causes (hemochromatosis, autoimmune, viral, biliary and alcohol-induced liver cirrhosis) (Wakolbinger et al. 2019; Schmidt et al. 2018; Jandl et al. 2020; Schmidt et al. 2021). Considering the frequency and clinical relevance of femoral and vertebral fractures, it is important to analyze cortical and trabecular microstructural bone properties of the proximal femora and lumbar vertebrae in patients suffering from different stages of alcoholic and non-alcoholic (cardiac) CLD. Moreover, in the current literature, a comparison of regional micro-architectural and mechanical differences of the proximal femora is absent. Still, this analysis could be required in order to elucidate the morphological basis for the increased occurrence of certain types of femoral fractures in CLD patients.

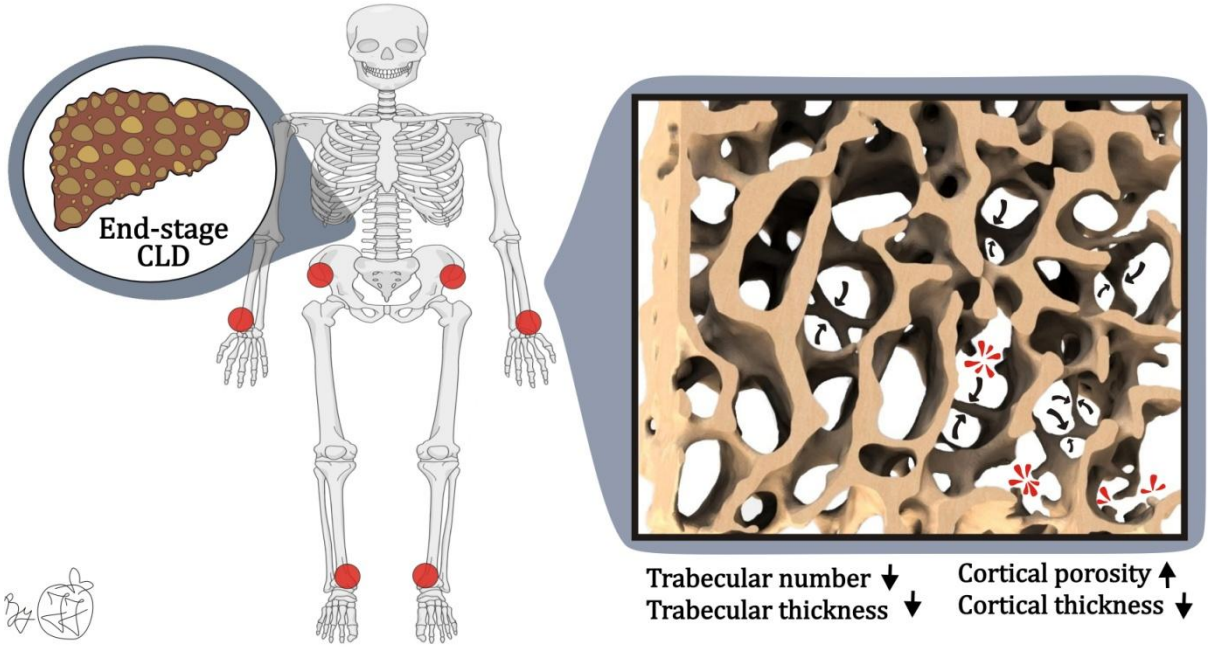


**Figure 01. Bone microstructure alteration in patients with various end-stage CLD (liver cirrhosis)**

Abbreviations: CLD – chronic liver disease;

The direct toxic effect of alcohol consumption on the skeletal system is not negligible, although some previous histomorphometry studies did not show significant alterations in biopsied iliac bone samples collected from patients with chronic alcoholism (Crilly et al. 1988). Still, heavy alcohol intake is known to significantly reduce osteoblastic activity and negatively affect the formation of mineralized bone (Crilly et al. 1988), which was recently

confirmed in the iliac bone biopsies of persons prone to heavy alcohol consumption (Ulhøi et al. 2017). However, the data about the comparison of bone changes between individuals with alcoholic and non-alcoholic end-stage CLD are scarce (Mahmoudi et al. 2011; Guañabens & Parés 2011), so further investigation is required.

Additionally, it is important to note that some authors found an association between progressive bone loss and clinical and laboratory parameters of hepatocellular insufficiency that reflect the severity of clinical manifestations and the duration of liver disease (Child-Pugh and Model for End-Stage Liver Disease /MELD/ score) in patients with various types of end-stage CLD (liver cirrhosis), including people with alcoholic etiology of the disease (Schmidt et al. 2018; Culafić et al. 2014). However, the opposite results were previously obtained (Díez-Ruiz et al. 2010; Wakolbinger et al. 2019), and further research is required to elucidate the role of CLD stage in bone loss among these individuals.

### *1.6. Bone micro-hardness as a contributing factor for compromised bone strength in CLD patients*

Bone strength is a result of complex interactions between many different determinants (Ibrahim et al. 2020; Weiner & Wagner 1998). Besides external and structural bone properties (bone size, bone mass, bone density, geometry, trabecular/cortical micro-architecture), intrinsic compositional (material) bone properties (degree of bone matrix mineralization, collagen fiber structure and collagen fiber organization) have a significant influence on the mechanical competence and strength of the bones (Weiner & Wagner 1998; Wang et al. 2019). Bone hardness is considered as an important factor affecting bone's ability to resist fracture, which could be assessed at the macro-, micro-, and nano-level (Arnold et al. 2017). In contrast to nano-indentation that assesses mechano-structural parameters at the lamellar level (Boivin et al. 2008; Milovanovic et al. 2013), micro-indentation allows the investigation of bone mechanical properties at the level of the bone structural unit. It has been believed that bone micro-hardness is a measure of bone tissue resistance to deformation by indentation (Wang et al. 2019), encompassing two components: elastic deformation and plastic deformation (Boivin et al. 2008; Dall'Ara et al. 2012). Vickers micro-indentation test is

a convenient method for conducting non-destructive measurements of the bone resistance to plastic deformation under constant mechanical loading (Wu et al. 2019; Dall'Ara et al. 2007). Previous studies analyzed site-specific (Wu et al. 2019; Yin et al. 2019) and age-associated (Huja et al. 2006) micro-hardness alterations in cancellous and cortical human bone specimens (Dall'Ara et al. 2012; Boivin et al. 2008; Dall'Ara et al. 2007). However, the comparison of Vickers micro-hardness values between the CLD patients and healthy age- and sex-matched controls was not previously conducted.

### *1.7. The etiopathogenetic mechanisms of CLD-induced bone deterioration*

The complex mechanisms underlying the development of osteoporosis in patients with various CLD stages are constantly in the focus of attention of numerous research teams. However, these etiopathogenetic mechanisms are still insufficiently elucidated. Most often, the development of CLD-induced skeletal damage is described as a disorder of the bone remodeling process, in which disbalance between bone resorption and bone formation is leading to decrease in bone mass, subsequently causing osteopenia/osteoporosis associated with CLD (Emkey 2018). The majority of leading scientific teams believe that the etiopathogenetic mechanisms of bone loss may be variable in CLD of various causes (Guañabens & Parés 2018; López-Larramona et al. 2011). Namely, it has been shown that impaired osteoblast function and impaired bone matrix synthesis are the main etiopathogenetic mechanisms of bone loss in patients with cholestatic liver disease, Wilson's disease, and hemochromatosis (Kawelke et al. 2008; Parés & Guañabens 2018; Hegedus et al. 2002; Valenti et al. 2009), leading to low-turnover osteoporosis. On the other hand, in patients with viral etiology of cirrhosis, the more dominant effect has increased osteoclast activity and a consequent increase in bone resorption - high-turnover osteoporosis (Corazza et al. 2000; Gallego-Rojo et al. 1998; Nakchbandi 2014).

The critical problem in the etiopathogenesis of bone loss in patients with CLD of alcoholic origin could be that in addition to liver disease, alcohol intake also directly affects bone tissue. Namely, previous studies noted that dose-dependent toxic effects of alcohol on function, differentiation, proliferation and maturation of osteoblastic cell lines could cause

decreased bone formation (Figure 02) (Luo et al. 2017; Chakkalakal 2005). In addition, low vitamin D levels, reduced physical activity, unbalanced diet (low calcium and protein intake), malabsorption syndrome, and intestinal microbiome disorders combined with various hormonal and metabolic disorders (such as increased PTH levels, hypogonadism and hypercorticism) associated with ALD, could be significant contributing factor for impaired bone metabolism among alcohol abuse patients (Luo et al. 2017; Alvisa-Negrín et al. 2009; Jeong & Kim 2019). Likewise, altering the ratio between the receptor activator for nuclear factor kappa B ligand (RANKL) and osteoprotegerin (OPG) in patients with liver disorders may play a significant role in increased osteoclast activity (Figure 02) and bone matrix degradation in patients with liver cirrhosis (Moschen et al. 2005). It is also considered that pro-inflammatory cytokines (interleukins (IL), tumor necrosis factor-α (TNF-α), interferons (INF), and others) may be involved in bone loss in patients with end-stage CLD (Figure 02). Namely, it has been shown that the hyperproduction of IL-1, IL-2, and IL-6 present in alcoholic end-stage CLD directly stimulates osteoclast activity, while bone resorption could be enhanced indirectly due to disturbed OPG/RANKL balance (Fábrega et al. 2005; Luo et al. 2017; Díez-Ruiz et al. 2010). Also, serum levels of tumor necrosis factor receptor p55 (sTNFR-55) and neopterin were significantly higher in ALC patients (Guañabens & Parés 2018). At the same time, these factors were positively associated with increased serum concentrations of bone resorption markers (Díez-Ruiz et al. 2010). In contrast, previous histomorphometry studies combined with electron microscopy have shown a reduced number of osteoblasts (Bihari et al. 2018) and a reduced rate of osteoid formation, indicating a reduced possibility of new bone formation in ALC patients (Chappard et al. 1991). These histological data are consistent with other publications showing reduced serum osteocalcin concentrations (a biochemical marker of bone formation) in these patients (Culafić et al. 2014). Osteoblast dysfunction may be the result of altered production of trophic factors in the liver, such as insulin-like growth factor 1 (IGF-1) or oncofetal fibronectin. Also decreased bone formation could be a consequence of the toxic effect of the bilirubin and bile acids stasis present in patients with end-stage CLD (Figure 02) (Mitchell et al. 2011; Santori et al. 2008; Sens et al. 2017).

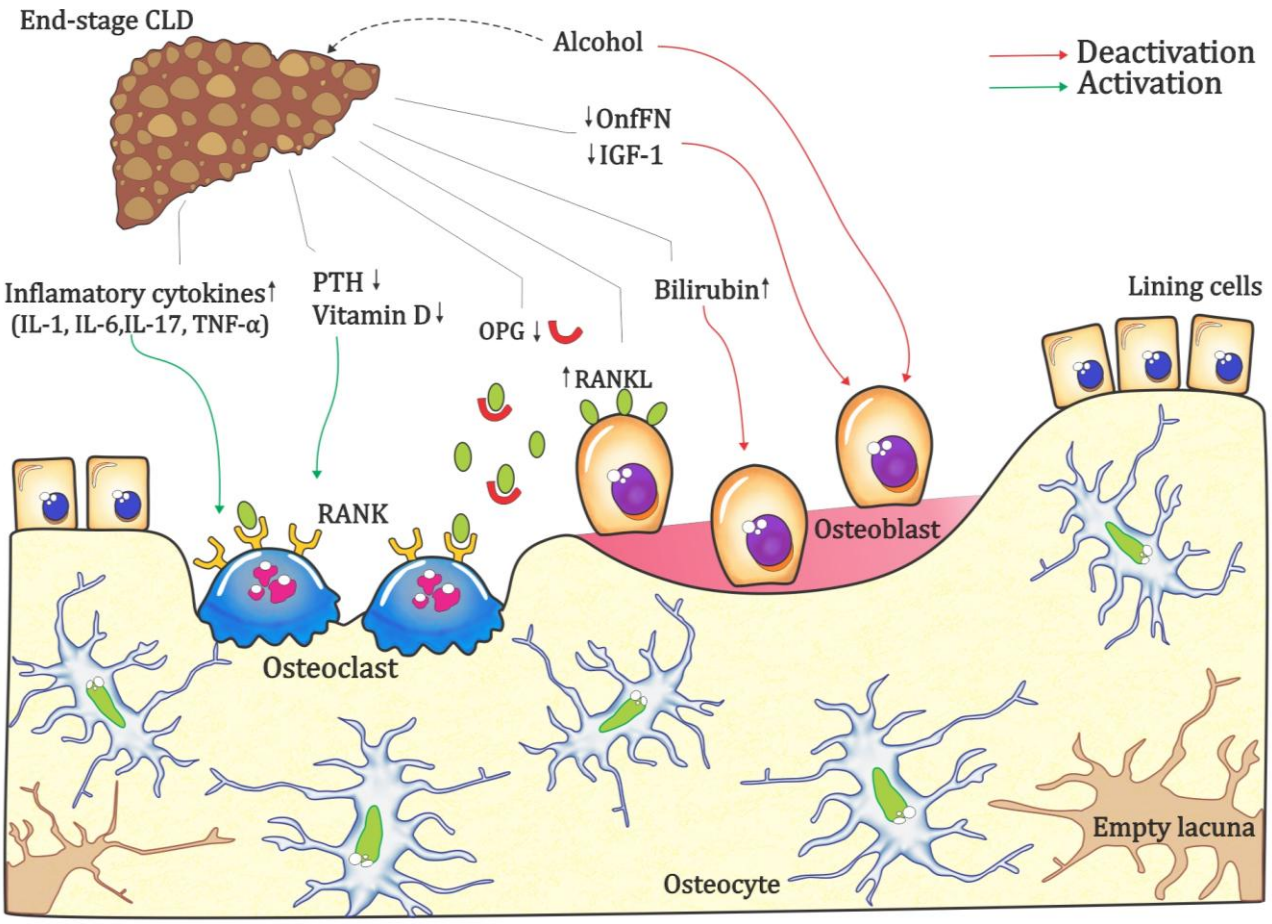


**Figure 02. The etiopathogenetic mechanisms of bone loss in alcohol-induced CLD**

Abbreviations: CLD – chronic liver disease; IL-interleukins; TNF – tumor necrosis factors; PTH – parathyroid hormone; OPG – osteoprotegerin; RANK –receptor activation of nuclear factor–κB; RANKL – receptor of nuclear factor–κB ligand; Onf FN- oncofetal fibronectin; IGF-1 – insulin like growth factor–1;

In order to fully understand the etiopathogenesis of bone impairment associated with CLD, the assessment of osteocytic network and osteocyte functionality could be of importance. It has been known that inter-cellular communication in bone and functional integrity of the osteocytic network is maintained by gap junctions (Stains et al. 2019; Stains et al. 2014). Gap junctions are intercellular channels formed by the two hemichannels (called connexons), located in the plasma membrane of two adjacent cells (Figure 03a). Hence, gap junctions are forming an aqueous pore between the cytoplasm of two bone cells which enables exchange of small (<1 kDalton) molecules, ions and nutrients (Stains et al. 2019; Stains et al. 2014). The connexons are formed by six monomeric subunits called connexins (Figure 03a). In human genome, 21 connexin genes were encoded, of which at least four are expressed in bone cells (Plotkin 2011). Those are connexin 37, connexin 40, connexin 45 and most frequently

expressed - connexin 43 (Cx43) (Stains et al. 2019; Stains et al. 2014; Plotkin 2011). Previous data showed that Cx43 molecule is an important part of intracellular machinery responsible for the signal transduction in bone, as a result of various stimuli (e.g. drugs, hormones and mechanical stress) (Plotkin 2011). Altered expression of Cx43 has been discovered in bone and liver cells among various animal models of ageing and disease (Davis et al. 2018; Cooreman et al. 2020; Balasubramaniyan et al. 2013) and in human liver tissue samples of patients with liver cirrhosis (Hernández-Guerra et al. 2019; Yanguas et al. 2016). Additionally, altered Cx43 expression has been discovered in cardiomyocytes of humans with chronic left heart failure (Kostin et al. 2004). Still, the osteocytic Cx43 expression in bone samples obtained from patients with various stages of alcoholic and non-alcoholic (cardiac) CLD has not been performed in the past.

Recently it has been suggested that sclerostin, the product of sclerostin-encoding (SOST) gene, may be involved in the pathogenesis of osteoporosis and bone impairment among patients with various CLD (González-Reimers et al. 2013; Wakolbinger et al. 2020). Sclerostin is an osteocyte-derived regulator of the Wnt/ß-catenin signaling pathway which binds to low-density lipoprotein receptor-related proteins 5/6 (LRP5/6), thereby inhibits bone formation (Ehnert et al. 2019). Thus, increased sclerostin is assumed in CLD patients with a tendency to induce decrease in bone mass (Figure 03b). Indeed, increased serum concentration of sclerostin were noted in patients with various stages of alcoholic and non-alcoholic CLD (González-Reimers et al. 2013; Wakolbinger et al. 2020; Yousry et al. 2016). Moreover, increased expression of sclerostin was recently observed in the liver tissue samples from patients with primary biliary cirrhosis (Guañabens et al. 2016). Additionally, previous studies shown that serum concentrations of sclerostin correlate with advanced bone loss among patients with ALD (González-Reimers et al. 2013) and in patients with liver cirrhosis of various etiology (Wakolbinger et al. 2020). However, serum assessment is depicting the sclerostin of extra-osseus origin, and the expression of sclerostin in bone samples (and bone cells) of men with alcoholic and non-alcoholic (cardiac) CLD could contribute to better understanding of the mechanisms leading to bone loss among these individuals.

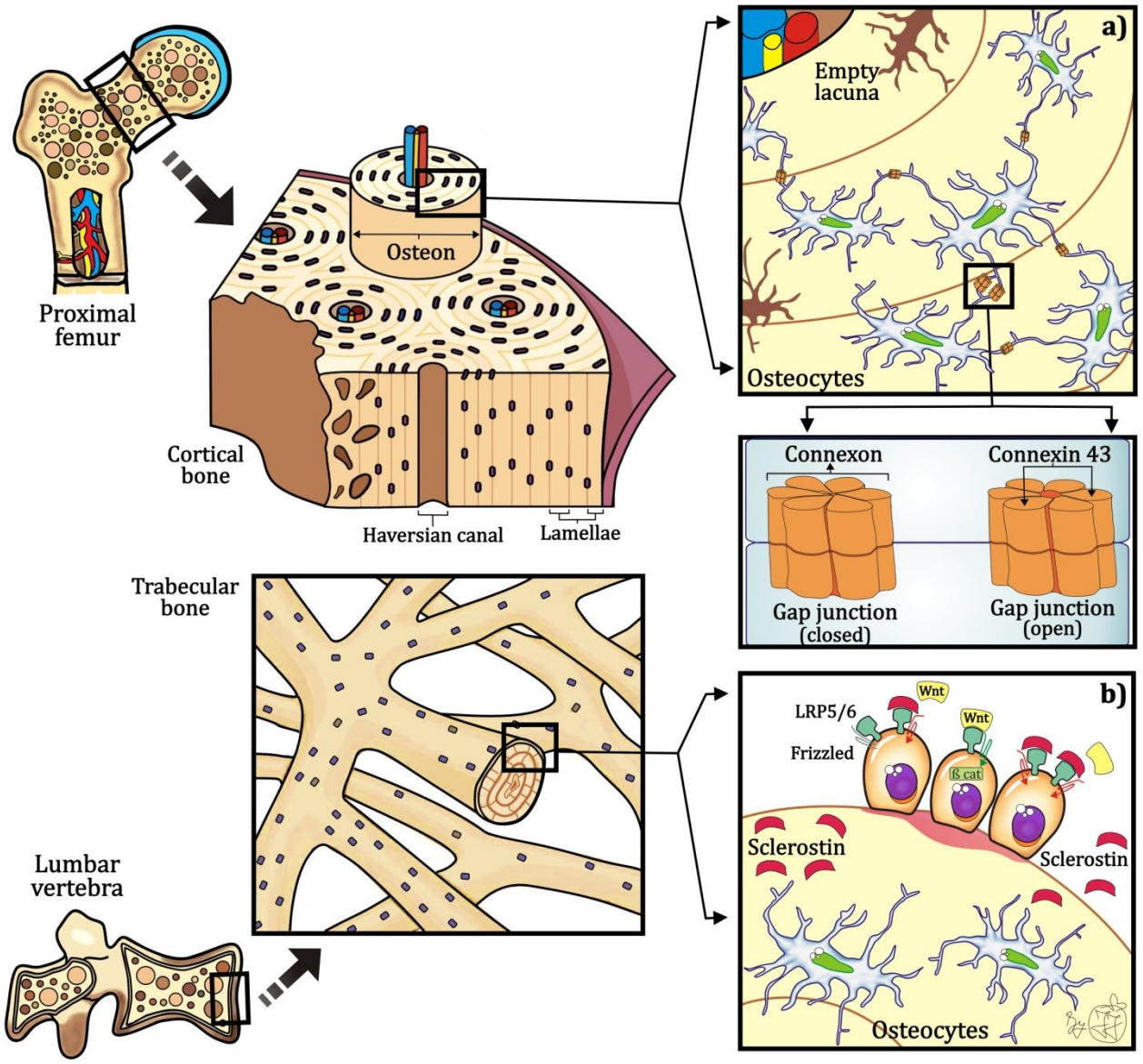


**Figure 03. The schematic representation of the role of connexin 43 and sclerostin in bone metabolism**

a) The connexin monomer (such as connexin 43) is a transmembrane protein of osteocytes, which forms hexameric connexon or hemichannel in each cell's plasma membrane. Two hemichannels on adjacent osteocytes form a continuous aqueous channel between the cytoplasm of two osteocyte, known as a *gap junction*. Trough open aqueous channel exchange of small molecules, ions and nutrients is enabled allowing efficient inter-cellular signal transduction triggered by various stimuli.

b) If Wnt ligand binds to a receptor complex, consisting of LDL-receptor related protein 5/6 (LRP-5/6) and Frizzled, it will cause accumulation of unphosphorylated β-catenin (β-cat), ensuring gene transcription and subsequent bone formation. In the presence of sclerostin, secreted by osteocytes, the Wnt ligand could not be bound to the LRP-5/6-Frizzled receptor complex, which decreases bone formation and subsequently leads to reduced bone mass.

## 2. RESEARCH AIMS

To characterize the bone changes in individuals with CLD of alcoholic and non-alcoholic origin, the specific objectives of this thesis were:

- to examine the differences of bone mineral density, bone mineral content, and HSA parameters of proximal femora in persons with various ALD stages and healthy age- and sex-matched controls.
- to examine the significance of changes in the cortical and trabecular micro-architecture in the lumbar vertebrae and proximal femora of individuals with various stages of alcoholic and non-alcoholic (cardiac) CLD.
- to analyze the association between the micro-architectural changes in the lumbar vertebrae and the severity of pathological changes in the liver of patients with end-stage CLD of alcoholic and non-alcoholic (cardiac) origin.
- to test whether the vertebral bone impairment is more prominent in individuals with end-stage CLD of alcoholic origin, when compared to non-alcoholic (cardiac) CLD.
- to examine the significance of the difference in the morphology of osteocyte lacunar network and in the expression of osteocyte-specific molecules (Cx43 and Sclerostin) in persons with end-stage CLD of alcoholic and non-alcoholic (cardiac) origin.
- to examine the significance of the difference in the mechanical bone properties (Vickers micro-hardness) of the proximal femora of persons with ALD compared to the age- and sex-matched controls.
- to examine the significance of the difference in the mechano-structural femoral bone properties between persons with initial ALD stage (FLD) and end-stage ALD (ALC).
- to determine the existence of regional mechano-structural specificities of the proximal femora in persons with various ALD stages compared to healthy age- and sex-matched control individuals.
- to test whether the changes in the osteocyte lacunar network and in the expression of osteocyte-specific molecules (Cx43 and Sclerostin) could contribute to bone loss among ALD individuals.

## 3. MATHERIAL AND METHODS

### *3.1. Study sample*

This cross-sectional study analyzed samples of the lumbar vertebrae body (n=55) and partially excised proximal femora (n=33) collected from male adult cadaveric donors (age range between 29 and 89 years) during routine autopsies at the Institute of Forensic Medicine in Belgrade, Serbia. The sample collection process for this study was approved by the Ethics Committee of Faculty of Medicine, University of Belgrade, Serbia (no. 1322/V-1). In addition, this study was carried out following the 1964 Helsinki declaration (and its later amendments) and the Directive of the European Parliament.

Lumbar vertebrae bodies were collected postmortem for microstructural and immunohistochemistry analysis, from adult individuals divided into the following groups:

- ALC group (men with end-stage CLD of alcoholic origin, n=20),
- non-ALC group (men with end-stage CLD of non-alcoholic (cardiac) origin, n=15), and
- control group (healthy sex-matched individuals without any form of liver disease, n=20).

Partially excised proximal femora were obtained from cadaveric donors divided into the following groups:

- ALD group (adult men with alcoholic liver disease, n=13), and
- control group (healthy age-matched men without known liver disorder, n=20).

To assess the effect of the various ALD stages on mechano-structural properties of femoral bone, samples of proximal femora obtained from persons with ALD were further classified into the following subgroups:

- ALC group (persons with pathohistologically confirmed liver cirrhosis of alcoholic origin, n=7), and

- FLD group (persons with pathohistologically confirmed fatty liver disease of alcoholic origin, n=6).

Finally, femoral samples for immunohistochemistry analysis were collected from adult cadaveric men divided into the following groups:

- ALC group (men with end-stage CLD of alcoholic origin, n=17), and
- control group (healthy age-matched men without liver disease, n=14).

Initial inclusion criteria for the alcohol-induced CLD donors were macroscopic signs of chronic alcoholism present at the autopsy, in combination with heteroanamnestic or clinical data on long-term alcohol abuse (more than 50g of pure alcohol />3 units/ per day for more than 5 years). Only after pathohistological confirmation of end-stage CLD (liver cirrhosis) these individuals were included in the ALC group, while individuals with pathohistological confirmation of fatty liver disease (at least 5% of liver tissue affected by steatosis) were included in the FLD group.

Inclusion criteria for a non-ALC group were macroscopic signs of liver disease present at autopsy (e.g., nutmeg liver) in adult men with available clinical data on previous congestive heart failure (due to hereditary and/or acquired valvular heart defect), accompanied by pathological verification of liver damage known as congestive hepatopathy and/or cardiac fibrosis.

In contrast, adult cadaveric men with an absence of macroscopic signs and clinical data about liver disorders, chronic alcoholism and/or congestive heart failure at the time of autopsy could be included in the control group only if the pathohistological analysis of liver tissue was in physiological range and without signs of hepatic disorder. Also, according to our best knowledge, the causes of death of all individuals included in the study encompassed sudden death, natural causes of death or traumatic injuries that cannot directly negatively interfere with the study results. General exclusion criteria included a positive history of previous fragility fracture (especially vertebral and hip low trauma fracture), the presence of solitary and metastatic cancerous bony lesions (for instance: chondrosarcoma) and data suggesting the any kind of donor's immobility, lower limb paralysis and wheelchair

dependence. In addition, positive history of endocrine and metabolic diseases that could negatively affect the musculoskeletal system (for instance: hyperparathyroidism, hypogonadism, thyroid dysfunction, diabetes mellitus, obesity and metabolic syndrome, autoimmune, hereditary, or viral liver disease) was considered as general exclusion criteria. According to our best knowledge, all included donors did not routinely use bone-affecting therapy (for instance: antiepileptic drugs, cytostatic, antiviral nucleoside analogs, antipsychotics, vitamin D, glucocorticoids, reproductive hormonal treatment, bisphosphonates and/or other antiresorptive therapy). Only exceptions from this rule were non-ALC donors who followed prescribed antihypertensive regimen (for instance: beta-blockers and diuretics) which could influence the bone turn-over. Specifically, clinical or heteroanamnestic data about alcohol consumption and binge drinking were considered as exclusion criteria for donors of control and non-ALC group.

### *3.2. Pathohistological analysis of the liver tissue samples*

During the autopsy, one tissue sample per liver lobe was obtained from all included cadaveric donors. The liver tissue samples were fixed in standard formaldehyde solution, paraffin-embedded, and sliced in 5-μm-thick-sections that were mounted on slides and routinely stained with Hematoxylin & Eosin technique in collaboration with the Institute of Forensic Medicine, University of Belgrade, Serbia. These liver tissue slides were analyzed under an optic microscope (DM 1000 LED, Leica Microsystems, Germany) equipped with HDMI digital camera (Leica ICC500W version, Leica Microsystems, Germany), in collaboration with the Institute for Pathology in Belgrade, Serbia. To ensure correct pathohistological analysis, expert pathologist was not informed about the specific macroscopic signs for each donor included in the study.

In each liver tissue specimen, the following pathohistological features were analyzed: (a) periportal and bridging hepatocellular necrosis; (b) intralobular degeneration and focal hepatocellular necrosis; (c) portal inflammation, and (d) degree of fibrosis. Moreover, the presence of steatosis, ballooned hepatocytes, canalicular cholestasis and accumulation of

Mallory hyaline in perisinusoidal spaces (spaces of Disse) were analyzed in these liver tissue samples as previously described (Knodell et al. 1981; Goodman 2007).

The Knodell's scoring system was used to estimate the severity of liver tissue disturbances (pathohistological stage of liver disease) in our individuals (Knodell et al. 1981). Namely, a numerical score for each previously described histological category was assigned to each liver biopsy specimen, and the combined score of the first three categories (periportal and bridging hepatocellular necrosis, intralobular degeneration, focal hepatocellular necrosis, and portal inflammation) formed the necroinflammatory score (grading from 0 to 18) for that biopsy specimen. The degree of fibrosis (classified as 0 - no fibrosis, 1 - fibrous portal expansion, 3 - bridging fibrosis and 4 - cirrhosis) was added to the necro-inflammatory score to form Histology Activity Index (HAI) used in statistical analysis as a marker of the severity of the liver tissue disturbances (Knodell et al. 1981; Goodman 2007).

### *3.3. Dual-energy X-ray absorptiometry (DXA) and Hip structure analysis (HSA)*

Bone mineral density of partially excised proximal femora was evaluated in collaboration with the staff at the Institute of Endocrinology, Diabetes and Metabolic Diseases, Clinical Centre of Serbia, by *ex vivo* measurement on Hologic QDR 1000/W DXA device. In accordance to previous suggestions, femoral specimens were positioned with consistent orientation and submerged in water bath to simulate surrounding soft tissue present *in vivo* (Beck et al. 1990; Culafić et al. 2014). The scans were auto-evaluated by build-in software of the standard femoral sub-regions (neck, inter-trochanteric and total, Figure 04a). The following osteodensitometry parameters were provided:

- Bone mineral content (g) – measure of the inorganic mineral content in the bone tissue of proximal femora
- Areal BMD (g/cm2) – represents a bone mineral content per femoral bone area. Thus, it depends on the size of proximal femora and its bone mineral content.

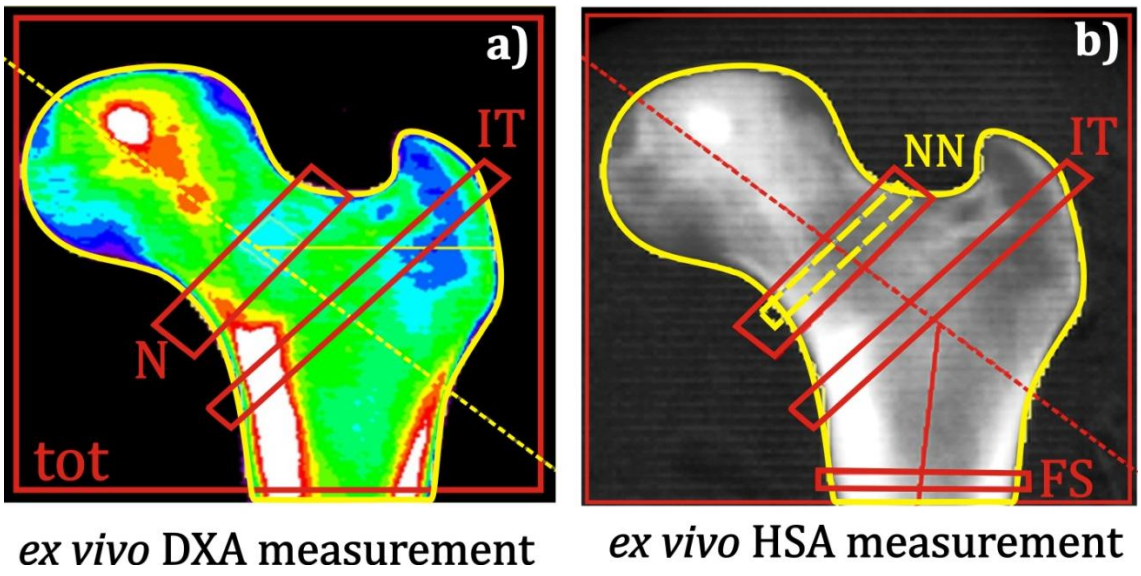


**Figure 04. The regions of interest in DXA (a) and HSA (b) measurement**

Abbreviations: N – femoral neck; NN – narrow neck (located at the narrowest diameter of the femoral neck region); IT – inter-trochanteric region (located at the section of femoral shaft and femoral neck axes); FS – femoral shaft (located 1.5 times minimum neck diameter distal to the intersection of the axes passing through the middle of femoral neck and femoral shaft); tot – total proximal femora; DXA – Dual-energy X-ray absorptiometry; HSA – Hip structure analysis;

HSA measurement, originally invented by Beck and his colleagues, carried out with Hologic Apex software (version 2.0, Bedford, MA, USA) was utilized to estimate femoral geometry parameters (Beck et al. 1990) for each standard region of interest (narrow neck, inter-trochanteric region and femoral shaft, Figure 04b).

The following HSA parameters were determined:

- cross-sectional area ($cm^2$) – a measure of bone resistance to compressive load. Represents an area of bone surface in the cross section after excluding bone marrow spaces and trabecular bone.
- cross-sectional moment of inertia ($cm^4$) – an index of structural rigidity of the bone. It represents the measure of bone resistance to torsion and bending forces.
- section modulus ($cm^3$) – indicated the ability of proximal femora to resist bending and torsion stress applied.
- estimated cortical thickness (cm) - difference between periosteal and endocortical diameter of the proximal femora.

- buckling ratio (dimensionless) - indicates bone instability due to thinning of the cortical bone. This parameter is used as an indicator of the compensatory bone remodeling in the proximal femora, which redistributes bone mass to counteract the bone loss in order to preserve bending strength.

### *3.4. Bone specimen preparation*

Obtained samples of lumbar vertebrae and proximal femora were stored in a standard formaldehyde solution at a constant (room) temperature, manually cleaned of soft tissues, and cut into separate samples of the anterior-mid transverse portion of the lumbar vertebrae (Figure 05), full-length samples of femoral neck (lateral part and medial part) and samples of the inter-trochanteric femoral region, which were than prepared for further analysis. Bone samples (both vertebral and femoral), consisted of cortical compartment and attached trabeculae, were approximately 10 mm thick and approximately 10 mm wide. The length of bone samples was 1 cm for lumbar vertebrae, and at least 2 cm for femoral samples included in the further evaluation. The cutting was performed by oscillating autopsy saw (Kugel Medical HB-740, Kugel Medical GmbH, Germany) in Laboratory of Bone Biology and Bioanthropology in Belgrade, Serbia.

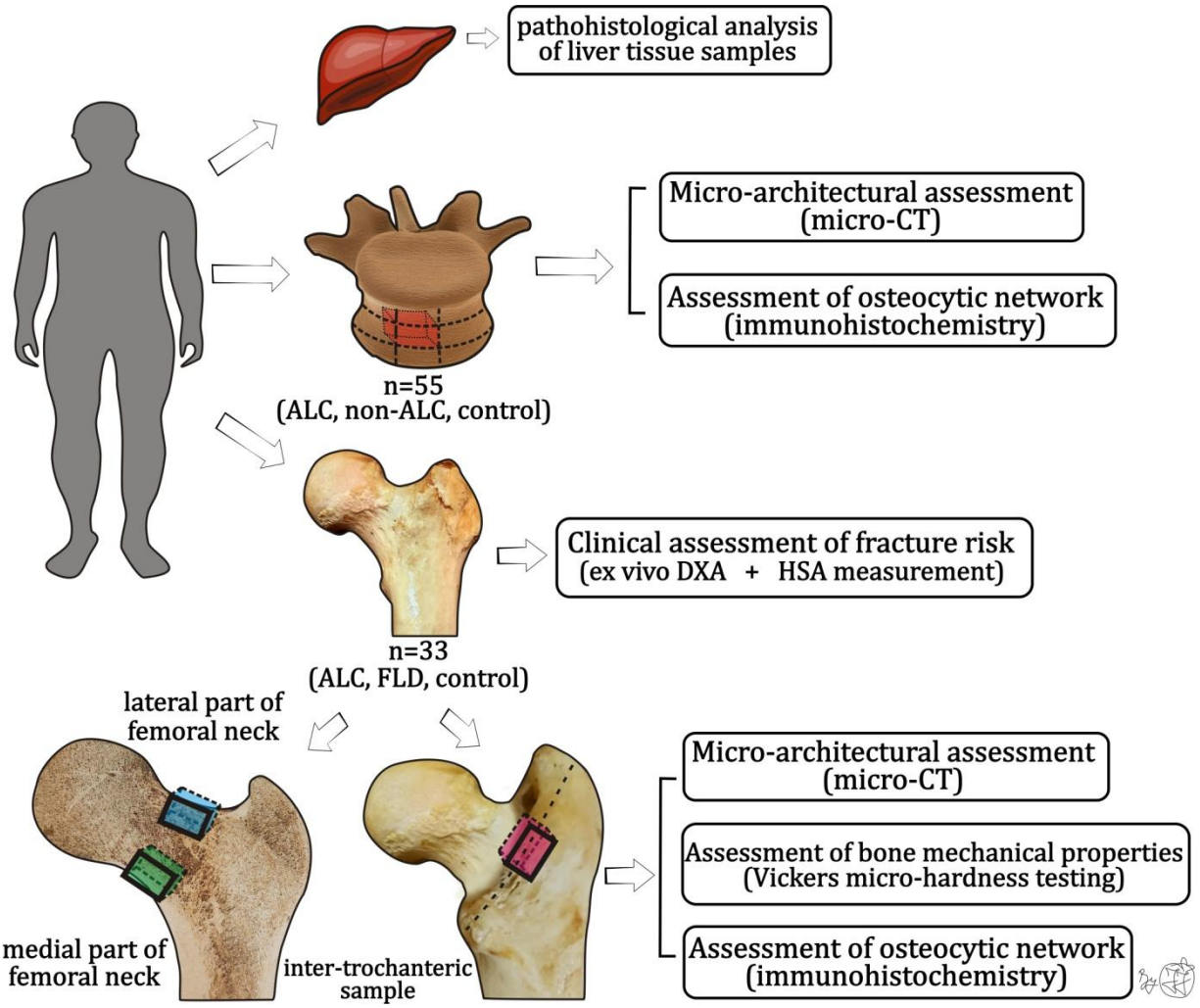


**Figure 05. The bone sampling process and bone assessing methodology used in this study**

Abbreviations: micro-CT – micro-computed tomography; DXA – dual-energy X-ray absorptiometry; HSA – hip structure analysis; ALC – alcoholic liver cirrhosis; FLD – fatty liver disease;

### *3.5. Micro-computed tomography imaging of the lumbar vertebrae*

Each vertebral bone sample (anterior mid-transverse part of vertebral body, Figure 06) was covered with a thin layer of parafilm and placed on a sample holder with a consistent orientation in specimen chamber. These samples were scanned with a micro-CT system (Sky Scan 1172, Bruker, Belgium) under following scanning conditions: 90 kV, 112 μA, 10 W, pixel size of 10 μm, isotropic resolution of 2000 × 1332 pixels per slice, with an aluminum-copper (Al-Cu) filter, 0.4° rotation step, triple frame averaging, in accordance to previous scanning protocols (Jadzic, Mijucic, et al. 2021; Cvetković et al. 2020). Following the scanning, the reconstruction of the projection images was done using software NRecon version 1.6.9.8

(Bruker, Belgium) with beam hardening correction of 20% and adequate thermal drift, misalignment, and ring artifact compensation.

Using CT analyzer software (CT.An 1.14.4.1 version, Bruker, Belgium), trabecular and cortical regions of interest (ROI) on the lumbar vertebrae were marked for the analysis. As shown in Figure 06, the appropriate three-dimensional regions, i.e., volumes of interest (VOI) of 700 slices in total (central ± 350 slices) were selected (approximately 7 mm in total). VOI for trabecular bone was selected as a manually adapted ROI in the center of the trabecular zone in order to avoid damaged marginal tissue, while VOI selection for cortical bone analysis was manually adapted in the same frame range (Figure 06). The transient zone was consistently excluded from micro-architectural assessments. The threshold value was carefully considered and set at 95/255, meaning that the gray level values between 0 and 95 were considered as non-mineralized or bone marrow spaces, whereas gray levels between 95 and 255 were considered as mineralized tissue (bone). This threshold was used for all vertebral samples allowing inter-individual comparison of micro-architectural parameters. The appropriateness of chosen threshold values was evaluated by comparing with original micro-CT scanning images.

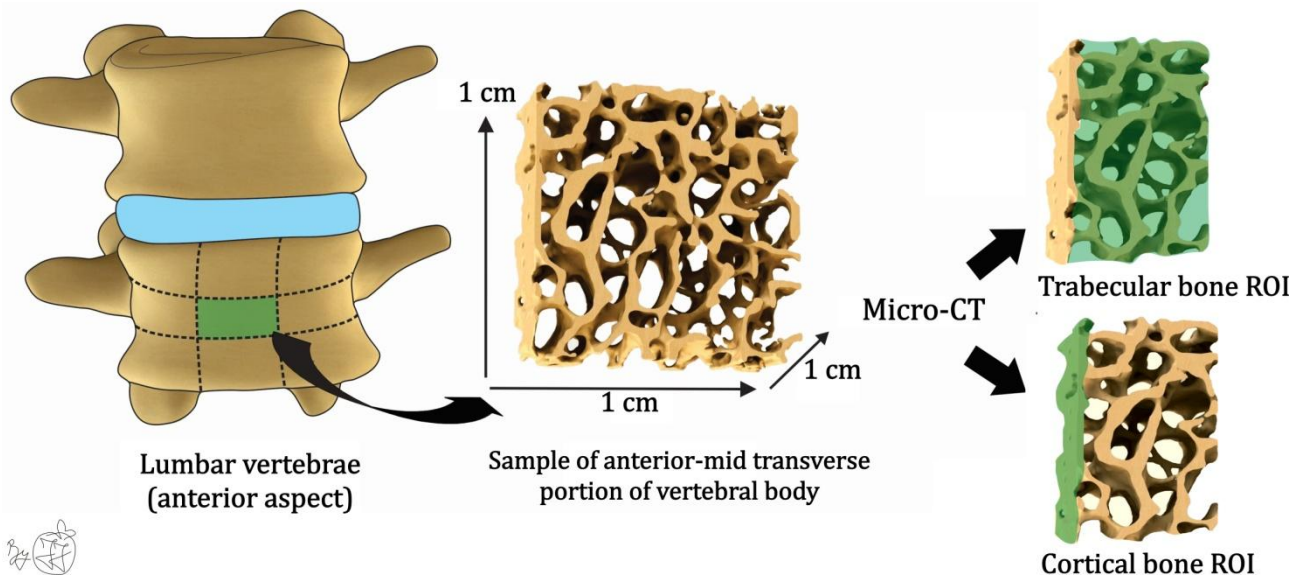


**Figure 06. Methodological steps in micro-CT assessment of lumbar vertebrae**

Abbreviations: ROI – region of interest;

As previously suggested (Djukic et al. 2015), following parameters of cortical and trabecular micro-architecture were determined in samples of lumbar vertebrae:

- bone volume fraction (BV/TV, %) - the ratio of the trabecular bone volume in total VOI;
- trabecular number (Tb.N, 1/mm) - the average number of trabeculae per unit length;
- trabecular thickness (Tb.Th, mm) - the mean thickness of the trabeculae;
- trabecular separation (Tb.Sp, mm) - the mean distance between the trabeculae;
- specific bone surface (BS/BV, 1/mm) – a measure of bone surface per total trabecular bone volume;
- degree of anisotropy (DA, dimensionless) - describes the orientation of the trabeculae;
- fractal dimension (FD, dimensionless) - describes the degree of trabecular complexity;
- trabecular bone pattern factor (TbPf, 1/mm) - measure of trabecular connectivity;
- structure model index (SMI, dimensionless) - an indicator of the trabecular shape;
- cortical porosity (Ct.Po, %) - the ratio of pore volume in total cortical VOI;
- pore diameter (Po.Dm, mm) - the average diameter of the pores in cortex;
- pore spacing (Po.Sp, mm) - the average thickness of cortical bone between the pores;
- cortical thickness (Ct.Th, mm) - the average thickness of the cortical bone.

### *3.6. Micro-computed tomography of proximal femora*

After DXA and HSA measurement were adequately performed, the 1cm-thick full-length samples of lateral and medial part of femoral neck and approximately 1cm-thick-2cm-long bone sample of inter-trochanteric region (Figure 07) were collected from the same individuals for further analysis. These femoral samples (Figure 07) were scanned with the same micro-computed tomography system (1172 version, Bruker, Belgium) under the following conditions: oversized scan, 80 kV, 124 μA, 10W, exposure time of 1200 μs, with an isotropic resolution of 10 μm and applying Al-Cu filter, as previously suggested (Cvetkovic et al. 2020). Using CT-analyzing software (CT.An 1.14.4.1 version, Bruker, Belgium) VOIs of femoral neck samples were standardized in the range of 1800 slices (central slice ± 900; approximately 18 mm), while analysis of inter-trochanteric region was limited in 1200 slice range (central ± 600 slices, approximately 12 mm). On each femoral part, trabecular and

cortical VOIs were established using manually adapted ROI (Figure 07). In short, damaged marginal tissue and transient cortico-trabecular zone was excluded from ROI. The same threshold value used in micro-CT assessment of lumbar vertebrae (95/225) was chosen for distinguishing the mineralized and non-mineralized tissue in the femoral samples as well, which allowed inter-individual comparison of femoral micro-architecture in ALD and control individuals. Using the same 3D morphometry software (CT.An 1.14.4.1 version, Bruker, Belgium), we analyzed cortical porosity (%), pore diameter (mm), pore spacing (mm) and cortical thickness (mm) in all three investigated femoral regions. Furthermore, the following trabecular micro-architectural parameters were calculated for all investigated femoral samples: bone volume fraction (%), trabecular thickness (mm), trabecular number (1/mm), trabecular separation (mm), trabecular bone pattern factor (dimensionless), structural model index (SMI, dimensionless) and fractal dimension (dimensionless).

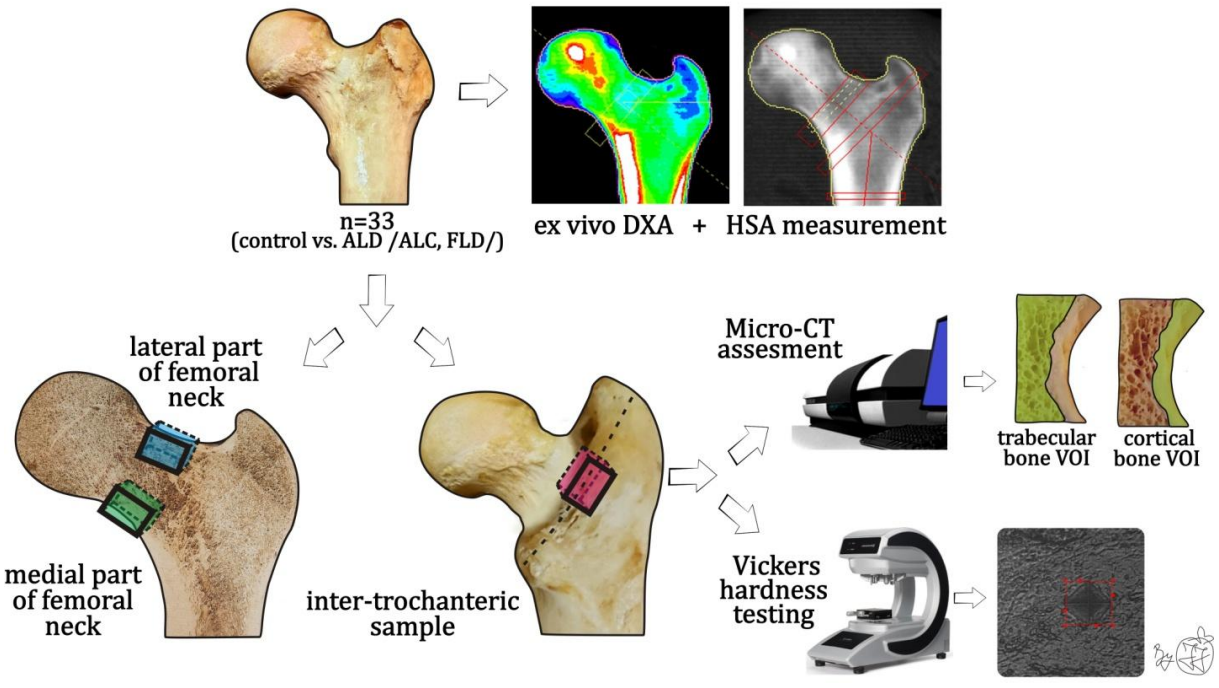


**Figure 07. Multi-scale assessment of femoral bone changes**

Abbreviations: ALD – alcoholic liver disease; ALC – alcoholic liver cirrhosis; FLD – fatty liver disease; DXA – dual-energy X-ray absorptiometry; HSA – hip structure analysis; micro-CT – micro-computed tomography; VOI – volume of interest;

### *3.7. The assessment of bone mechanical properties*

Following the adequate micro-CT assessment, lateral part of the femoral neck, medial part of the femoral neck and inter-trochanteric femoral bone samples were progressively polished by sand paper (up to 2000 grit) using water cooled polishing machine (EQ-Unipol 810 polishing machine, MTI corporation, USA). Micro-indentation on the cortical surface of these bone samples (Figure 07) was generated using Vickers micro-hardness tester (HMV-G version, Schimadzu, Japan) in Laboratory of Bone biology and Bioanthropology in Belgrade, Serbia. The cortical bone micro-hardness was measured as the auto-calculated Vickers hardness value (HV or kgf/mm$^2$). According to previous studies (Yin et al. 2019; Zwierzak et al. 2009; Dall'Ara et al. 2012), micro-indentation was performed with mechanical load of 50g applied for 12s of indentation time. Five effective indentations were performed in intact bone surface per bone sample and mean HV value was calculated for each investigated bone sample. The indentations were carefully placed in a minimum 2.5 diagonals between indentations to avoid overlapping and boundary effect, and in a minimum of 60 μm distance from the Haversian canal to assure absence of border effect. Indentations in which one diagonal was more than 10% longer than the other (Figure 08) were discarded and indentation was repeated. Thus, 495 effective indentations in total were performed in cortical part of all femoral bone samples included in the study (medial part of the femoral neck, lateral part of the femoral neck and inter-trochanteric bone samples).

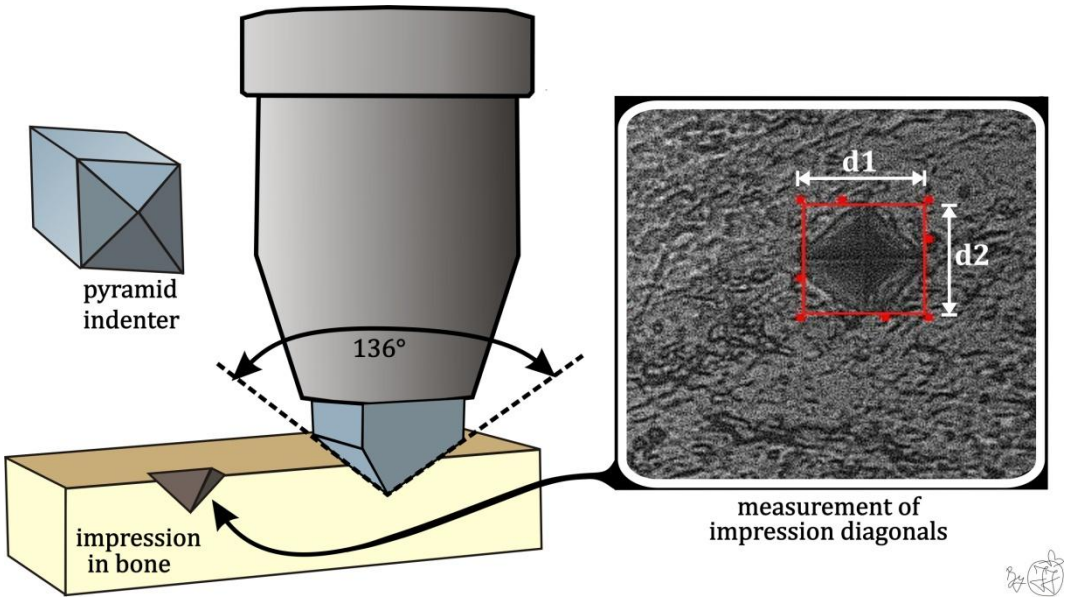


**Figure 08. Vickers micro-hardness testing of the cortical compartment of femoral bone samples**

### *3.8. Immunohistochemistry analysis of bone tissue*

Using oscillating electric autopsy saw (Kugel Medical HB-740, Kugel Medical GmbH, Germany), bone samples of the lumbar vertebrae and proximal femora were additionally cut into 1-2 mm-thick bone chips used for immunohistochemistry analysis. These bone samples were decalcified in Ethylenediaminetetraacetic acid (EDTA) based solution (USEDECALC, Medite, USA) under constant temperature ($37^0$C) in ultrasonic bath unit (SONOCOOL 255, Bandelin electronic, Germany). The endpoint for bone decalcification was established by the bending test and radiography assessment in collaboration with the Department of Diagnostic Radiology, Faculty of Dental Medicine, University of Belgrade, Serbia. Further, all decalcified bone samples were embedded in paraffin. Ultra-thin sections of bone tissue (5 μm-thik) mounted on the slides were stained using specially adapted immunohistochemistry protocol for staining bone samples at the Laboratory of Bone Biology and Bioanthropology in Belgrade, Serbia.

In short, bone sections were deparaffinized, rehydrated and treated with trypsin and TWEEN 20 solution for antigen retrieval. Hydrogen peroxide solution (3%) was used to block activity of endogenous peroxidase, while bovine serum antigen (BSA) solution was utilized to block the non-specific staining. Thereafter, tissue sections were incubated overnight at 4°C with rabbit anti-human monoclonal primary antibodies bounding to connexin 43 (antibody that targeted an osteocytic membrane protein that participate in intercellular osteocytic communication trough gap-junctions), and rabbit anti-human monoclonal primary antibodies bounding to sclerostin (antibody targeted an inhibitor of osteoblastic bone formation). For indirect protein detection, the samples were incubated for 30 min with biotin-conjugated goat anti-rabbit secondary IgG antibody diluted in 1% BSA in phosphate buffered saline (PBS) buffer (1:200). After horseradish peroxidase (HRP) conjugated streptavidin solution (DAKO, Denmark) was applied, staining was developed with diaminobenzidine (DAB) as the chromogen solution. Incubation with the pure antibody diluents without the primary antibody (1% BSA in PBS) served as a negative control, while aqueous hematoxylin dilution (1:5) was used for counterstaining.

Using freely available ImageJ software equipped with BoneJ plug-in (version 2, for Windows operative system), quantitative analysis was performed, including determination of the number of positive bone cells (brown-colored) and negative bone (purple-colored) cells per bone area (n/mm$^2$) (Figure 09). Additionally, the total number of osteocytes per bone area (N.Ot/B.Ar; n/ mm$^2$), the number of empty lacunae per bone area (N.Em.Lc/B.Ar; n/mm$^2$) and total number of osteocyte lacunas per bone area (N.Lc/B.Ar; n/mm$^2$) were determined in collected bone samples, as previously suggested (Wölfel et al. 2020). The total number of osteocytes per bone area were defined as a number of lacunae with visible nuclei present in certain bone area, while number of empty lacunae were defined as a number of lacunae without visible nuclei presented in analyzed bone area.

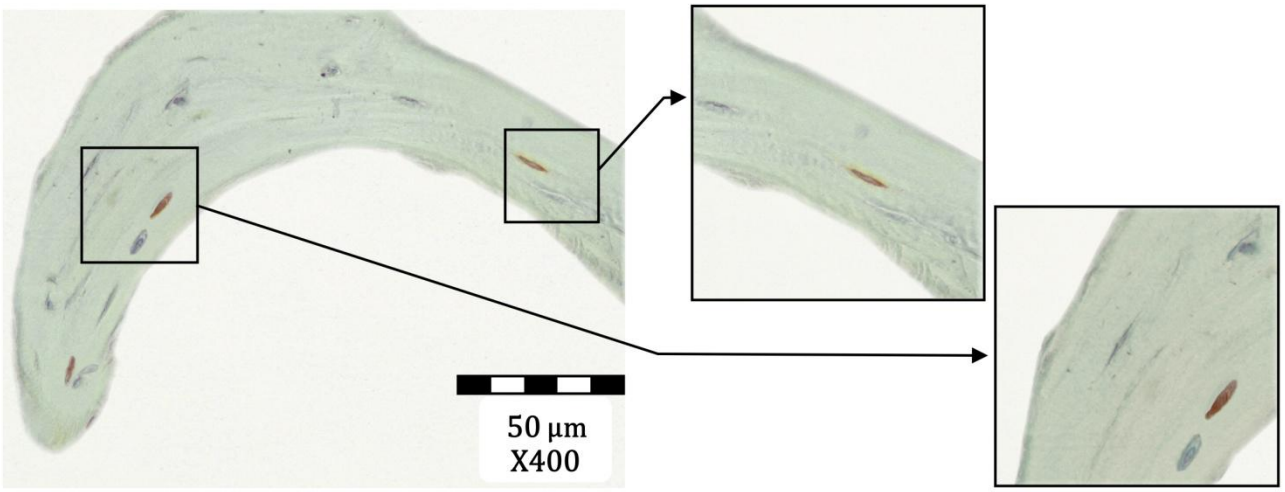


**Figure 09. Representative immunohistochemistry images of the vertebral samples**

Detail is showing a comparison of the Cx43 positive (brown colored) and Cx43 negative osteocytes (blue colored) in the isolated trabecula of the lumbar vertebrae.

### *3.9. Statistical analysis*

**Sample size**: Using the statistical software G*Power (version 3.1.9.6, for Windows operating system) for one-way analysis of variance (ANOVA), a sample size of 15 participants in ALC, non-ALC, and control group was required for microstructural analysis to achieve a power of at least 80% at a 0.05 level of significance ($\beta = 0.2$, $\alpha = 0.05$, three groups, one measurement, intended effect size of 0.48 for presented BV/TV values). With the same G*Power software for repeated measures ANOVA (two groups, three measurements, intended

effect size of 0.30 for Ct.Po), it was indicated that a minimum of 11 individuals in ALD and control group was required to ensure type one error of 0.05 and type two error of 0.2 during the present study.

**Statistical analysis of the data:** To verify the data distribution normality, coefficient of variation, skewness, kurtosis and Kolmogorov-Smirnov test were applied. Parametric tests (Student's t test, one way ANOVA, ANOVA for repeated measurements) in the case of normal distributed data were used for assessing the differences in pathohistological, densitometric, HSA, microstructural, mechanical and immunohistochemical parameters between the investigated groups. In the case of post-hoc ANOVA analysis, Bonferroni correction was applied. ANCOVA with Bonferroni post hoc test was applied for age-adjustment of micro-CT parameters in order to assess the difference between ALC, non-ALC and control group. Given that the dimensions of the femur, and its cross-sectional properties depend, at least partially, on the donor's height and weight, DXA and HSA parameters were BMI-adjusted to avoid the covariant influence of these parameters on the results. Besides the assessment of inter-group differences, repeated measures ANOVA with Bonferroni posthoc correction for pairwise comparisons was conducted to evaluate the significance of the site-specific differences in mechano-structural parameters between the investigated regions (lateral part of the femoral neck, medial part of the femoral neck, and inter-trochanteric region), and their interaction (site * group). Pearson's correlation analysis was conducted to estimate the correlation between the pathohistological score of liver disease and micro-CT parameters that complied with normal distribution. All statistical tests were performed in Statistical Package for the Social Sciences (SPSS, version 17 for Windows operative system) at a 0.05 level of significance ($p<0.05$ was considered statistically significant).

# 4. RESULTS

## *4.1. Pathohistological analysis of liver tissue samples*

Pathohistological features of significant liver damage were absent in the liver samples of control group (Figure 10a), while the presence of severe bridging fibrosis was a hallmark of liver damage confirmed in all individuals with end-stage CLD of alcoholic and non-alcoholic (cardiac) origin (Figure 10b and Table 01). In addition, focal lytic necrosis, intermediate portal tract inflammation (Figure 10b and Figure 10d), canalicular cholestasis (Figure 10c), and moderate balloon degeneration of hepatocytes (Figure 10d) were frequently observed in donors with alcoholic and non-alcoholic (cardiac) end-stage CLD (ALC and non-ALC group). The presence of Mallory bodies was noted in alcoholic end-stage CLD (ALC group, Figure 10e), while liver congestion was a hallmark of liver damage in individuals with non-alcoholic (cardiac) end-stage CLD (Figure 10f). On the other side, the significant presence of macro- and micro-vesicular steatosis (Figure 10c) was confirmed in all cadaveric men sorted into FLD group (more than 5% of fatty change in liver specimen).

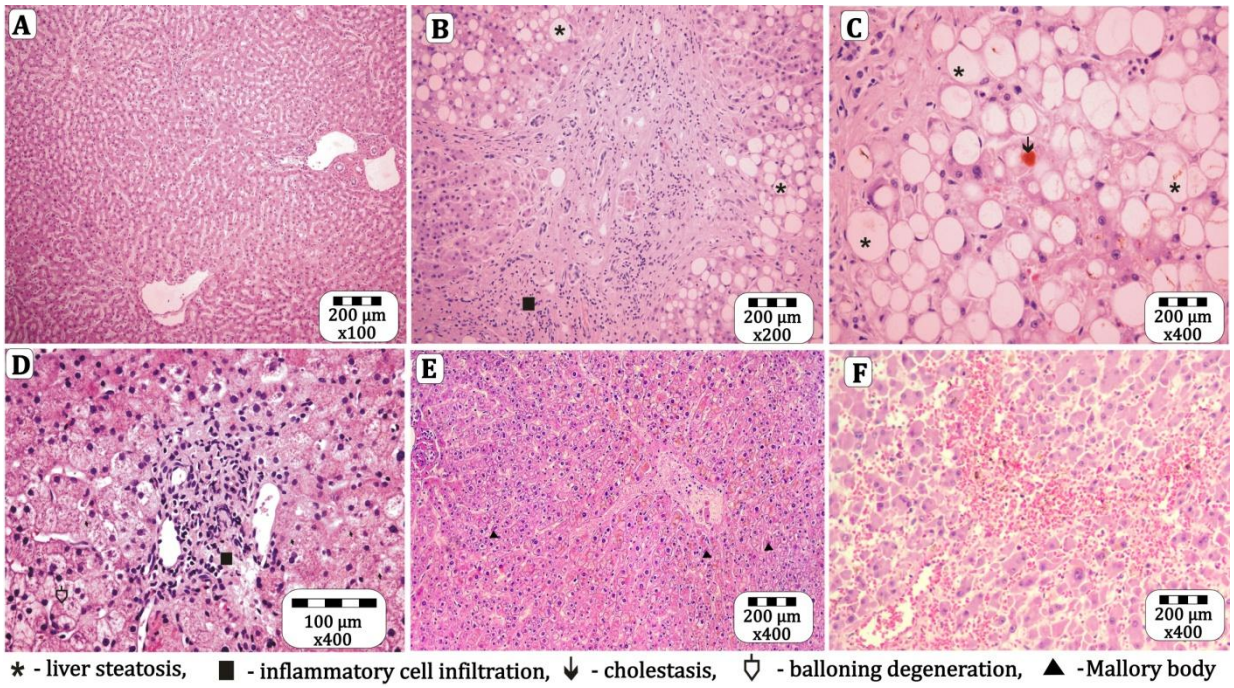


**Figure 10. Representative Hematoxylin&Eosin-stained liver tissue samples**

Absence of pathological changes was noted in liver samples of control group (a), while the presence of severe bridging fibrosis (b), moderate inflammation (b, d), canalicular cholestasis (c) and ballooning degeneration of hepatocytes (d) were observed in donors with end-stage alcoholic and non-alcoholic CLD. In addition, presence of micro- and macrovesicular steatosis (c) was a hallmark of liver damage in cadaveric donors with alcoholic fatty liver disease, Mallory body were noted in CLD of alcoholic origin (e), while liver congestion was a hallmark of liver damage in individuals with non-alcoholic (cardiac) liver cirrhosis (f).

*4.2. Pathohistological scoring of the liver damage in individuals with end-stage alcoholic and non-alcoholic CLD*

In order to evaluate the severity of liver tissue disturbances and hepatocellular damage present in donors with end-stage CLD, scoring system developed by Knodell was used. While increased HAI was observed in men with non-alcoholic (cardiac) end-stage CLD compared with the control group, even more severe liver tissue disturbances were indicated by increased HAI values in individuals with end-stage CLD of alcoholic origin, in comparison with both non-ALC and control group (Table 01, $p<0.05$, ANOVA with Bonferroni post-hoc tests). In addition, the severity of the necroinflammatory features (periportal and bridging necrosis, intralobular degeneration, and portal inflammation), given by necroinflammatory score, was higher in ALC group than in non-ALC and control groups (Table 01, $p<0.05$, ANOVA with Bonferroni post-hoc tests).

**Table 01. Results of pathohistological analysis of liver tissue samples from ALC, non-ALC and healthy cadaveric men**

| | Score | *Control* | *Non-ALC group* | *ALC group* |
|---|---|---|---|---|
| ***Piecemeal necrosis*** | n (%) | | | |
| None | 0 | 4 (20%) | 2 (13.33%) | 1 (5%) |
| Mild | 1 | 12 (60%) | 8 (53.33%) | 2 (10%) |
| Moderate | 3 | 2 (10%) | 3 (20.00%) | 5 (25%) |
| Marked | 4 | 2 (10%) | 1 (6.67%) | 7 (35%) |
| Moderate + bridging necrosis | 5 | 0 (0%) | 0 (0.00%) | 3 (15%) |
| Marked + bridging necrosis | 6 | 0 (0%) | 1 (6.67%) | 2 (10%) |
| Multilobular necrosis | 10 | 0 (0%) | 0 (0.00%) | 0 (0%) |
| ***Intralobular degeneration and focal necrosis*** | n (%) | | | |
| None | 0 | 20 (100%) | 13 (87.67%) | 6 (30%) |
| Mild | 1 | 0 (0%) | 2 (13.33%) | 11 (55%) |
| Moderate | 3 | 0 (0%) | 0 (0.00%) | 2 (10%) |
| Marked | 4 | 0 (0%) | 0 (0.00%) | 1 (5%) |
| ***Portal inflammation*** | n (%) | | | |
| None | 0 | 7 (35%) | 1 (6.67%) | 1 (5%) |
| Mild | 1 | 9 (45%) | 6 (40.00%) | 7 (35%) |
| Moderate | 3 | 4 (20%) | 5 (33.33%) | 9 (45%) |
| Marked | 4 | 0 (0%) | 3 (20.00%) | 3 (15%) |
| ***Necroinflammatory score*** | Mean ± SD | 2±2 | 4±3 | 7±3*# |
| ***Fibrosis*** | n (%) | | | |
| No fibrosis | 0 | 15 (75%) | 0 (0.00%) | 0 (0%) |
| Fibrous portal expansion | 1 | 5 (25%) | 0 (0.00%) | 0 (0%) |
| Bridging fibrosis | 3 | 0 (0%) | 0 (0.00%) | 0 (0%) |
| Cirrhosis | 4 | 0 (0%) | 15 (100%) | 20 (100%) |
| ***Histology Activity Index*** | Mean ± SD | 3±2 | 8±3* | 11±3*# |

Statistical significance was estimated using one-way ANOVA with Bonferroni post hoc test (* $p<0.05$ vs. control; # $p<0.05$ vs. non-ALC).

### *4.3. The comparison of clinical imaging tools in fracture risk assessment of the healthy individuals and donors with alcoholic liver disease*

In this study we analyzed femoral BMD and HSA parameters of the 33 cadaveric men belonging to: ALD group (n=13; age=57±13 years) and control group (n=20; age= 54±13 years). Donor's age, weight (78±21 kg vs. 82±20 kg), height (175±9 cm vs. 173±11 cm) and Body Mass Index (BMI, 25.58±7.06 kg/m$^2$ vs. 27.18±6.02 kg/m$^2$) was not significantly different between individuals belonging to ALD and control group ($p>0.05$, Student's *t* test).

As presented in Table 02 and 03, DXA and HSA parameters showed normal distribution in ALD and control group, while Levene's test confirmed homogeneity of the variance of presented results ($p>0.05$).

**Table 02.** DXA and HSA parameters of ALD group: Data distribution normality testing

| | **BMC** (g) | | | **BMD** (g/cm$^2$) | | | **CSA** (cm$^2$) | | **CTh** (cm) | | **BR** | |
|---|---|---|---|---|---|---|---|---|---|---|---|---|
| Region | N | IT | Tot | N | IT | Tot | NN | IT | NN | IT | NN | IT |
| CV | 0.327 | 0.241 | 0.220 | 0.270 | 0.192 | 0.189 | 0.277 | 0.386 | 0.294 | 0.371 | 0.386 | 0.281 |
| Skewness | 0.486 | -0.016 | -0.099 | 0.471 | -0.462 | -0.068 | 0.382 | 0.742 | 0.520 | 0.243 | 1.580 | 0.316 |
| Kurtosis | -1.130 | -0.840 | -0.866 | -0.320 | -0.870 | -1.261 | -0.642 | -0.321 | -0.321 | -1.485 | 3.945 | -1.816 |
| KS test (p value) | 0.847 | 0.828 | 0.820 | 0.534 | 0.902 | 0.952 | 0.930 | 0.900 | 0.750 | 0.669 | 0.514 | 0.695 |

Abbreviations: BMC – bone mineral content; BMD – areal bone mineral density; CSA – cross-sectional area; CSMI – cross-sectional moment of inertia; CTh – estimated cortical thickness; BR – buckling ratio; N – femoral neck; NN – narrow neck; IT – inter-trochanteric region; Tot – total proximal femora; CV – coefficient of variation; KS test – Kolmogorov-Smirnov test;

**Table 03.** DXA and HSA parameters of control group: Data distribution normality testing

| | **BMC** (g) | | | **BMD** (g/cm$^2$) | | | **CSA** (cm$^2$) | | **CTh** (cm) | | **BR** | |
|---|---|---|---|---|---|---|---|---|---|---|---|---|
| Region | N | IT | Tot | N | IT | Tot | NN | IT | NN | IT | NN | IT |
| CV | 0.167 | 0.326 | 0.274 | 0.158 | 0.157 | 0.149 | 0.108 | 0.250 | 0.188 | 0.273 | 0.230 | 0.303 |
| Skewness | -0.120 | 0.332 | 0.172 | -0.178 | -0.634 | -0.192 | 1.283 | 0.030 | -0.120 | -0.370 | 0.454 | 0.774 |
| Kurtosis | 0.305 | -0.634 | -0.551 | 0.127 | 0.053 | -0.109 | 1.137 | 0.299 | -0.362 | -1.184 | -0.184 | -0.363 |
| KS test (p value) | 0.916 | 0.820 | 0.914 | 0.970 | 0.901 | 0.994 | 0.347 | 0.995 | 0.927 | 0.822 | 0.829 | 0.987 |

Abbreviations: BMC – bone mineral content; BMD – areal bone mineral density; CSA – cross-sectional area; CSMI – cross-sectional moment of inertia; CTh – estimated cortical thickness; BR – buckling ratio; N – femoral neck; NN – narrow neck; IT – inter-trochanteric region; Tot – total proximal femora; CV – coefficient of variation; KS test – Kolmogorov-Smirnov test;

According to widely known World Health Organization (WHO) recommendations (Danford et al. 2019), *ex vivo* DXA assessment performed during this study suggested that eight ALD men could meet diagnostic criteria for osteopenia (n=6) or osteoporosis (n=2), while in the control group, four individuals had findings suggesting age-associated osteopenia and one had finding in osteoporotic range. Still, our data did not reveal extremely prominent osteodensitometry changes in ALD individuals (Table 04), due to significant BMI associated covariant effect on our results.

**Table 04a. Comparison of DXA and HSA assessment of proximal femora obtained from ALD donors with age-matched healthy controls (data not adjusted)**

| | Femoral subregion | **ALD group** (Mean ± SD) | **Control group** (Mean ± SD) | **P value** |
|---|---|---|---|---|
| **BMC** (g) | N | 3.836±1.255 | 4.668±0.781 | **p=0.025** |
| | IT | 37.845±9.126 | 42.830±13.970 | p>0.05 |
| | Tot | 48.404±10.671 | 54.889±15.021 | p>0.05 |
| **BMD** ($g/cm^2$) | N | 0.680±0.184 | 0.839±0.134 | **p=0.007** |
| | IT | 0.988±0.188 | 1.132±0.179 | p>0.05 |
| | Tot | 0.909±0.172 | 1.027±0.154 | **p=0.048** |
| **CSA** ($cm^2$) | NN | 2.889±0.161 | 3.508±0.130 | **p=0.005** |
| | IT | 5.989±2.317 | 6.969±1.744 | p>0.05 |
| | FS | 4,519±1,106 | 4,974±1,185 | p>0.05 |
| **CSMI** ($cm^4$) | NN | 3.810±1.172 | 3.913±0.889 | p>0.05 |
| | IT | 29.249±18.786 | 28.835±13.171 | p>0.05 |
| | FS | 4,656±1,216 | 4,938±0,889 | p>0.05 |
| **CTh** (cm) | NN | 0.158±0.046 | 0.192±0.036 | **p=0.027** |
| | IT | 0.478±0.178 | 0.591±0.162 | p>0.05 |
| **Z** ($cm^3$) | NN | 1.755±0.514 | 1.967±0.322 | p>0.05 |
| | IT | 7.076±3.496 | 7.320±2.544 | p>0.05 |
| | FS | 2.674±0.627 | 3.023±0.437 | p>0.05 |
| **BR** (dimensionless) | NN | 14.200±5.488 | 10.785±3.270 | **p=0.032** |
| | IT | 8.736±2.460 | 7.395±1.705 | p>0.05 |
| | FS | 3.561±1.407 | 2.726±0.845 | **p=0.044** |

Abbreviations: BMC – bone mineral content; BMD – areal bone mineral density; CSA – cross-sectional area; CSMI – cross-sectional moment of inertia; CTh – estimated cortical thickness; Z – section modulus; BR – buckling ratio; N – femoral neck; NN – narrow neck; IT – inter-trochanteric region; FS – Femoral shaft; Tot – total proximal femora; ALD – Alcoholic liver disease;
Statistical significance was estimated using one-way ANOVA (significant difference was presented in bold font).

As shown in the Table 04b, after the BMI adjustment, only values of bone mineral density and cross-sectional area remained significantly decreased in the femoral neck region of ALD individuals when compared to healthy controls, suggesting real ALD-induced bone loss. Although we observed deterioration trend in other osteodensitometry and HSA

parameters of proximal femora collected from ALD donors (Table 04a), statistical significance faded away after BMI adjusting (p>0.05, one-way ANOVA).

**Table 04b. Comparison of DXA and HSA assessment of proximal femora collected from adult cadaveric ALD men and age-matched healthy control male individuals (data adjusted for BMI)**

| | Femoral subregion | **ALD group** (Mean ± SE) | **Control group** (Mean ± SE) | **P value** |
|---|---|---|---|---|
| BMC (g) | N | 3.895±0.277 | 4.631±0.223 | p>0.05 |
| | IT | 38.891±3.214 | 42.150±2.580 | p>0.05 |
| | Tot | 49.616±3.477 | 54.101±2.791 | p>0.05 |
| BMD ($g/cm^2$) | N | 0.693±0.042 | 0.831±0.034 | **p=0.017** |
| | IT | 1.004±0.048 | 1.122±0.038 | p>0.05 |
| | Tot | 0.923±0.042 | 1.019±0.034 | p>0.05 |
| CSA ($cm^2$) | NN | 2.932±0.158 | 3.480±0.127 | **p=0.012** |
| | IT | 6.286±0.470 | 6.766±0.387 | p>0.05 |
| | FS | 4,591±0,303 | 4,925±0,250 | p>0.05 |
| CSMI ($cm^4$) | NN | 3.880±0.360 | 3.868±0.289 | p>0.05 |
| | IT | 31.235±4.058 | 27.476±3.338 | p>0.05 |
| | FS | 4.688±0.288 | 4.916±0.237 | p>0.05 |
| CTh (cm) | NN | 0.162±0.11 | 0.190±0.009 | p>0.05 |
| | IT | 0.504±0.046 | 0.568±0.043 | p>0.05 |
| Z ($cm^3$) | NN | 1.768±0.113 | 1.959±0.091 | p>0.05 |
| | IT | 7.234±0.795 | 7.212±0.656 | p>0.05 |
| | FS | 2.699±0.141 | 3.006±0.117 | p>0.05 |
| BR (dimensionless) | NN | 14.062±1.223 | 10.875±0.982 | p>0.05 |
| | IT | 8.671±0.588 | 7.432±0.447 | p>0.05 |
| | FS | 3.500±0.295 | 2.768±0.244 | p>0.05 |

Abbreviations: BMC – bone mineral content; BMD – areal bone mineral density; CSA – cross-sectional area; CSMI – cross-sectional moment of inertia; CTh – estimated cortical thickness; Z – section modulus; BR – buckling ratio; N – femoral neck; NN – narrow neck; IT – inter-trochanteric region; FS – Femoral shaft; Tot – total proximal femora; ALD – alcoholic liver disease;
Statistical significance was estimated using one-way ANOVA, while data were BMI-adjusted to avoid the covariant effect on the study results (BMI value appearing in corrected model was 26.55 $kg/m^2$). Data were presented as mean ± standard error (SE).

As shown in Figure 11, the femoral neck bone mineral density and cross-sectional area alterations observed in our ALD group originated from included ALC donors, in whom these parameters were significantly lower when compared to healthy controls (p<0.05, ANOVA with Bonferroni post hoc test, Figure 11). Additionally, significantly decreased cross-sectional area and thinner cortex was noted in the inter-trochanteric region of donors with end-stage ALD, compared with healthy age- and sex-matched controls (p<0.05, ANOVA with Bonferroni post hoc test, Figure 11). In contrast, we did not observe any significant difference in densitometry and geometry parameters either between individuals with initial ALD stage (FLD group) and

healthy controls (Figure 11), or between individuals with initial and end-stage of ALD (FLD vs. ALC group p>0.05, ANOVA with Bonferroni post hoc test).

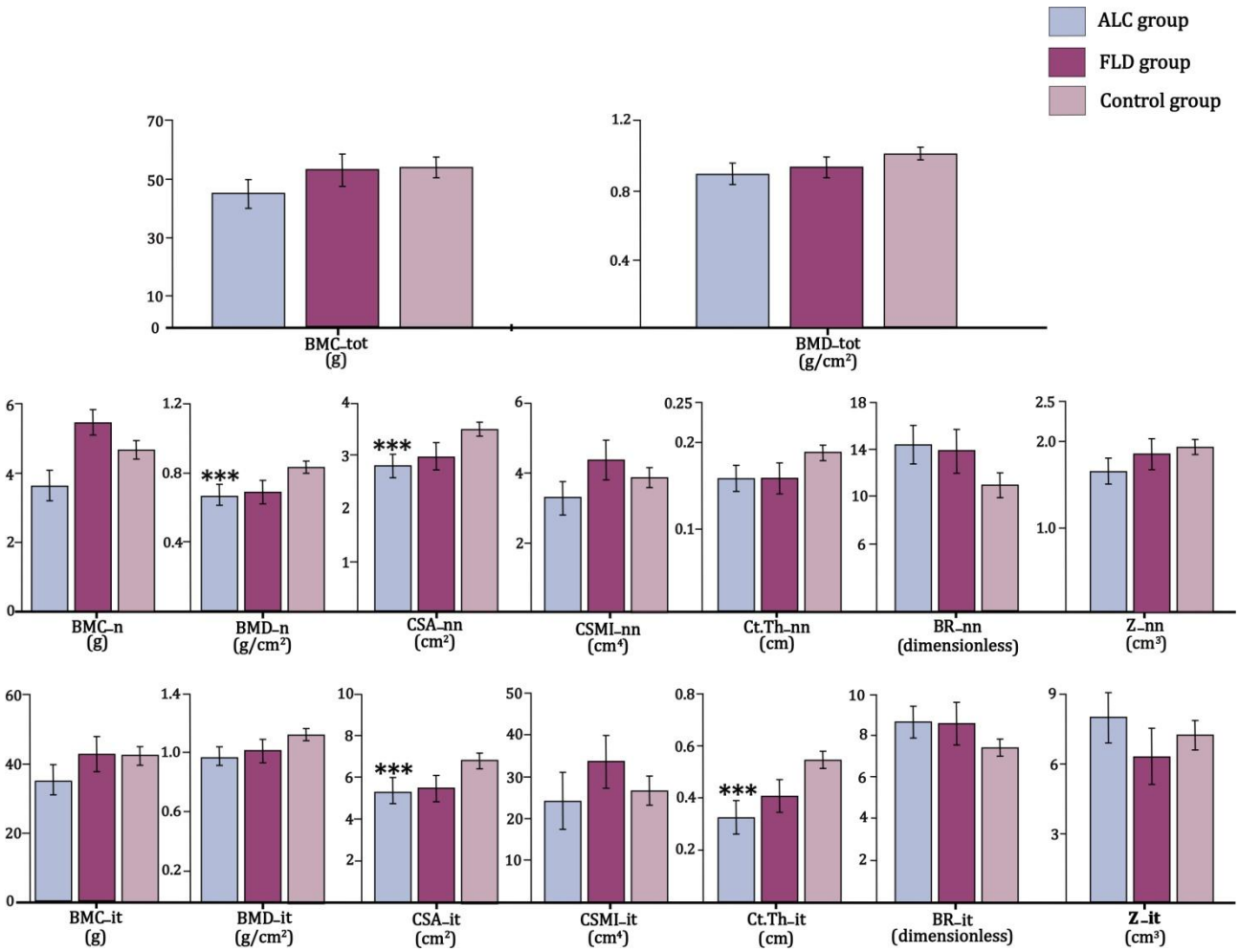


**Figure 11. Comparison of DXA and HSA assessment of proximal femora collected from adult cadaveric men with various ALD stages and age-matched healthy control men**

Abbreviations: BMC – bone mineral content; BMD – areal bone mineral density; CSA – cross-sectional area; CSMI – cross-sectional moment of inertia; CTh – estimated cortical thickness; Z – section modulus; BR – buckling ratio; N – femoral neck; NN – narrow neck; IT – inter-trochanteric region; Tot – total proximal femora; ALC – alcoholic liver cirrhosis; FLD – fatty liver disease;
Statistical significance was estimated using one-way ANOVA with Bonferroni post hoc test, while data were BMI-adjusted to avoid the covariant effect on the study results (***p<0.05 vs. control).

### *4.4. The changes of trabecular and cortical microstructure in lumbar vertebrae collected from men with end-stage CLD of alcoholic and non-alcoholic origin*

In this study, we analyzed micro-architectural parameters of anterior mid-transverse part of lumbar vertebrae body collected from 55 cadaveric men belonging to: ALC group (n=20; age= 59±8 years), non-ALC group (n=15; age= 69±10 years) and control group (n=20; age= 60±7 years). These donors included into our ALC, non-ALC and control group were well

matched for weight (87± 20 kg vs. 76±13 vs. 80±12 kg), height (177±7 cm vs. 173±7 cm vs. 176±10 cm) and BMI (27.90±6.41 kg/m$^2$ vs. 25.28±4.38 kg/m$^2$vs. 25.64±2.72 kg/m$^2$) ($p>0.05$, one-way ANOVA with Bonferroni post-hoc test). In contrast, due to the specific pathogenesis of end-stage CLD of non-alcoholic (cardiac) origin, the non-ALC donors were older than donors of control ($p=0.004$) and ALC group ($p=0.002$; one-way ANOVA with Bonferroni post-hoc test). Thus, to control for potential influence of age-associated differences in bone micro-architecture on our results, analyzed micro-CT parameters were age-adjusted.

As presented in Table 05-07, analyzed trabecular and cortical micro-architectural parameters in lumbar vertebrae of individuals divided into ALC, non-ALC and control group showed normal distribution, while Levene's test confirmed homogeneity of variance of the presented results ($p>0.05$).

**Table 05.** Main micro-architectural parameters in lumbar vertebrae of ALC group: Data distribution normality testing

| | **BV/TV** (%) | **Tb.Th** (μm) | **Tb.N** (1/mm) | **Ct.Po** (%) | **Po.Dm** (μm) | **Ct.Th** (mm) |
|---|---|---|---|---|---|---|
| CV | 0.250 | 0.184 | 0.299 | 0.396 | 0.290 | 0.414 |
| Skewness | -0.290 | 0.178 | -0.577 | 0.801 | 0.076 | -0.201 |
| Kurtosis | 0.150 | 1.381 | 1.010 | 0.787 | -0.558 | 0.614 |
| KS test (p value) | 0.964 | 0.802 | 0.947 | 0.961 | 0.982 | 0.887 |

Abbreviations: BV/TV – trabecular bone volume fraction; Tb.Th – trabecular thickness; Tb.N – trabecular number; Ct. Po – cortical porosity; Po.Dm – cortical pore diameter; Ct.Th – cortical thickness; CV – coefficient of variation; KS test – Kolmogorov-Smirnov test;

**Table 06.** Main micro-architectural parameters in lumbar vertebrae of non-ALC group: Data distribution normality testing

| | **BV/TV** (%) | **Tb.Th** (μm) | **Tb.N** (1/mm) | **Ct.Po** (%) | **Po.Dm** (μm) | **Ct.Th** (mm) |
|---|---|---|---|---|---|---|
| CV | 0.313 | 0.145 | 0.247 | 0.294 | 0.589 | 0.228 |
| Skewness | 1.139 | 0.731 | 0.336 | -0.096 | 3.238 | 2.222 |
| Kurtosis | 2.277 | 0.400 | -0.899 | 0.133 | 11.477 | 6.545 |
| KS test (p value) | 0.715 | 0.571 | 0.719 | 0.887 | 0.068 | 0.320 |

Abbreviations: BV/TV – trabecular bone volume fraction; Tb.Th – trabecular thickness; Tb.N – trabecular number; Ct. Po – cortical porosity; Po.Dm – cortical pore diameter; Ct.Th – cortical thickness; CV – coefficient of variation; KS test – Kolmogorov-Smirnov test;

**Table 07.** Main micro-architectural parameters in lumbar vertebrae of control group: Data distribution normality testing

| | **BV/TV** (%) | **Tb.Th** (μm) | **Tb.N** (1/mm) | **Ct.Po** (%) | **Po.Dm** (μm) | **Ct.Th** (mm) |
|---|---|---|---|---|---|---|
| CV | 0.311 | 0.184 | 0.174 | 0.329 | 0.370 | 0.227 |
| Skewness | 1.983 | 0.678 | 0.429 | 0.252 | 1.068 | 0.497 |
| Kurtosis | 4.840 | -1.070 | -0.453 | -1.271 | 0.467 | -0.282 |
| KS test (p value) | 0.388 | 0.259 | 0.881 | 0.803 | 0.304 | 0.974 |

Abbreviations: BV/TV – trabecular bone volume fraction; Tb.Th – trabecular thickness; Tb.N – trabecular number; Ct. Po – cortical porosity; Po.Dm – cortical pore diameter; Ct.Th – cortical thickness; CV – coefficient of variation; KS test – Kolmogorov-Smirnov test;

Micro-CT analysis showed a significant reduction in trabecular bone volume fraction, accompanied by the reduced trabecular number and thickness, noted in the lumbar vertebrae body collected from donors with alcoholic and non-alcoholic (cardiac) end-stage CLD (ALC and non-ALC group), when compared to healthy control individuals ($p<0.05$, one-way ANOVA with Bonferroni post-hoc test , Table 08 and Figure 13). The observed differences in these micro-CT parameters remained significantly different after age-adjustment between control group and individuals suffering from end-stage CLD of alcoholic and non-alcoholic (cardiac) origin, indicating real trabecular deterioration in lumbar vertebrae induced by alcoholic and non-alcoholic (cardiac) liver cirrhosis ($p<0.05$; ANCOVA with Bonferroni correction for age-adjustment, Table 08). Still, parameters of trabecular micro-architecture were not significantly different in lumbar vertebrae collected from persons with alcoholic end-stage CLD and non-alcoholic (cardiac) end-stage CLD ($p>0.05$; one way ANOVA with Bonferroni post hoc test, Figure 13).

In addition, minor inter-group differences were observed in trabecular complexity and connectivity parameters. Namely, an increasing trend of specific bone surface and trabecular separation was observed in persons with end-stage CLD of alcoholic and non-alcoholic origin, in comparison to healthy controls. However, this increasing trend reached statistical significance only in the individuals with alcohol-induced end-stage CLD (liver cirrhosis) after age adjustment ($p<0.05$, ANCOVA with Bonferroni correction for age-adjustment, Table 08). In contrast, the differences in DA, FD, TbPf and SMI were not observed between controls and individuals with alcoholic and non-alcoholic end-stage CLD ($p>0.05$, Table 08). Moreover,

these parameters were without any correlation to the severity of the observed pathohistological changes in the liver tissue of the same individuals (p>0.05, Pearson correlation analysis).

**Table 08. Comparison of trabecular micro-architectural parameters of lumbar vertebrae from ALC, non-ALC and control group**

| | **Control group** (Mean ± SD) | **Non-ALC group** (Mean ± SD) | **ALC group** (Mean ± SD) |
|---|---|---|---|
| **BV/TV** (%) | 15.11±4.71 | 9.91±3.11*** | 9.69±2.42*** |
| **Tb.Th** (μm) | 158.8±29.1 | 128.0±18.7*** | 121.9±22.6*** |
| **Tb.N** (1/mm) | 1.02±0.18 | 0.77±0.19* | 0.70±0.21*** |
| **TbPf** (1/mm) | 3.52±1.97 | 4.77±2.35 | 5.26±1.66* |
| **FD** | 2.32±0.09 | 2.22±0.13 | 2.28±0.09 |
| **DA** | 1.97±0.24 | 1.99±0.40 | 1.94±0.33 |
| **SMI** | 1.49±0.87 | 1.31±0.41 | 1.47±0.48 |
| **Tb.Sp** (μm) | 691.5±137.6 | 864.3±142.4* | 907.3±144.2*** |
| **BS/BV** (1/mm) | 23.77±3.36 | 27.86±3.58 | 28.30±7.76* |
| Micro-CT parameters adjusted for age (62.2 years) | | | |
| **BV/TV** (%) | 14.96±0.81 | 10.36±1.02*** | 9.50±0.82*** |
| **Tb.Th** (μm) | 158.0±6.0 | 129.0±7.0*** | 121.0±6.0*** |
| **Tb.N** (1/mm) | 1.01±0.04 | 0.80±0.05* | 0.69±0.04*** |
| **TbPf** (1/mm) | 3.67±0.44 | 4.35±0.55 | 5.43±0.44 |
| **FD** | 2.31±0.02 | 2.23±0.03 | 2.28±0.02 |
| **DA** | 1.96±0.07 | 1.93±0.07 | 2.03±0.09 |
| **SMI** | 1.52±0.14 | 1.22±0.18 | 1.51±0.14 |
| **Tb.Sp** (μm) | 699.0±32.0 | 834.0±40.0 | 916.0±32.0* |
| **BS/BV** (1/mm) | 23.84±1.25 | 27.65±1.56 | 28.39±1.26* |

Abbreviations: BV/TV – trabecular bone volume fraction; Tb.Th – trabecular thickness; Tb.N – trabecular number; FD – fractal dimension; TbPf – trabecular bone pattern facto; SMI – structure model index; Tb.Sp – trabecular separation; BS/BV – specific bone surface; ALC – alcoholic liver cirrhosis; non-ALC – non-alcoholic (cardiac) liver cirrhosis;
Statistical significance was estimated using one-way ANOVA with Bonferroni post-hoc test (* p<0.05; *** p<0.001 vs. control), and ANCOVA with Bonferroni correction for age-adjustment (* p<0.05; ***p<0.001 vs. control).

As shown in Figure 12, Pearson correlation analysis has shown an inverse correlation between histology activity index and trabecular bone quantity parameters (BV/TV, Tb.Th and Tb.N) in bone samples of lumbar vertebral body obtained from individuals suffering from alcoholic and non-alcoholic end-stage liver disorder (r=-0.510, r=-0.513, r=-0.506 respectively; p<0.001).

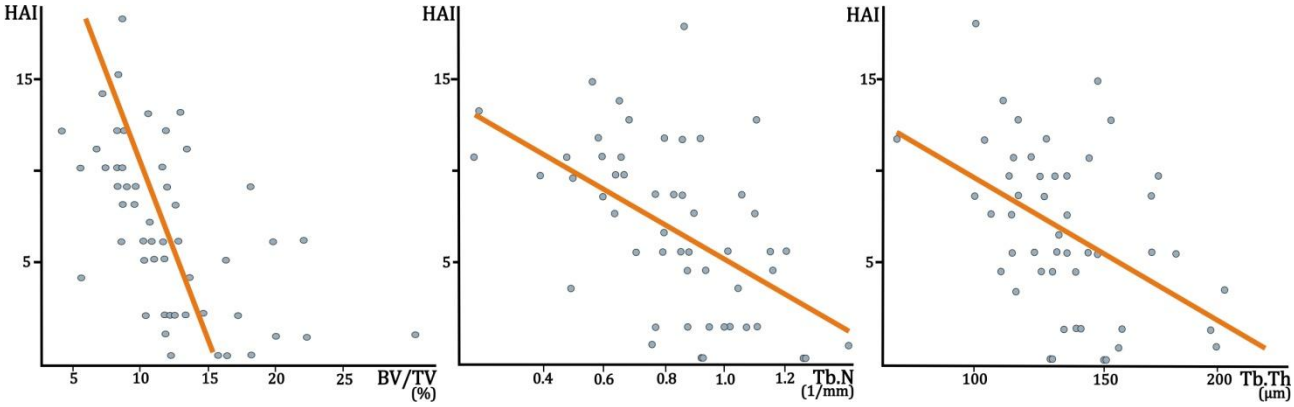


**Figure 12. Inverse association between liver pathohistological scores and trabecular micro-structural parameters in our vertebral samples, presented by scatter plots** (Pearson correlation analysis, p<0.001);

Abbreviations: HAI – histology activity index; BV/TV – trabecular bone volume fraction; Tb.Th – trabecular thickness; Tb.N – trabecular number;

In contrast to trabecular bone, our results indicated that cortical micro-architecture of lumbar vertebrae was not susceptible for significant liver cirrhosis induced bone deterioration (Figure 13). Namely, all parameters of cortical micro-architecture did not show any significant difference between the lumbar vertebrae of individuals suffering from end-stage CLD and healthy control individuals (p>0.05, one-way ANOVA with Bonferroni post-hoc test, Table 09), regardless of the age adjustment.

**Table 09. Comparison of cortical micro-architectural parameters of lumbar vertebrae from ALC, non-ALC and control group**

| | **Control group** (Mean ± SD) | **Non-ALC group** (Mean ± SD) | **ALC group** (Mean ± SD) | **P value** |
|---|---|---|---|---|
| **Ct.Po** (%) | 30.57±10.05 | 33.08±9.72 | 37.63±14.92 | p>0.05 |
| **Po.Dm** (µm) | 181.9±67.4 | 208.2±121,7 | 179.6±52.0 | p>0.05 |
| **Po.Sp** (µm) | 171.2±97.6 | 208.5±30.1 | 205.0±57.2 | p>0.05 |
| **Ct.Th** (mm) | 1.875±0.425 | 1.790±0.409 | 1.645±0.682 | p>0.05 |
| Parameters adjusted for age (62.2 years) | | | | |
| **Ct.Po** (%) | 30.68±2.75 | 32.75±3.44 | 37.76±2.77 | p>0.05 |
| **Po.Dm** (µm) | 185.0±19.0 | 199.0±23.0 | 183.0±19.0 | p>0.05 |
| **Po.Sp** (µm) | 172.0±29.0 | 205.0±36.0 | 206.0±29.0 | p>0.05 |
| **Ct.Th** (mm) | 1.897±0.120 | 1.725±0.151 | 1.672±0.121 | p>0.05 |

Abbreviations: Ct.Po – cortical porosity; Po.Dm – cortical pore diameter; Po.Sp – cortical pore separation; Ct.Th – cortical thickness; ALC – alcoholic liver cirrhosis; non-ALC – non-alcoholic (cardiac) liver cirrhosis; Statistical significance was estimated using one-way ANOVA with Bonferroni post-hoc test (p>0.05) and ANCOVA with Bonferroni correction for age-adjustment (p>0.05).

Nonetheless, our data may suggest a mild trend in cortical thickness deterioration, accompanied by bland tendency to increased cortical porosity, and pore diameter (Table 09) in ALC and non-ALC donors. Moreover, micro-CT assessed parameters of cortical microstructure were not significantly different between individuals with alcoholic and non-alcoholic liver cirrhosis ($p>0.05$, one-way ANOVA with Bonferroni post-hoc test, Table 09). Finally, Pearson correlation analysis did not reveal any significant association between any of the Knodell's pathohistological scores and cortical microstructure in individuals with alcoholic and non-alcoholic (cardiac) end-stage CLD ($p>0.05$).

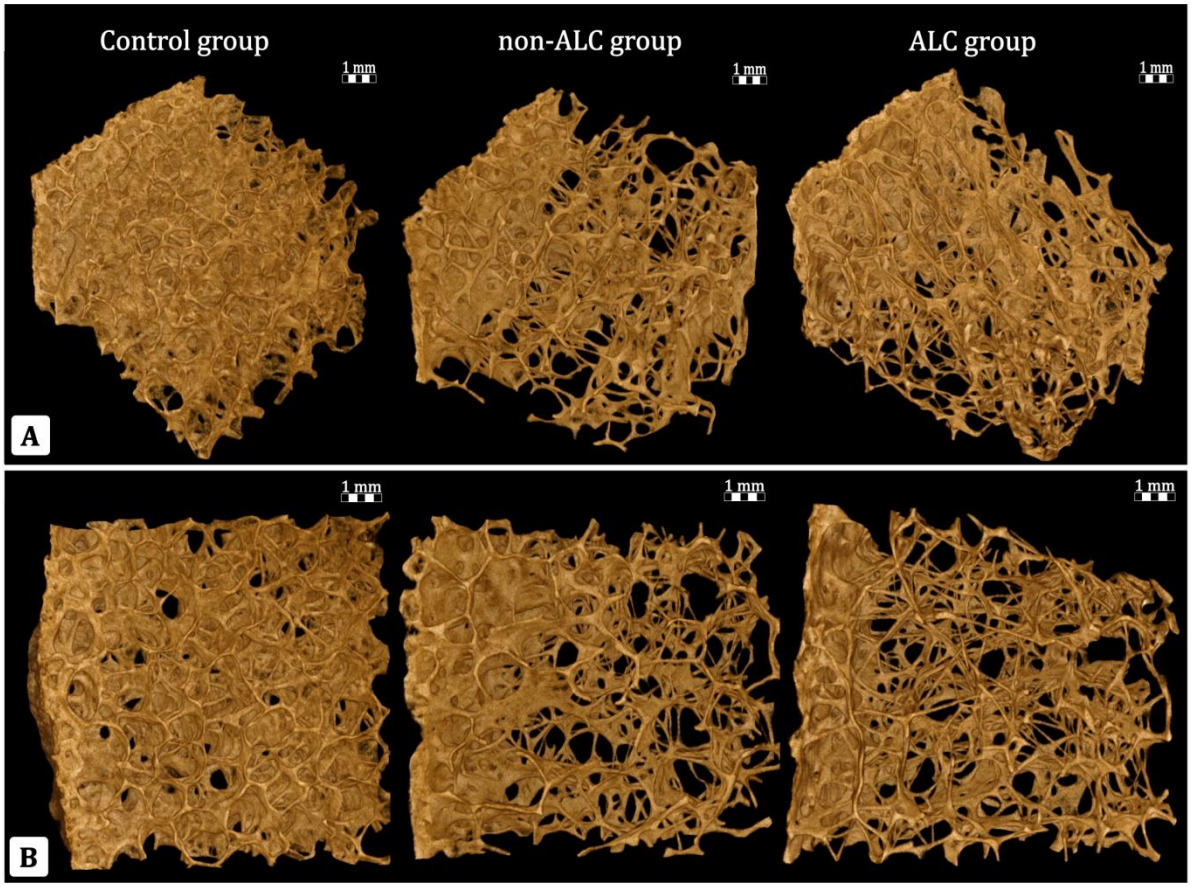


**Figure 13. Representative 3D model of lumbar vertebrae sampled from ALC, non-ALC and healthy control donors – whole harvested bone sample (a) and view from above (b)**

Significant trabecular bone loss is represented in decreased trabecular bone volume fraction, reduced trabecular number, and trabecular thickness in men with end-stage alcoholic and non-alcoholic (cardiac) CLD in comparison to healthy controls (* $p<0.05$ vs. control, ANOVA with Bonferroni post-hoc analysis, Figure 2c). Still, the micro-architecture of lumbar cortical shell was not significantly different between investigated groups. It is notable that bone loss in the ALC group is not substantially different from the non-ALC group.

### *4.5. The micro-architectural alteration of proximal femora obtained from men with alcoholic liver disease*

Following osteodensitometry and HSA measurements, we analyzed femoral microstructural parameters of the 33 cadaveric men divided into: ALD group (n=13) and control group (n=20).

As presented in Table 10-13, parameters of femoral micro-architecture showed normal distribution in ALD and control group, while Levene's test confirmed homogeneity of variance of the presented results ($p>0.05$).

**Table 10** Trabecular micro-architectural parameters in three regions of proximal femora obtained from ALD donors: Test for data distribution normality

| | **BV/TV** (%) | | | **Tb.Th** (μm) | | | **Tb.N** (1/mm) | | |
|---|---|---|---|---|---|---|---|---|---|
| Femoral region | **LN** | **MN** | **IT** | **LN** | **MN** | **IT** | **LN** | **MN** | **IT** |
| CV | 0.190 | 0.180 | 0.252 | 0.185 | 0.173 | 0.185 | 0.139 | 0.152 | 0.175 |
| Skewness | 0.475 | -0.457 | 0.292 | 0.230 | 0.546 | 0.857 | 0.368 | 0.978 | 0.137 |
| Kurtosis | 1.808 | -1.080 | -1.563 | -0.153 | -0.222 | -0.256 | -0.849 | 0.893 | 0.202 |
| KS test (p value) | 0.685 | 0.848 | 0.309 | 0.999 | 0.715 | 0.467 | 0.765 | 0.515 | 0.676 |

Abbreviations: BV/TV – trabecular bone volume fraction; Tb.Th – trabecular thickness, Tb.N – trabecular number; LN – lateral part of the femoral neck; MN – medial part of the femoral neck; IT – inter-trochanteric region; CV – coefficient of variation; KS test – Kolmogorov-Smirnov test;

**Table 11** Trabecular micro-architectural parameters in three regions of proximal femora obtained from control donors: Test for data distribution normality

| | **BV/TV** (%) | | | **Tb.Th** (μm) | | | **Tb.N** (1/mm) | | |
|---|---|---|---|---|---|---|---|---|---|
| Femoral region | **LN** | **MN** | **IT** | **LN** | **MN** | **IT** | **LN** | **MN** | **IT** |
| CV | 0.215 | 0.255 | 0.221 | 0.145 | 0.130 | 0.103 | 0.099 | 0.207 | 0.178 |
| Skewness | 1.935 | 0.329 | 0.368 | 0.714 | 0.342 | -0.223 | 0.298 | -0.196 | -0.014 |
| Kurtosis | 4.951 | 0.406 | -0.320 | 2.928 | -0.219 | 0.048 | -0.222 | 0.364 | -0.664 |
| KS test (p value) | 0.262 | 0.916 | 0.979 | 0.547 | 0.792 | 0.500 | 0.974 | 0.995 | 0.928 |

Abbreviations: BV/TV – trabecular bone volume fraction; Tb.Th – trabecular thickness, Tb.N – trabecular number; LN – lateral part of the femoral neck; MN – medial part of the femoral neck; IT – inter-trochanteric region; CV– coefficient of variation; KS test – Kolmogorov-Smirnov test;

**Table 12** Cortical micro-architectural parameters in three regions of proximal femora obtained from ALD donors: Test for data distribution normality

| | **Ct.Po** (%) | | | **Po.Dm** (μm) | | | **Ct.Th** (mm) | | |
|---|---|---|---|---|---|---|---|---|---|
| Femoral region | **LN** | **MN** | **IT** | **LN** | **MN** | **IT** | **LN** | **MN** | **IT** |
| CV | 0.305 | 0.440 | 0.262 | 0.252 | 0.208 | 0.232 | 0.251 | 0.397 | 0.181 |
| Skewness | 0.868 | 0.187 | 0.280 | 0.748 | 0.145 | 0.149 | -0.116 | 0.347 | -0.063 |
| Kurtosis | -0.422 | -1.472 | 0.452 | 0.617 | -0.669 | -0.447 | -0.169 | -1.374 | -0.788 |
| KS test (p value) | 0.504 | 0.829 | 0.801 | 0.818 | 0.995 | 0.997 | 0.638 | 0.347 | 0.861 |

Abbreviations: Ct.Po – cortical porosity; Po.Dm – cortical pore diameter; Ct.Th – cortical thickness; LN – lateral part of the femoral neck; MN – medial part of femoral neck; IT – inter-trochanteric region; CV – coefficient of variation; KS test – Kolmogorov-Smirnov test;

**Table 13** Cortical micro-architectural parameters in three regions of proximal femora obtained from control donors: Test for data distribution normality

| | **Ct.Po** (%) | | | **Po.Dm** (μm) | | | **Ct.Th** (mm) | | |
|---|---|---|---|---|---|---|---|---|---|
| Femoral region | **LN** | **MN** | **IT** | **LN** | **MN** | **IT** | **LN** | **MN** | **IT** |
| CV | 0.321 | 0.321 | 0.297 | 0.164 | 0.245 | 0.209 | 0.183 | 0.216 | 0.182 |
| Skewness | 0.218 | 0.412 | 0.181 | -0.506 | 0.693 | -0.552 | 0.184 | 0.036 | 0.261 |
| Kurtosis | -1.078 | 1.056 | 0.469 | -0.590 | -0.248 | -0.107 | 0.984 | 0.241 | -0.249 |
| KS test (p value) | 0.924 | 0.897 | 0.955 | 0.388 | 0.251 | 0.810 | 0.787 | 0.943 | 0.979 |

Abbreviations: Ct.Po – cortical porosity; Po.Dm – cortical pore diameter; Ct.Th – cortical thickness; LN – lateral part of the femoral neck; MN – medial part of the femoral neck; IT – inter-trochanteric region; CV – coefficient of variation; KS test – Kolmogorov-Smirnov test;

Our data revealed statistically significant ALD-induced trabecular bone loss in investigated regions of proximal femora, illustrated by lower trabecular bone volume fraction (group p=0.002, ANOVA for repeated measurements, Table 14), decreased trabecular number and increased trabecular separation (group p<0.001, ANOVA for repeated measurements, Table 14), in comparison to healthy control men. Moreover, ALD-induced microstructural deterioration of femoral cortical compartment was illustrated in significant cortical porosity and cortical pore diameter increase (group p<0.001, repeated measures ANOVA, Figure 14), accompanied with cortical thickness and pore separation reduction (p=0.011, p=0.055 vs. control, repeated measures ANOVA, Table 14). Most preserved cortical and trabecular micro-architecture was noted in the medial part of femoral neck, while most significant ALD-associated difference was noted in inter-trochanteric region (Figure 14). Namely, significant deterioration trend was observed in trabecular bone volume fraction, trabecular number and cortical thickness of inter-trochanteric region when compared to medial and lateral part of the femoral neck (p<0.001, repeated measures ANOVA with Bonferroni post hoc).

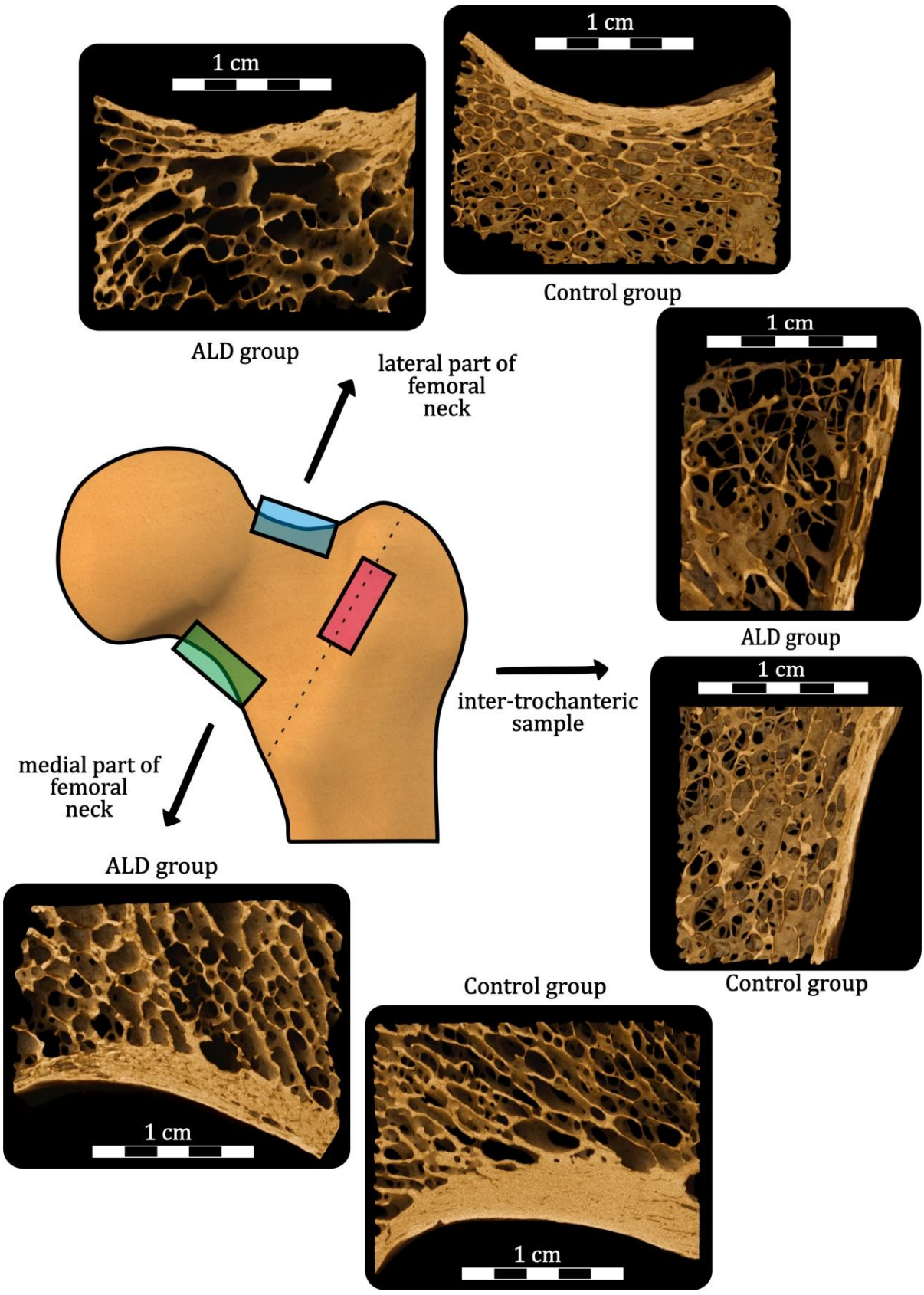


**Figure 14. The comparison of a representative 3D model of femoral bone samples obtained from healthy control and donor with alcoholic liver disease.**

Note significant cortical and trabecular micro-architectural deterioration in the investigated regions of the proximal femora, with particular accent on inter-trochanteric region of ALD men.

In addition, interaction of ALD-associated effect and assessed femoral region showed pronounced difference for trabecular number (site*group p=0.059), trabecular bone pattern factor (site*group p=0.058), cortical porosity (site*group p=0.029) and pore diameter (site*group p=0.047, ANOVA for repeated measurements, Table 14), reflecting trend to less numbered and poorly connected trabeculae, in combination with more porous cortex in inter-trochanteric region than in two femoral neck regions, predominantly observed in ALD men (Table 14). On the other side, alteration of trabecular thickness, structure model index and fractal dimension failed to reach statistical significance between ALD and control group in any of the assessed femoral regions (p>0.05, repeated measures ANOVA, Table 14).

**Table 14. Micro-architectural parameters of analyzed sub-regions in proximal femora collected from individuals with alcoholic liver disease and healthy age-matched control men**

| | Femoral region | ALD group (Mean ± SD) | Control group (Mean ± SD) | P value |
|---|---|---|---|---|
| **Ct.Po** (%) | LN | 26.685±8.146 | 17.758±5.697 | Group **p<0.001** |
| | MN | 14.183±6.240 | 8.201±2.636 | Site **p<0.001** |
| | IT | 32.801±8.589 | 20.188±6.007 | Site*Group **p=0.029** |
| **Po.Dm** (µm) | LN | 242.31±60.9 | 221.0±36.2 | Group **p<0.001** |
| | MN | 207.9±43.5 | 176.9±43.3 | Site **p<0.001** |
| | IT | 213.8±49.8 | 142.0±29.7 | Site*Group **p=0.047** |
| **Po.Sp** (µm) | LN | 274.1±32.3 | 294.9±26.4 | Group p=0.055 |
| | MN | 353.5±86.3 | 383.4±52.8 | Site **p<0.001** |
| | IT | 251.1±35.1 | 271.5±29.4 | Site*Group p=0.918 |
| **Ct.Th** (mm) | LN | 2.710±0.680 | 3.221±0.589 | Group **p=0.011** |
| | MN | 4.931±1.961 | 6.061±1.306 | Site **p<0.001** |
| | IT | 2.172±0.393 | 2.531±0.462 | Site*Group p=0.347 |
| **BV/TV** (%) | LN | 13.950±2.655 | 18.313±3.943 | Group **p=0.002** |
| | MN | 19.204±3.455 | 22.746±5.818 | Site **p<0.001** |
| | IT | 10.358±2.607 | 12.907±2.855 | Site*Group p=0.153 |
| **Tb.Th** (µm) | LN | 171.5±31.9 | 175.3±25.4 | Group p=0.596 |
| | MN | 206.8±35.9 | 226.4±29.6 | Site **p<0.001** |
| | IT | 152.0±27.9 | 138.8±14.2 | Site*Group p=0.105 |
| **Tb.N** (1/mm) | LN | 0.836±0.116 | 1.030±0.102 | Group **p<0.001** |
| | MN | 0.920±0.140 | 0.984±0.204 | Site **p<0.001** |
| | IT | 0.682±0.119 | 0.927±0.165 | Site*Group p=0.059 |
| **Tb.Sp** (µm) | LN | 938.1±84.5 | 830.1±85.9 | Group **p<0.001** |
| | MN | 858.5±84.2 | 816.4±132.2 | Site p=0.084 |
| | IT | 955.6±146.2 | 779.2±89.0 | Site*Group p=0.255 |
| **TbPf** (dimensionless) | LN | 2.670±1.475 | 2.682±1.146 | Group p=0.872 |
| | MN | 0.826±1.434 | 1.769±2.527 | Site **p<0.001** |
| | IT | 5.095±2.560 | 4.363±1.517 | Site*Group p=0.058 |
| **SMI** (dimensionless) | LN | 1.049±0.374 | 1.079±0.310 | Group p=0.907 |
| | MN | 0.699±0.458 | 0.953±0.754 | Site **p<0.001** |
| | IT | 1.521±0.408 | 1.197±0.267 | Site*Group **p=0.012** |
| **FD** (dimensionless) | LN | 2.346±0.052 | 2.362±0.065 | Group p=0.411 |
| | MN | 2.395±0.058 | 2.398±0.087 | Site **p<0.001** |
| | IT | 2.276±0.089 | 2.307±0.088 | Site*Group p=0.753 |

Abbreviations: Ct. Po – cortical porosity; Po.Dm – cortical pore diameter; Po.Sp – cortical pore separation; Ct.Th – cortical thickness; BV/TV – bone volume fraction; Tb.Th – trabecular thickness; Tb.N – trabecular number; Tb.Sp – trabecular separation; TbPf – trabecular bone pattern factor; SMI – structure model index; FD – fractal dimension; LN – lateral part of the femoral neck; MN – medial part of the femoral neck; IT – inter-trochanteric region;

Statistical analysis of the differences in micro-architectural bone parameters between the investigated site, investigated groups and their interaction (site*group) was performed using analysis of variance (ANOVA) for repeated measurements with Bonferroni post-hoc test (significant difference is given in bold).

*4.6. The comparison of microstructural changes in different regions of proximal femora obtained from end-stage and initial-stage of alcoholic liver disease*

In order to assess the potential negative effect of various ALD stages on femoral bone, individuals were subdivided into: ALC group (n=7; age=56±13 years), FLD group (n=6; age=59±15 years) and control group (n=20; age=54±13 years).

As presented in Table 15-20, parameters of femoral micro-architecture showed normal distribution in donors with various ALD stages and control group, while Levene's test confirmed homogeneity of the variance of the presented data (p>0.05).

**Table 15.** Trabecular micro-architectural parameters in three regions of proximal femora obtained from ALC donors: Test for data distribution normality

| | **BV/TV** (%) | | | **Tb.Th** (μm) | | | **Tb.N** (1/mm) | | |
|---|---|---|---|---|---|---|---|---|---|
| Femoral region | **LN** | **MN** | **IT** | **LN** | **MN** | **IT** | **LN** | **MN** | **IT** |
| CV | 0.161 | 0.212 | 0.260 | 0.146 | 0.107 | 0.211 | 0.116 | 0.160 | 0.129 |
| Skewness | -0.964 | 0.518 | 0.108 | -0.074 | -0.126 | 0.506 | -0.412 | 1.619 | -0.936 |
| Kurtosis | 1.780 | -1.373 | -2.035 | -0.788 | -1.627 | -1.162 | -0.978 | 2.420 | 1.828 |
| KS test (p value) | 0.734 | 0.910 | 0.670 | 0.998 | 0.978 | 0.955 | 0.987 | 0.540 | 0.742 |

Abbreviations: BV/TV – trabecular bone volume fraction; Tb.Th – trabecular thickness, Tb.N – trabecular number; LN – lateral part of the femoral neck; MN – medial part of the femoral neck; IT – inter-trochanteric region; CV – coefficient of variation; KS test – Kolmogorov-Smirnov test;

**Table 16.** Trabecular micro-architectural parameters in three regions of proximal femora obtained from FLD donors: Test for data distribution normality

| | **BV/TV** (%) | | | **Tb.Th** (μm) | | | **Tb.N** (1/mm) | | |
|---|---|---|---|---|---|---|---|---|---|
| Femoral region | **LN** | **MN** | **IT** | **N** | **MN** | **IT** | **LN** | **MN** | **IT** |
| CV | 0.169 | 0.087 | 0.257 | 0.125 | 0.124 | 0.143 | 0.085 | 0.153 | 0.229 |
| Skewness | 1.262 | 0.164 | 0.582 | 0.481 | 0.353 | 0.921 | -0.165 | 0.264 | 0.241 |
| Kurtosis | 0.138 | -1.765 | -1.059 | -0.598 | -1.480 | -1.329 | 1.520 | -1.014 | -0.648 |
| KS test (p value) | 0.369 | 0.863 | 0.696 | 0.960 | 0.991 | 0.344 | 0.839 | 0.802 | 0.936 |

Abbreviations: BV/TV – trabecular bone volume fraction; Tb.Th – trabecular thickness, Tb.N – trabecular number; LN – lateral part of femoral neck; MN – medial part of femoral neck; IT – inter-trochanteric region; CV– coefficient of variation; KS test – Kolmogorov-Smirnov test;

**Table 17.** Trabecular micro-architectural parameters in three regions of proximal femora obtained from control donors: Test for data distribution normality

| | **BV/TV** (%) | | | **Tb.Th** (μm) | | | **Tb.N** (1/mm) | | |
|---|---|---|---|---|---|---|---|---|---|
| Femoral region | **LN** | **MN** | **IT** | **LN** | **MN** | **IT** | **LN** | **MN** | **IT** |
| CV | 0.215 | 0.255 | 0.221 | 0.145 | 0.130 | 0.103 | 0.099 | 0.207 | 0.178 |
| Skewness | 1.935 | 0.329 | 0.368 | 0.714 | 0.342 | -0.223 | 0.298 | -0.196 | -0.014 |
| Kurtosis | 4.951 | 0.406 | -0.320 | 2.928 | -0.219 | 0.048 | -0.222 | 0.364 | -0.664 |
| KS test (p value) | 0.262 | 0.916 | 0.979 | 0.547 | 0.792 | 0.500 | 0.974 | 0.995 | 0.928 |

Abbreviations: BV/TV – trabecular bone volume fraction; Tb.Th – trabecular thickness, Tb.N – trabecular number; LN – lateral part of the femoral neck; MN – medial part of the femoral neck; IT – inter-trochanteric region; CV – coefficient of variation; KS test – Kolmogorov-Smirnov test;

**Table 18.** Cortical micro-architectural parameters in three regions of proximal femora obtained from ALC donors: Test for data distribution normality

| | **Ct.Po** (%) | | | **Po.Dm** (μm) | | | **Ct.Th** (mm) | | |
|---|---|---|---|---|---|---|---|---|---|
| Femoral region | **LN** | **MN** | **IT** | **LN** | **MN** | **IT** | **LN** | **MN** | **IT** |
| CV | 0.341 | 0.385 | 0.338 | 0.292 | 0.171 | 0.272 | 0.247 | 0.378 | 0.231 |
| Skewness | 0.391 | -0.126 | 0.052 | 1.061 | -0.511 | -0.747 | -0.323 | 1.364 | -0.045 |
| Kurtosis | -1.878 | -1.499 | -0.678 | 1.949 | -0.768 | -0.457 | -2.478 | 1.191 | -1.677 |
| KS test (p value) | 0.933 | 0.994 | 0.926 | 0.594 | 0.991 | 0.730 | 0.693 | 0308 | 0.938 |

Abbreviations: Ct. Po – cortical porosity; Po.Dm – cortical pore diameter; Ct.Th – cortical thickness; LN – lateral part of the femoral neck; MN – medial part of the femoral neck; IT – inter-trochanteric region; CV – coefficient of variation; KS test – Kolmogorov-Smirnov test;

**Table 19.** Cortical micro-architectural parameters in three regions of proximal femora obtained from FLD donors: Test for data distribution normality

| | **Ct.Po** (%) | | | **Po.Dm** (μm) | | | **Ct.Th** (mm) | | |
|---|---|---|---|---|---|---|---|---|---|
| Femoral region | **LN** | **MN** | **IT** | **LN** | **MN** | **IT** | **LN** | **MN** | **IT** |
| CV | 0.218 | 0.512 | 0146 | 0.222 | 0.207 | 0.115 | 0.166 | 0.289 | 0.122 |
| Skewness | 0.822 | 0.742 | 0.644 | 0.149 | -0.523 | 0.369 | 0.407 | -0.701 | 1.002 |
| Kurtosis | 0.645 | -0.869 | -0.363 | -1.731 | -0.963 | 0.324 | 0.061 | 0.141 | -1.109 |
| KS test (p value) | 0.966 | 0.828 | 0.997 | 0.957 | 0.848 | 0.993 | 0.860 | 0.976 | 0.450 |

Abbreviations: Ct.Po – cortical porosity; Po.Dm – cortical pore diameter; Ct.Th – cortical thickness; LN – lateral part of the femoral neck; MN – medial part of the femoral neck; IT – inter-trochanteric region; CV – coefficient of variation; KS test – Kolmogorov-Smirnov test;

**Table 20.** Cortical micro-architectural parameters in three regions of proximal femora obtained from control donors: Test for data distribution normality

| | **Ct.Po** (%) | | | **Po.Dm** (μm) | | | **Ct.Th** (mm) | | |
|---|---|---|---|---|---|---|---|---|---|
| Femoral region | **LN** | **MN** | **IT** | **LN** | **MN** | **IT** | **LN** | **MN** | **IT** |
| CV | 0.321 | 0.321 | 0.297 | 0.164 | 0.245 | 0.209 | 0.183 | 0.216 | 0.182 |
| Skewness | 0.218 | 0.412 | 0.181 | -0.506 | 0.693 | -0.552 | 0.184 | 0.036 | 0.261 |
| Kurtosis | -1.078 | 1.056 | 0.469 | -0.590 | -0.248 | -0.107 | 0.984 | 0.241 | -0.249 |
| KS test (p value) | 0.924 | 0.897 | 0.955 | 0.388 | 0.251 | 0.810 | 0.787 | 0.943 | 0.979 |

Abbreviations: Ct.Po – cortical porosity; Po.Dm – cortical pore diameter; Ct.Th – cortical thickness; LN – lateral part of the femoral neck; MN – medial part of the femoral neck; IT – inter-trochanteric region; CV – coefficient of variation; KS test – Kolmogorov-Smirnov test;

We observed minor microstructural alteration in inter-trochanteric region of FLD donors illustrated in higher values of cortical porosity, pore diameter and trabecular separation, in combination with decreased trabecular number, when compared to control individuals (group $p<0.05$, repeated measures ANOVA with Bonferroni correction, Table 21).

**Table 21. Femoral micro-architectural changes of healthy individuals in comparison with donors suffering from alcoholic liver cirrhosis and fatty liver disease**

| | Femoral region | ALC group (Mean ± SD) | FLD group (Mean ± SD) | Control group (Mean ± SD) | P value |
|---|---|---|---|---|---|
| **Ct.Po** (%) | LN | 28.876±9.864 | 24.129±5.273 | 17.757±5.696 | Group **p<0.001** |
| | MN | 15.958±6.149 | 12.111±6.207 | 8.200±2.636 | Site **p<0.001** |
| | IT | 33.454±11.323 | 32.040±4.680 | 20.188±6.007 | Site*Group p=0.109 |
| **Po.Dm** (μm) | LN | 242.9±70.9 | 241.7±53.6 | 221.0±36.2 | Group **p=0.001** |
| | MN | 189.7±32.6 | 229.2±47.5 | 176.9±43.3 | Site **p=0.002** |
| | IT | 229.3±62.6 | 195.7±22.6 | 142.0±29.7 | Site*Group **p=0.022** |
| **Po.Sp** (μm) | LN | 253.1±29.1# | 298.5±12.7 | 294.9±26.4 | Group **p=0.001** |
| | MN | 302.4±53.5 # | 413.2±68.3 | 383.4±52.8 | Site **p<0.001** |
| | INTT | 244.7±43.6 | 258.5±23.6 | 271.5±29.4 | Site*Group **p=0.047** |
| **Ct.Th** (mm) | LN | 2.329±0.574# | 3.154±0.523 | 3.221±0.589 | Group **p=0.001** |
| | MN | 3.859±1.460 | 6.181±1.784 | 6.061±1.306 | Site **p<0.001** |
| | IT | 2.147±0.497 | 2.201±0.268 | 2.531±0.462 | Site*Group **p=0.006** |
| **BV/TV** (%) | LN | 12.597±2.034*** | 15.529±2.530 | 18.313±3.943 | Group **p=0.005** |
| | MN | 17.506±3.711* | 21.186±1.836 | 22.746±5.818 | Site **p<0.001** |
| | INTT | 10.749±2.792 | 9.901±2.549* | 12.907±2.855 | Site*Group p=0.183 |
| **Tb.Th** (μm) | LN | 151.1±22.1 | 195.3±24.3* | 175.3±25.4 | Group **p=0.011** |
| | MN | 182.6±19.4***## | 235.2±29.4 | 226.4±29.6 | Site **p<0.001** |
| | IT | 158.7±33.3 | 144.2±20.1 | 138.8±14.2 | Site*Group **p=0.002** |
| **Tb.N** (1/mm) | LN | 0.906±0.105*# | 0.754±0.064*** | 1.030±0.102 | Group **p<0.001** |
| | MN | 0.940±0.150 | 0.897±0.137 | 0.984±0.204 | Site **p<0.001** |
| | IT | 0.675±0.087*** | 0.689±0.158*** | 0.927±0.165 | Site*Group **p=0.041** |
| **Tb.Sp** (mm) | LN | 0.907±0.093 | 0.974±0.062*** | 830.1±85.9 | Group **p=0.050** |
| | MN | 0.847±0.0874 | 0.872±0.086 | 816.4±132.2 | Site **p=0.001** |
| | IT | 0.968±0.124*** | 0.941±0.179* | 779.2±89.0 | Site*Group p=0.110 |
| **TbPf** (dimensionless) | LN | 2.757±1.426 | 2.569±1.663 | 2.682±1.146 | Group p=0.897 |
| | MN | 1.276±1.428 | 0.302±1.369 | 1.769±2.527 | Site **p<0.001** |
| | IT | 4.999±3.319 | 5.207±1.649 | 4.363±1.517 | Site*Group p=0.517 |
| **SMI** (dimensionless) | LN | 0.964±0.294 | 1.418±0.459 | 1.079±0.310 | Group p=0.979 |
| | MN | 0.763±0.338 | 0.624±0.595 | 0.953±0.754 | Site **p<0.001** |
| | IT | 1.501±0.454 | 1.544±0.389 | 1.197±0.267 | Site*Group **p=0.047** |
| **FD** (dimensionless) | LN | 2.370±0.056 | 2.318±0.032 | 2.362±0.065 | Group p=0.537 |
| | MN | 2.386±0.069 | 2.405±0.045 | 2.398±0.087 | Site **p<0.001** |
| | IT | 2.294±0.082 | 2.255±0.100 | 2.307±0.088 | Site*Group p=0.531 |

Abbreviations: Ct.Po – cortical porosity; Po.Dm – cortical pore diameter; Po.Sp – cortical pore separation; Ct.Th – cortical thickness; BV/TV – bone volume fraction; Tb.Th – trabecular thickness; Tb.N – trabecular number; Tb.Sp – trabecular separation; LN – lateral part of the femoral neck; MN – medial part of the femoral neck; IT – inter-trochanteric region;

Statistical analysis of the inter-group differences (group), site-specific differences in micro-architectural bone parameters between investigated groups (site) and their interaction (site*group) was performed using ANOVA for repeated measurements with Bonferroni post-hoc test (bold font indicate significant difference). Repeated measures ANOVA with Bonferroni correction was performed to estimate the differences in microstructural parameters between donors with two ALD stages - alcoholic liver cirrhosis and fatty liver disease and control group (* p<0.05, *** p<0.01 vs. control; # p<0.05, ### p<0.01 vs. FLD group).

At the same time, our data suggested even more severe deterioration in femoral micro-architecture in the inter-trochanteric region of ALC donors (Figure 15). Additionally, bone deterioration illustrated in cortical thickness, pore separation changes in the lateral part of femoral neck, combined with changes in trabecular thickness and pore separation in the medial part of femoral neck, was observed in ALC donors when compared to FLD group (group $p<0.05$, repeated measures ANOVA with Bonferroni correction, Table 21). Other femoral microstructural parameters were not significantly altered between ALC and FLD donors (group $p>0.05$, repeated measures ANOVA with Bonferroni correction, Table 21).

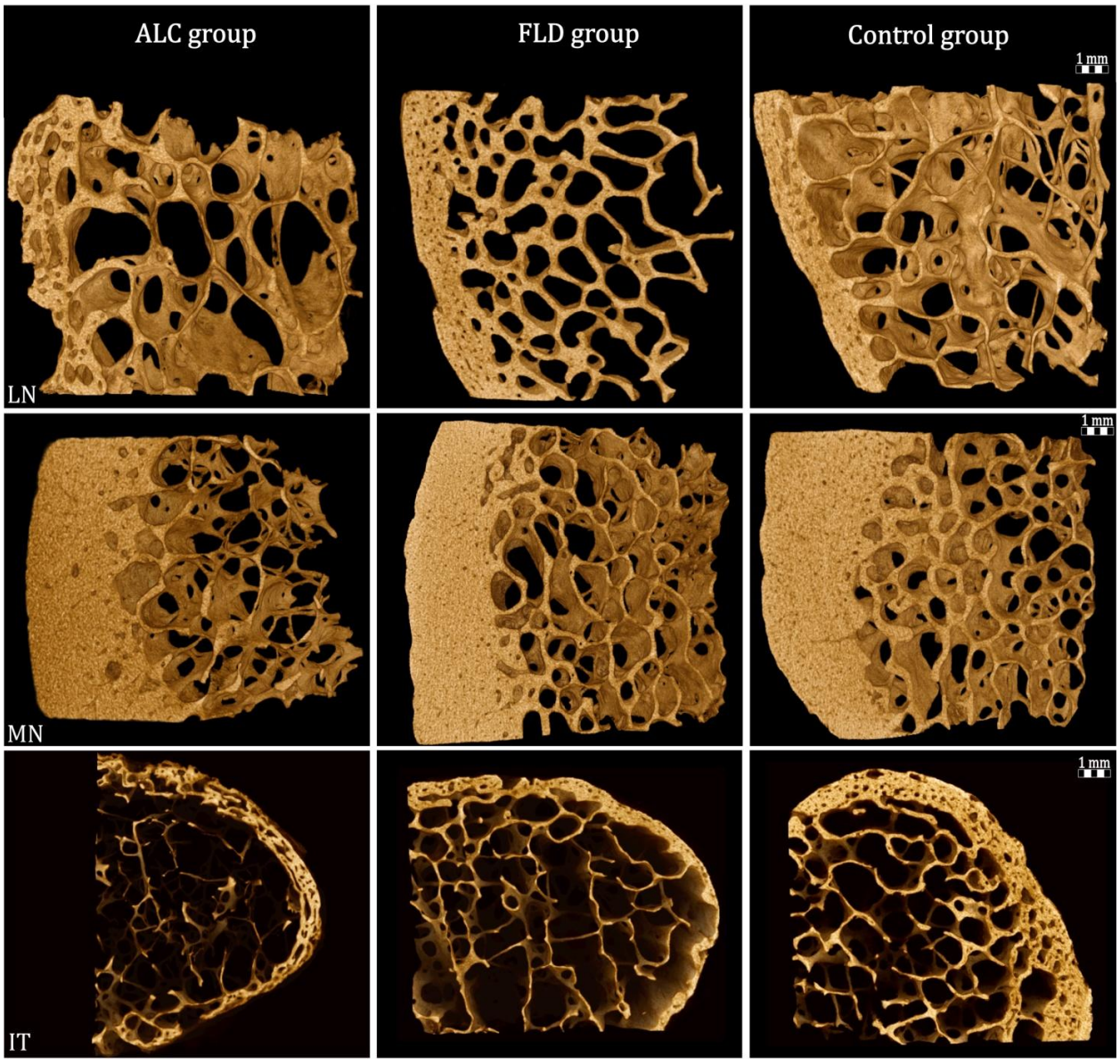


**Figure 15. The comparison of a representative transversal cross-section of femoral bone samples obtained from donors with various ALD stages.**

Note more pronounced cortical and trabecular micro-architectural deterioration in the investigated regions of the proximal femora collected from ALC individuals, with particular accent on inter-trochanteric region.

### *4.7. The changes in mechanical properties of femoral bone samples obtained from donors with alcoholic liver disease*

During this study we analyzed cortical Vickers micro-hardness of the three femoral regions sampled from the ALD men and healthy age-matched individuals. Additionally, to assess the effect of ALD stage, we analyzed cortical Vickers micro-hardness of the three femoral regions sampled from the individuals divided into ALC, FLD and control group.

As shown on Table 22-25, our data showed normal distribution, while Levene's test confirmed homogeneity of the variance of presented results ($p>0.05$) (Table 22-25).

**Table 22.** Vickers micro-hardness in three regions of proximal femora obtained from ALD donors: Test for data distribution normality

| | **Ct.VH of LN sample** ($kgf/mm^2$) | **Ct.VH of MN sample** ($kgf/mm^2$) | **Ct.VH of IT sample** ($kgf/mm^2$) |
|---|---|---|---|
| CV | 0.079 | 0.094 | 0.085 |
| Skewness | 0.485 | -0.296 | -0.294 |
| Kurtosis | 0.178 | -0.432 | 1.030 |
| KS test (p value) | 0.908 | 0.945 | 0.666 |

Abbreviations: Ct.VH – Vickers hardness value of the cortical bone; LN – lateral part of the femoral neck; MN – medial part of the femoral neck; IT – inter-trochanteric region; CV – coefficient of variation; KS test – Kolmogorov-Smirnov test;

**Table 23.** Vickers micro-hardness in three regions of proximal femora obtained from ALC donors: Test for data distribution normality

| | **Ct.VH of LN sample** ($kgf/mm^2$) | **Ct.VH of MN sample** ($kgf/mm^2$) | **Ct.VH of IT sample** ($kgf/mm^2$) |
|---|---|---|---|
| CV | 0.059 | 0.088 | 0.108 |
| Skewness | 0.006 | -0.373 | -0.142 |
| Kurtosis | -2.256 | -0.348 | 0.121 |
| KS test (p value) | 0.831 | 0.999 | 0.914 |

Abbreviations: Ct.VH – Vickers hardness value of the cortical bone; LN – lateral part of the femoral neck; MN – medial part of the femoral neck; IT – inter-trochanteric region; CV – coefficient of variation; KS test – Kolmogorov-Smirnov test;

**Table 24.** Vickers micro-hardness in three regions of proximal femora obtained from FLD donors: Test for data distribution normality

| | **Ct.VH of LN sample** (kgf/mm²) | **Ct.VH of MN sample** (kgf/mm²) | **Ct.VH of IT sample** (kgf/mm²) |
|---|---|---|---|
| CV | 0.105 | 0.089 | 0.108 |
| Skewness | 0.740 | -0.914 | -0.142 |
| Kurtosis | 0.117 | 1.870 | 0.121 |
| KS test (p value) | 0.998 | 0.758 | 0.914 |

Abbreviations: Ct.VH – Vickers hardness value of the cortical bone; LN – lateral part of the femoral neck, MN – medial part of the femoral neck; IT – inter-trochanteric region; CV – coefficient of variation; KS test – Kolmogorov-Smirnov test;

**Table 25.** Vickers micro-hardness in three regions of proximal femora obtained from control donors: Test for data distribution normality

| | **Ct.VH of LN sample** (kgf/mm²) | **Ct.VH of MN sample** (kgf/mm²) | **Ct.VH of IT sample** (kgf/mm²) |
|---|---|---|---|
| CV | 0.078 | 0.087 | 0.103 |
| Skewness | -0.444 | -0.497 | 0.451 |
| Kurtosis | -0.341 | 2.086 | -0.952 |
| KS test (p value) | 0.753 | 0.259 | 0.470 |

Abbreviations: Ct.VH – Vickers hardness value of the cortical bone; LN – lateral part of the femoral neck, MN – medial part of the femoral neck; IT – inter-trochanteric region; CV – coefficient of variation; KS test – Kolmogorov-Smirnov test;

As presented in Figure 16, significant ALD-induced reduction in cortical Vickers micro-hardness values was noted in cortical shell of all three assessed femoral regions ($p<0.001$ vs. control, Figure 16).

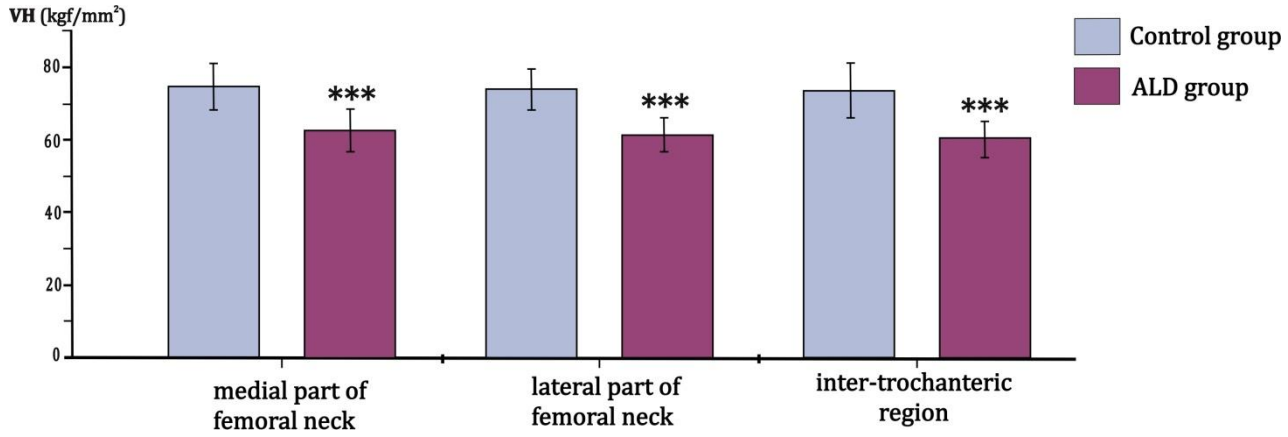


**Figure 16. The ALD-induced changes in mechanical properties of femoral bone samples**

Abbreviations: VH – Vickers hardness value of cortical bone; ALD – alcoholic liver disease;
Statistical analysis of the differences in Vickers hardness number between the investigated site, investigated groups and their interaction (site*group) was performed using analysis of variance (ANOVA) for repeated measurements (*** $p<0.05$ vs. control).

However, we did not find any region-specific significant difference in Vickers micro-hardness of investigated femoral samples either in ALD, or in control group (site p=0.476, ANOVA for repeated measurements, Figure 16). Additionally, our data suggested significant reduction in cortical Vickers micro-hardness in all three investigated regions of FLD and ALC donors (p<0.05 vs. control, ANOVA for repeated measurements, Figure 14). Still, cortical micro-hardness was not significantly different between donors with initial and end-stage of ALD (p>0.05, ANOVA for repeated measurements, Figure 17).

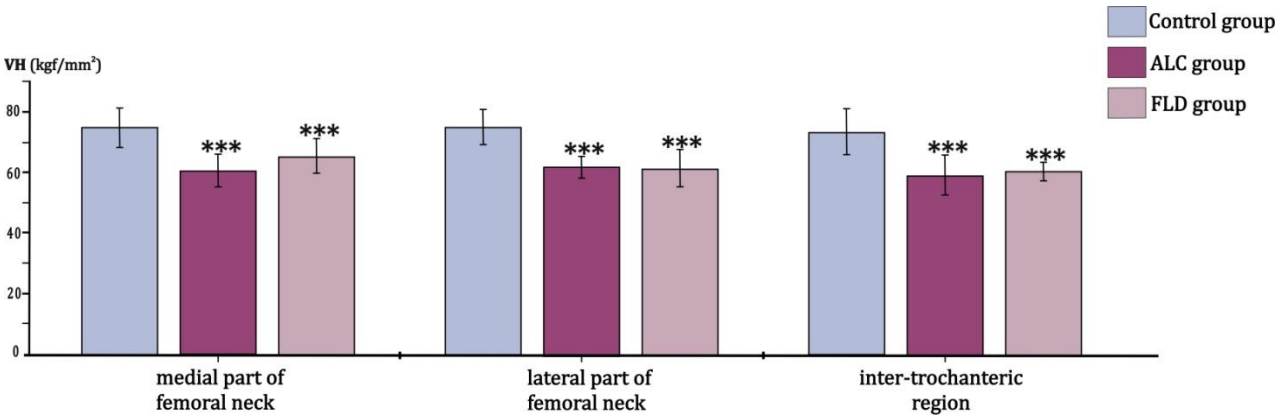


**Figure 17. The difference in mechanical properties of femoral bone samples between healthy men and donors with various stages of ALD (ALC and FLD)**

Abbreviations: VH – Vickers hardness value of cortical bone; ALC – alcoholic liver cirrhosis; FLD – fatty liver disease;
Statistical analysis of the differences in Vickers hardness number between the investigated site, investigated groups and their interaction (site*group) was performed using analysis of variance (ANOVA) for repeated measurements (*** p<0.05 vs. control).

### *4.8. The changes in the expression of osteocyte-specific molecules in persons with alcoholic and non-alcoholic end-stage CLD*

Following the micro-architectural assessment, in this study was analyzed the expression of osteocyte-specific molecules (Cx43 and sclerostin) in the lumbar vertebrae collected from 55 cadaveric donors divided into the ALC group, non-ALC group and control group. Additionally, the comparison of osteocytic network was done in lumbar vertebrae obtained from individuals with alcoholic end-stage CLD, non-alcoholic (cardiac) end-stage CLD and control group.

As presented in Table 26-28, our data complied with the normal distribution, while Levene's test confirmed homogeneity of the variance of presented data (p>0.05).

**Table 26.** The expression of osteocyte-specific molecules in lumbar vertebrae samples obtained from ALC donors: Test for data distribution normality

| | **Positive cells per bone area** (n/mm²) | | **Negative cells per bone area** (n/mm²) | | **Total lacunae number per bone area** (n/mm²) |
|---|---|---|---|---|---|
| | **Cx43** | **Sclerostin** | **Cx43** | **Sclerostin** | |
| CV | 0.428 | 0.344 | 0.334 | 0.769 | 0.289 |
| Skewness | 1.104 | 0.858 | 0.892 | 1.521 | 1.104 |
| Kurtosis | 1.338 | 1.061 | 0.700 | 1.076 | 0.779 |
| KS test (p value) | 0.363 | 0.361 | 0.835 | 0.074 | 0.664 |

Abbreviations: Cx43 – Connexin 43; CV – coefficient of variation; KS test – Kolmogorov-Smirnov test;

**Table 27.** The expression of osteocyte-specific molecules in lumbar vertebrae samples obtained from non-ALC donors: Test for data distribution normality

| | **Positive cells per bone area** (n/mm²) | | **Negative cells per bone area** (n/mm²) | | **Total lacunae number per bone area** (n/mm²) |
|---|---|---|---|---|---|
| | **Cx43** | **Sclerostin** | **Cx43** | **Sclerostin** | |
| CV | 0.343 | 0.510 | 0.278 | 0.299 | 0.282 |
| Skewness | 0.506 | 2.091 | -0.158 | 0.517 | 1.724 |
| Kurtosis | -0.834 | 4.119 | 0.230 | 0.970 | 4.388 |
| KS test (p value) | 0.579 | 0.159 | 0.839 | 0.990 | 0.843 |

Abbreviations: Cx43 – Connexin 43; CV – coefficient of variation; KS test – Kolmogorov-Smirnov test;

**Table 28.** The expression of osteocyte-specific molecules in lumbar vertebrae samples obtained from healthy donors: Test for data distribution normality

| | **Positive cells per bone area** (n/mm²) | | **Negative cells per bone area** (n/mm²) | | **Total lacunae number per bone area** (n/mm²) |
|---|---|---|---|---|---|
| | **Cx43** | **Sclerostin** | **Cx43** | **Sclerostin** | |
| CV | 0.378 | 0.373 | 0.409 | 0.586 | 0.462 |
| Skewness | -0.129 | 0.587 | 0.537 | 0.897 | 1.347 |
| Kurtosis | -1.191 | -0.275 | -0.619 | -0.421 | 1.797 |
| KS test (p value) | 0.893 | 0.983 | 0.094 | 0.172 | 0.855 |

Abbreviations: Cx43 – Connexin 43; CV – coefficient of variation; KS test – Kolmogorov-Smirnov test;

Significant reduction in osteocytic Cx43 expression, accompanied by the increased osteocytic sclerostin expression was observed in the lumbar vertebrae collected from donors with end-stage CLD of alcoholic and non-alcoholic origin (Figure 18 and Figure 19), when compared to healthy control individuals ($p<0.001$, one-way ANOVA with Bonferroni post hoc test , Table 29).

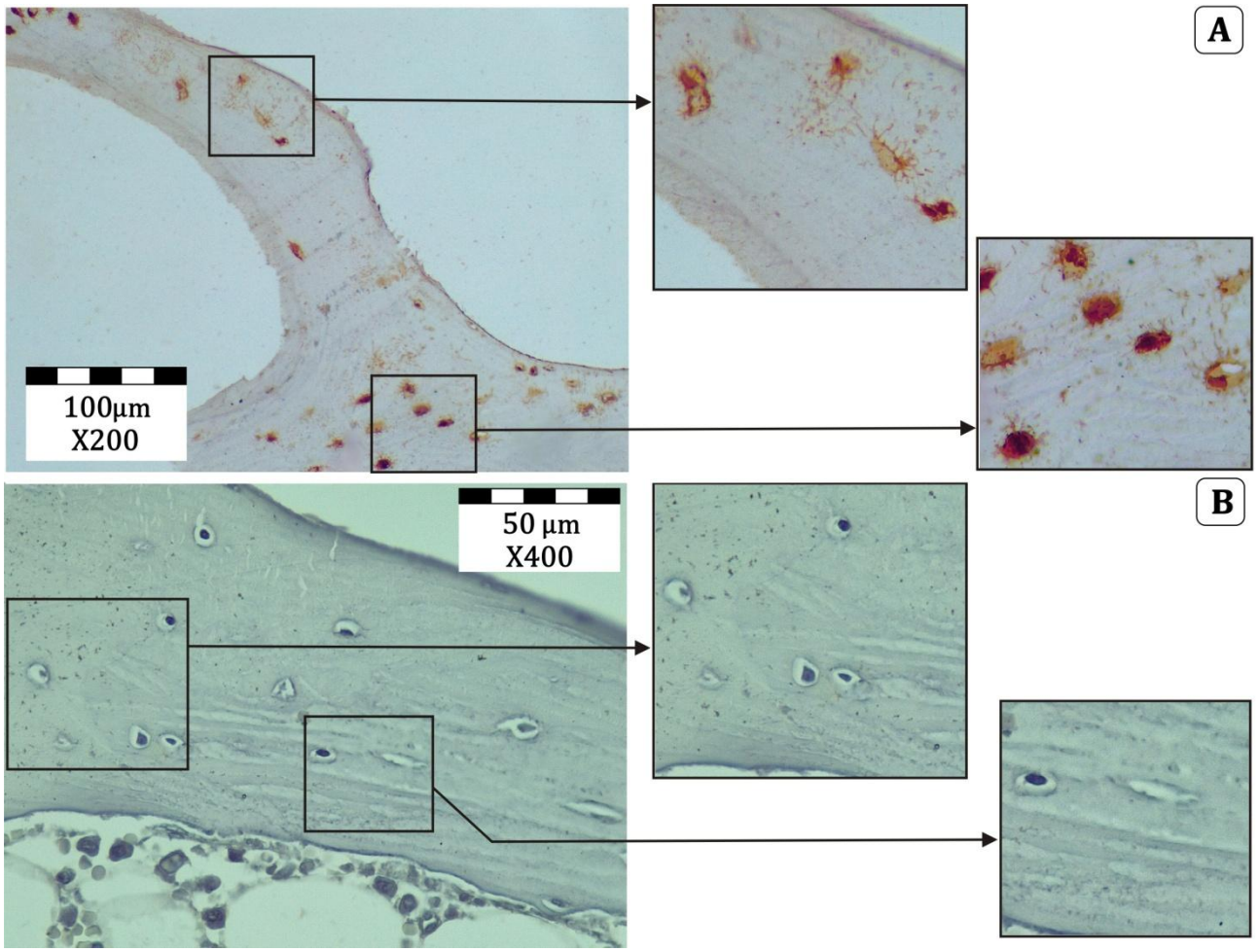


**Figure 18. Comparison of the representative vertebral immunohistochemistry findings in ALC and control group.**

Detail is showing the typical sclerostin positive (brown colored) and negative (blue colored) osteocytes in bone samples collected from ALC donor (a) and healthy control donor (b).

On the other side, total number of osteocytes per bone area was lower in non-ALC donors in comparison with ALC individuals. The difference in number of empty lacunas and the total number of osteocyte lacunas per vertebral bone area did not reach statistical significance between individuals of ALC, non-ALC and control group ($p>0.05$, one-way ANOVA with Bonferroni post hoc test ,Table 29).

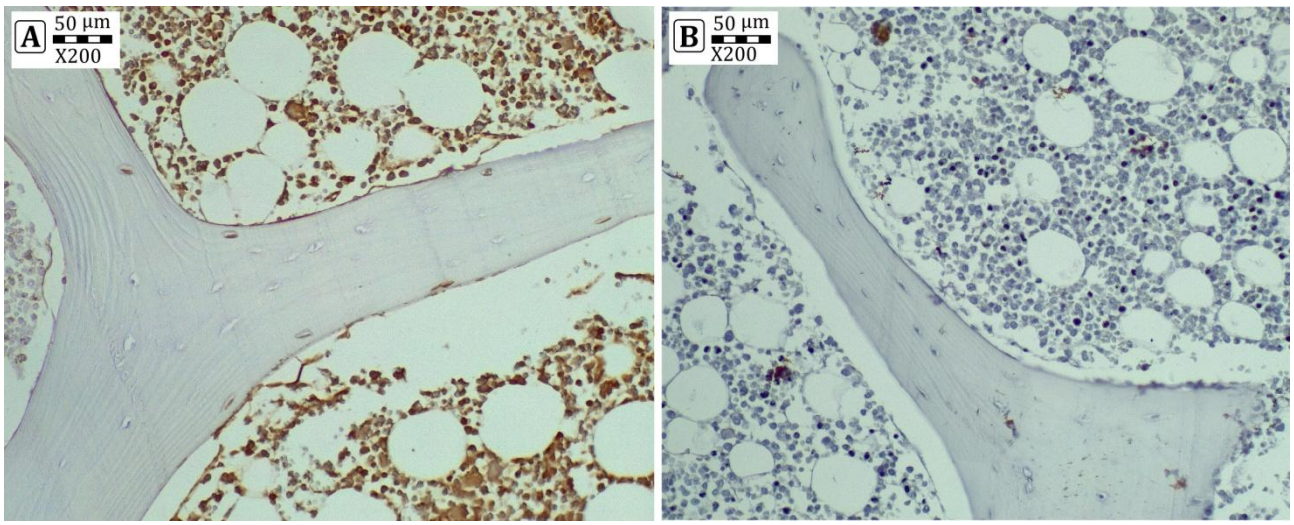


**Figure 19. Comparison of the representative immunohistochemistry findings in donor with non-alcoholic CLD and control group.**

Detail is showing the typical Cx43 positive (brown colored) and negative (blue colored) osteocytes in the trabecular compartment of the lumbar vertebrae obtained from healthy(a) and donor with non-ALC (b).

Still, the expression of Cx43 and sclerostin in osteocytic network of lumbar vertebrae was not significantly different between individuals with alcoholic and non-alcoholic (cardiac) end-stage CLD ($p>0.05$; one way ANOVA, Table 29), implying that alcoholic origin of the disease was not a crucial factor for bone deterioration noted in the same individuals.

**Table 29. Comparison of the immunohistochemistry findings in lumbar vertebrae collected from ALC, non-ALC and control group.**

| | **Control group** (Mean ± SD) | **Non-ALC group** (Mean ± SD) | **ALC group** (Mean ± SD) | ***P* value** |
|---|---|---|---|---|
| **Cx43 positive N.Ot/B.Ar** (n/ mm²) | 49±19 | 13±4 * | 17±7 * | ***p<0.001*** |
| **Cx43 negative N.Ot/B.Ar** (n/ mm²) | 76±31 | 87±40 | 119±40* # | ***p<0.001*** |
| **Sclerostin positive N.Ot/B.Ar** (n/ mm²) | 24±9 | 60±31 * | 56±19 * | ***p<0.001*** |
| **Sclerostin negative N.Ot/B.Ar** (n/ mm²) | 86±51 | 131±39 * | 63±48 # | ***p<0.001*** |
| **Tot.N.Ot/B.Ar** (n/ mm²) | 118±32 | 98±22 | 127±39 # | ***p=0.040*** |
| **N.Em.Lc/B.Ar** (n/ mm²) | 34±16 | 35±20 | 31±9 | *p>0.05* |
| **Tot.N.Lc/B.Ar** (n/ mm²) | 152±44 | 133±37 | 159±46 | *p>0.05* |

Abbreviations: Cx43 – Connexin 43; N.Ot/B.Ar – the number of osteocytes per bone area; Tot.N.Ot/B.Ar – the total number of osteocytes per bone area; N.Em.Lc/B.Ar – the number of empthy lacunae per bone area; Tot.N.Lc/B.Ar – total number of osteocyte lacunas per bone area;
Statistical significance was estimated using one-way ANOVA with Bonferroni post hoc test (* $p<0.05$ vs. control; # $p<0.05$ vs. non-ALC).

### *4.9. The assessment of osteocyte lacunar network in femoral bone sampled from individuals with end-stage alcoholic liver disease*

In this study, the assessment of osteocytic network was performed on the 17 femoral bone samples collected postmortem from men with ALC and 14 femoral bone samples collected postmortem from healthy control individuals.

As presented in Table 30 and Table 31, data complied with the normal distribution, while Levene's test confirmed homogeneity of the variance of presented data ($p>0.05$).

**Table 30.** The expression of osteocyte-specific molecules in femoral samples obtained from ALC donors: Test for data distribution normality

| | **Positive cells per bone area** (n/mm²) | | **Negative cells per bone area** (n/mm²) | | **Total lacunae number per bone area** (n/mm²) |
|---|---|---|---|---|---|
| | **Cx43** | **Sclerostin** | **Cx43** | **Sclerostin** | |
| CV | 0.399 | 0.369 | 0.511 | 0.392 | 0.374 |
| Skewness | 0.586 | 1.164 | 1.908 | 0.954 | 2.682 |
| Kurtosis | -0.408 | 1.829 | 4.241 | -0.579 | 8.617 |
| KS test (p value) | 0.857 | 0.882 | 0.360 | 0.094 | 0.495 |

Abbreviations: Cx43 – Connexin 43; CV – coefficient of variation; KS test – Kolmogorov-Smirnov test;

**Table 31.** The expression of osteocyte-specific molecules in femoral samples obtained from control donors: Test for data distribution normality

| | **Positive cells per bone area** (n/mm²) | | **Negative cells per bone area** (n/mm²) | | **Total lacunae number per bone area** (n/mm²) |
|---|---|---|---|---|---|
| | **Cx43** | **Sclerostin** | **Cx43** | **Sclerostin** | |
| CV | 0.425 | 0.379 | 0.506 | 0.342 | 0.212 |
| Skewness | 0.547 | 0.315 | 1.270 | 0.724 | 0.517 |
| Kurtosis | -0.718 | -0.729 | 2.052 | -0.431 | 0.236 |
| KS test (p value) | 0.975 | 0.824 | 0.704 | 0.419 | 0.400 |

Abbreviations: Cx43 – Connexin 43; CV – coefficient of variation; KS test – Kolmogorov-Smirnov test;

In femoral bone samples, we noted significant reduction in osteocytic Cx43 expression, in proximal femora collected from adult men with end-stage CLD of alcoholic origin, when compared to healthy age-matched control individuals ($p<0.05$, Student's *t* test; Figure 20). Moreover, we noted significantly higher osteocytic expression of sclerostin in femoral bone samples of ALC donors ($p<0.05$, Student's *t* test; Figure 20).

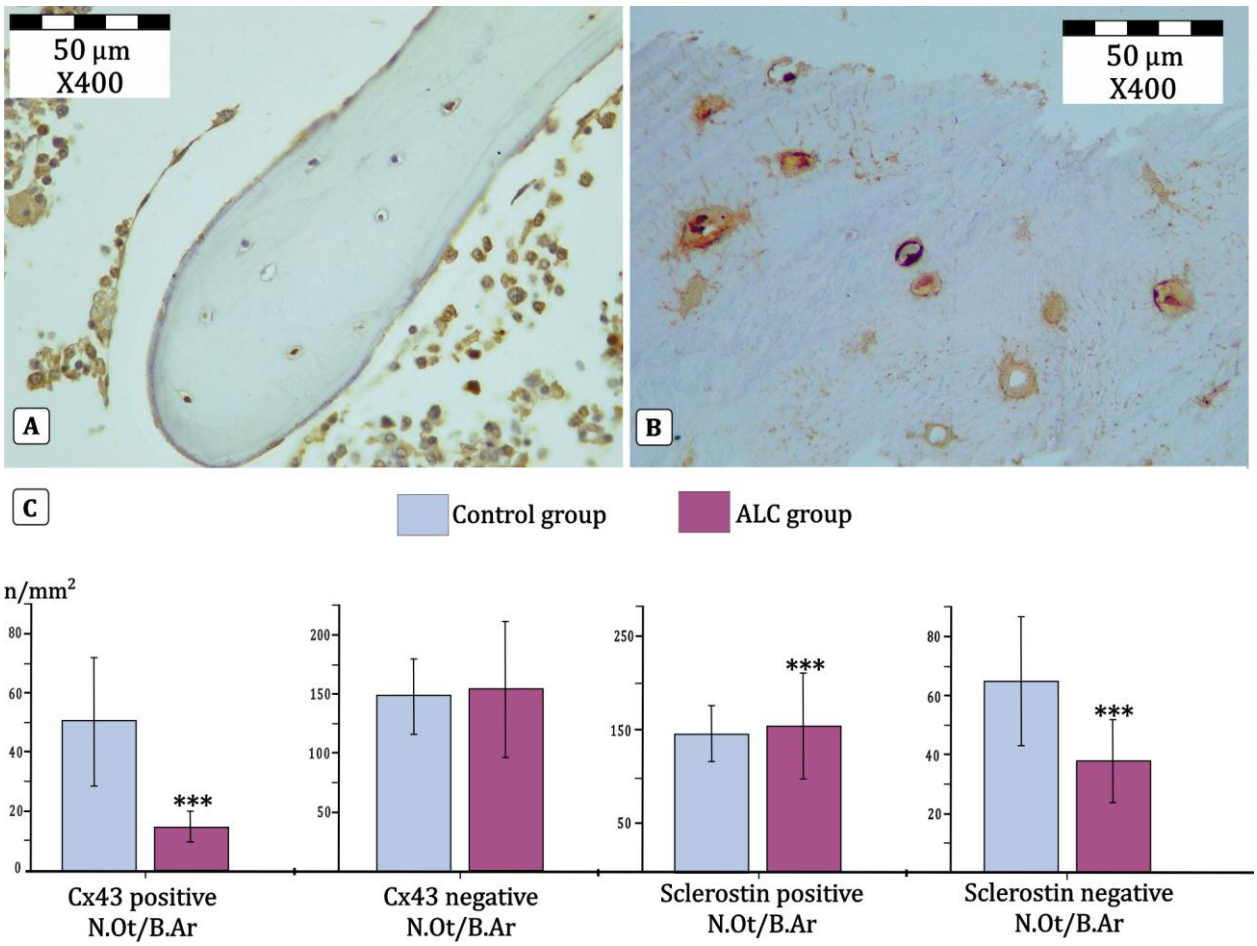


**Figure 20. The comparison of the expression of osteocyte-specific molecules in femoral samples collected from healthy individuals and individuals with ALC**

Detail is showing the typical Cx43 positive (brown colored, a), sclerostin positive (brown colored, b) and negative (blue colored) osteocytes in femoral bone samples collected from ALC donor. Our data suggested that decreased number of Cx43 positive osteocytes, coupled with increased number of sclerostin positive osteocytes, was present in femoral samples collected from individuals with end-stage alcoholic liver disorder, in comparison with healthy control individuals (c). Abbreviations: N.Ot/B.Ar – the number of osteocytes per bone area; Cx43 – Connexin 43; Statistical significance of the difference in immunohistochemistry findings between ALC and control group was estimated using Student's *t* test (*** $p<0.05$ vs. control).

Considering the morphology of osteocyte lacunar network in individuals with CLD of alcoholic origin, we noted some minor disruptions. Namely, the number of empty lacunas was significantly increased in bone samples collected from inter-trochanteric femoral region of adult male cadaveric individuals with end-stage ALD (p=0,021, Student's *t* test). Still, the difference in total number of osteocytes per bone area and the total number of osteocyte lacunas per bone area did not reach statistical significance between ALC and control individuals ($p>0.05$, Student's *t* test, Figure 21).

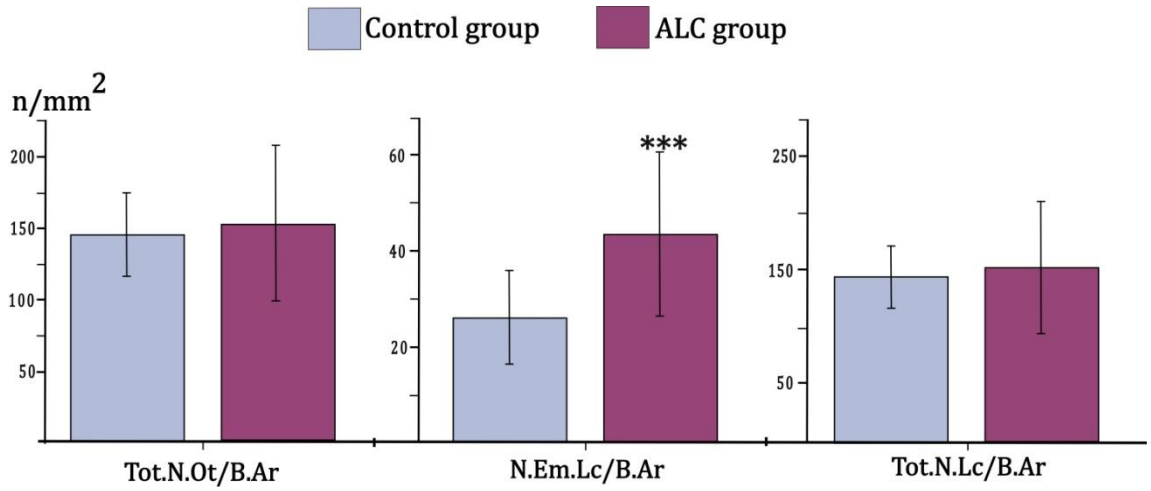


**Figure 21. The assessment of osteocytic network in femoral bone samples collected from individuals with ALC in comparison to healthy controls**

Abbreviations: Tot.N.Ot/B.Ar – the total number of osteocytes per bone area; N.Em.Lc/B.Ar – the number of empty lacunae per bone area; Tot.N.Lc/B.Ar – total number of osteocyte lacunas per bone area.
Statistical significance of the difference in femoral osteocytic network between ALC and control group was estimated using Student's *t* test ( *** indicated significant difference; $p<0.05$ vs. control).

## 5. DISCUSSION

This study has undertaken a various characterization of the lumbar vertebrae and femoral bone tissue changes in men with various stages of alcoholic and non-alcoholic (cardiac) chronic liver disorders. These assessments were conducted to contribute to a better understanding of increased bone fragility and low-trauma fracture susceptibility associated with CLD of alcoholic and non-alcoholic origin. Our approach comprised clinical assessment of fracture risk (using DXA and HSA measurement), analyses of the cortical and trabecular bone micro-architecture of lumbar vertebrae and proximal femora (using micro-CT), assessment of femoral bone mechanical competence (using Vickers micro-hardness indentation), as well as immunohistochemical assessment of the two osteocyte-specific molecules (Cx43 and sclerostin) in lumbar vertebrae and femoral samples obtained from individuals with alcoholic and non-alcoholic CLD and healthy controls. Altogether, this evaluation revealed evidence of the disruption of morphological, mechano-structural, and cellular indices for CLD-induced bone impairment that could be associated with increase in vertebral and femoral bone fragility.

Over the last decades, based on the numerous study results, a respectable amount of knowledge about the bone strength determinants and factors that could induce increased bone fragility in aged individuals and in individuals with different chronic diseases has been accumulated (Djuric et al. 2010; Djonic et al. 2011; Jadzic, Mijucic, et al. 2021). Leading research experts agree that this data set the path for future studies that will be used to develop various prevention programs and facilitate identifying high-fracture risk individuals in the future. According to its composition and structural design, bone is a unique biomechanical model that can simultaneously achieve adequate strength, hardness, and flexibility and provide ease of body movement against the force of gravity (Ammann & Rizzoli 2003; Milovanovic et al. 2015; Lin et al. 2020). From a biomechanical perspective, bones show exceptional strength when exposed to compressive and tension forces (Havaldar et al. 2014). Bone tissue is displaying its regenerative nature; that is, bone tissue has the ability to replace old with new bone in reaction to some form of stress (Lin et al. 2020). It is important to note that many factors affect the bone strength. However, the occurrence of a fragility fractures

primarily requires the action of several bone-strength determinants and their mutual interaction (Djonić et al. 2013; Ammann & Rizzoli 2003). Besides mechanical force characteristics, these intrinsic bone-strength determinants could be divided into micro-architectural changes and compositional (material) changes in bone tissue.

The WHO recommended that the DXA assessed BMD should be the "golden standard" for fracture risk assessment, as well as for the diagnosis of osteopenia and osteoporosis (as reduced bone mass conditions) (Jeon et al. 2016). However, numerous publications show that low trauma fractures could not be fully explained by BMD decrease (Ott 2016), suggesting that other factors could play a significant role in compromised bone strength (Djonić et al. 2013; Seeman 2003; Stone et al. 2003). Therefore, the pioneer studies analyzed influence of geometric bone characteristics on bone strength (Calis et al. 2004; Djonic et al. 2011; LaCroix et al. 2010). Based on that, Beck and his team invented a special software that provides data about bone resistance to compressive and bending mechanical forces (for example, the moment of inertia, section modulus, and buckling ratio) (Beck 2007). On the other hand, the disturbance of microstructure of the trabecular and cortical bone and accumulation of local non-traumatic microdamage (microfractures) are known as essential factors that contribute to increased risk for low-trauma fracture (Djuric et al. 2010; Jadzic, Mijucic, et al. 2021; Milovanovic et al. 2017).

As a tissue, bone is composed of an extracellular matrix and various bone cells (osteoblasts - bone-forming cells, osteoclasts - bone-resorbing cells, and the most numerous bone cells - osteocytes). Osteocytes are the most abundant bone cells that reside and interconnect within the osteocyte lacunar network formed of micron-sized pores (known as lacunae) and nanometer-sized channels (known as canaliculi)(Rolvien, vom Scheidt, et al. 2018). Signal transduction, molecular transport, and nutrient supply through the osteocyte lacunar network are recognized as essential for bone homeostasis (Milovanovic & Busse 2019); hence, disruption of the osteocyte lacunar network morphology and osteocyte functionality is considered as a contributing factor for compromised bone quality and substantial bone strength decline associated with aging and disease (Mullender et al. 1996).

Bone extracellular matrix could be considered complex material consisting of organic and

inorganic (mineralized) matter. The organic part of the bone extracellular matrix mainly consists of collagen (type I collagen predominantly), but also it contains non-collagenous proteins (such as osteopontin, phosphophoryn, and sialoprotein) (Viguet-Carrin et al. 2006; Daneault et al. 2017; Kalmey & Lovejoy 2002). An inorganic part of the bone primarily consists of carbonated hydroxyapatite crystals containing calcium and phosphorous. Due to its complexity, the physicochemical characteristics of bone tissue are drawing researchers' attention over the years. Namely, numerous research teams noted that various mineralization levels, the altered calcium and phosphorous content (and ratio), the change in mineral grain size, and collagen fibrils could contribute to age related compromised bone strength and reduced ability to resist to occurrence of low-trauma fracture (Zimmermann et al. 2021; Milovanovic et al. 2011; Milovanovic & Busse 2019).

To perform clinical assessment of fracture risk during the present study, we conducted and compared the *ex vivo* DXA and HSA findings of partially excised proximal femora collected from men with various ALD stages and healthy age- and sex-matched controls. Initially, we noted significantly reduced total BMD and deterioration trend in total BMC of proximal femora collected from ALD group, which faded away after BMI adjustment, suggesting that BMI influenced our data. The same significant covariant effect was noted in a previous study dealing with patients diagnosed with end-stage CLD of alcoholic origin (Culafić et al. 2014). However, our data suggest an actual ALD-induced BMD loss in the femoral neck region, regardless of the BMI adjustment. These data are in line with the results of previous clinical studies conducted on patients prone to drinking (Ulhøi et al. 2017; López-Larramona et al. 2013) and in patients with end-stage CLD of alcoholic (Culafić et al. 2014; Mahmoudi et al. 2011) and non-alcoholic origin (Mounach et al. 2008; González-Calvin et al. 2009; Gallego-Rojo et al. 1998).

Femoral neck HSA parameters (CSA, CTh and BR) were initially altered in ALD men, which is in accordance with previous observations on patients with alcohol-induced liver cirrhosis (Culafić et al. 2014). Still, after the BMI-adjustment, only narrow neck CSA in narrow neck remained significantly reduce in ALD individuals. Considering the CSA depend on periosteal diameter and BMD, and our data on BMD reduction, this finding is expected, and

suggest that femoral bone ability to resist axial loading could be compromised in our ALD donors. However, it could be hypothesized that external geometric parameters were not severely affected in our ALD men. Interestingly, in our study, the ALD-induced decline in CSA originated only from ALC men in whom narrow neck CSA was significantly lower than in healthy sex- and age-matched controls. On the other side, considering potential site-specific bone changes, our data did not depicture any significant difference in DXA and HSA parameters of the inter-trochanteric region when compared to the femoral neck region of our control and ALD group, which is following previous observations in non-alcoholic CLD patients (Ormarsdóttir et al. 2002). We failed to prove any significant difference in densitometry and geometry parameters either between FLD individuals and healthy controls or between FLD and ALC individuals. Even though the deterioration trend could not be denied, the recent meta-analysis suggests that osteodensitometry findings were not different in patients with and without alcohol-induced liver cirrhosis (Bang et al. 2015; Malik et al. 2009). However, the same authors noted increased fracture risk among ALD individuals (Bang et al. 2015), which could be associated with frequent falls in individuals prone to alcohol abuse (Cawthon et al. 2006).

Our osteodensitometry analysis may be limited by the cross-section nature of this autopsy study, meaning that we compared two or more groups at a particular moment in time, so we could not follow the bone impairment progression in individuals included in the study. Limited study sample is due to chosen autopsy design and analyzing the material of cadaveric origin. Prospective and multidisciplinary clinical studies are needed to reveal the true significance of the difference in DXA and HSA findings between individuals with various stages of alcohol-induced CLD and healthy age- and sex-matched controls. In addition, *ex vivo* DXA assessment was conducted on partially excised proximal femora submerged into a water bath. Still, it may be possible that *in situ* evaluation could slightly increase the value of osteodensitometry findings in this study.

Considering that clinical assessment of fracture risk is not always showing disturbed BMD findings in CLD individuals, we analyzed the micro-architectural characteristics of lumbar vertebral body and proximal femora. Our micro-CT assessment revealed that integrity

of trabecular micro-architecture was deteriorated in lumbar vertebrae and proximal femora of investigated CLD individuals. In lumbar vertebrae, these changes were primarily reflected in decreased trabecular bone volume, thinner trabeculae, and lower trabecular number in alcoholic and non-alcoholic (cardiac) end-stage CLD men. These data were in accordance with the results suggested by previous histomorphometry studies conducted on iliac bone biopsies collected from patients with various forms of CLD (Crilly et al. 1988; Guichelaar et al. 2002; Jorge-Hernandez et al. 1988). In addition, some novel studies, conducted in the controlled hospital settings, confirmed these results by applying different and more newel methodology (pQCT) in order to *in vivo* access CLD-induced micro-architectural changes in tibia and radius (Wakolbinger et al. 2019; Schmidt et al. 2018; Jandl et al. 2020). These data are nicely following our observation of significantly impaired integrity of trabecular micro-architecture (lower trabecular bone fraction, coupled with reduced trabecular number and increased trabecular separation) in proximal femora obtained from ALD individuals. These findings were in line with previous histomorphometry reports about compromised integrity of iliac crest micro-architecture in patients prone to alcohol abuse (Ulhøi et al. 2017), in patients with alcohol-induced pancreatitis (Schnitzler et al. 2010), and in patients with alcohol-induced end-stage CLD (Crilly et al. 1988). Based on the deteriorated trabecular micro-architecture, it is reasonable to assume that CLD men included in our study may have reduced bone strength and a greater chance to sustain a femoral and vertebral fragility fracture, which is in line with findings of various clinical studies (Alcalde Vargas et al. 2012; Crawford et al. 2003; Wibaux et al. 2011; Bang et al. 2015).

Micro-CT assessment performed in our study did not reveal any significant difference in vertebral cortical microstructure between healthy controls and individuals with alcoholic and non-alcoholic (cardiac) end-stage CLD. On other hand, we noticed a significantly thinner and more porous cortical shell of proximal femora collected from ALD men when compared to healthy controls. Previous studies conducted on distal tibia and radius also revealed deteriorated cortical bone microstructure among patients with various forms of CLD (Schmidt et al. 2018; Wakolbinger et al. 2019). Our conflicting results between CLD-induced cortical bone deterioration in lumbar vertebrae and proximal femora could stem from different

skeletal sites analyzed. Namely, previous results emphasized predominance of trabecular bone loss in the lumbar vertebral fracture development in aged men (Osterhoff et al. 2016), while cortical deterioration has a more significant biomechanical impact on the fracture occurrence in typical long bones (such as a femur, radius, and tibia) (Chen et al. 2013; Milovanovic et al. 2017; Milovanovic et al. 2014). These findings on vertebras could be also caused by prominent variability of cortical microstructure noted among individuals included in our study. Lastly, the concept of "different bone changes in a different time" has been previously recognized, indicating that in the pathogenesis of osteoporosis, trabecular bone loss initially occurs, and cortical bone impairment becomes more prominent with the evolution of the disease (Chen et al. 2013). Thus, we may speculate that with the progression of liver disorder, observed cortical micro-architectural alterations in lumbar vertebrae would become more pronounced and may influence vertebral strength in our CLD individuals.

Our data did not reveal any significant difference in vertebral microstructural parameters between men with alcoholic and non-alcoholic (cardiac) end-stage CLD, suggesting that alcoholic origin of the disease was not a crucial factor for bone alterations noted in our study. Recent pQCT study also show absence of significant microstructural differences between patients with end-stage CLD of various etiologies (Wakolbinger et al. 2019). In addition, previous histomorphometry analysis of individuals with chronic alcoholism did not reveal significant vertebral bone deterioration (Crilly et al. 1988). Based on these data, it may be assumed that adverse effects on bone status in our individuals with alcohol-induced CLD are more related to liver disease *per se* than the isolated alcohol intake negative effect. In contrast to our observations, previous histomorphometry studies noted that alcohol intake suppressed osteoblast activity and new bone formation in individuals who were prone to drinking (Ulhøi et al. 2017). Moreover, the findings of Crilly et al. suggested reduced osteoid surface in iliac crest bone biopsy samples of patients prone to chronic alcoholism (Crilly et al. 1988), so the harmful alcohol-induced effect on the bone tissue should not be neglected.

Micro-architectural analysis of lumbar vertebrae and proximal femora conducted during this thesis was limited by inherent restraints of the cross-sectional nature of this study, as it

does not track bone impairment over time, yet compares different groups of individuals at a specific point in time. The findings of our study could be limited by the lowest detectable values used in our micro-CT scanning protocol, so we could not detect changes bellow the resolution of 10 μm. Still, the resolution of micro-CT assessment used during present study was better (Wakolbinger et al. 2019; Jandl et al. 2020; Schmidt et al. 2018; Djuric et al. 2010) or comparable (Cvetkovic et al. 2020; Jadzic, Mijucic, et al. 2021; Jadzic, Milovanovic, et al. 2021) to scanning conditions used in many previous human studies. Later, as our data about the alcoholic origin of the disease were based on hetero-anamnestic data (units of alcoholic drink per day and duration of the drinking habits), these data may be subject to recall bias. The results of this cadaveric study may be subject to the covariant effect of unreported life habits (the drug and tobacco use, the level of physical activity) and undiagnosed health disturbances.

To test mechanical competence of the bone, we conducted Vickers micro-indentation testing on the cortical compartment of proximal femora collected from individuals with various ALD stages (FLD and ALC). Following our observation on altered cortical micro-architecture, Vickers micro-hardness decline was present in the femoral cortical shell of ALD individuals. Previous studies using a variety of bone samples suggested that decreased bone micro-hardness could be associated with altered mineral content and therefore reduced ability of bone tissue to resist plastic deformation under constant mechanical loading (Arnold et al. 2017; Boivin et al. 2008; Zwierzak et al. 2009; Yin et al. 2019). With that in mind, we may speculate that our data may suggest declined femoral ability to resist plastic deformation under constant mechanical loading, coupled with a poor level of bone mineralization (Boivin et al. 2008) in the cortical compartment of femoral samples collected from our ALD men. Reduced vitamin D levels, gut microbiota disturbances, hypogonadism, and poor nutrition associated with CLD and chronic alcoholism could induce micro-indentation findings in our ALD group (Guañabens & Parés 2011; Yadav & Carey 2013; Eshraghian 2017; González-Reimers et al. 2011). These assumptions are more likely to be true, if we take into consideration that our study revealed significant micro-hardness reduction in a cortical compartment of proximal femora collected both from men with FLD and ALC. On the other

side, our data did not reach statistical significance in the difference between individuals with initial and end-stage alcoholic liver disorder (ALC vs. FLD group) suggesting that mechanical competence of the bone is affected even in initial stage of ALD. Our data also did not reveal significant site-specific alterations in cortical Vickers micro-hardness of proximal femora in ALD men. Nevertheless, previous studies suggested a significantly heterogeneous and site-specific mineral composition of the bone matrix in proximal femora of aged individuals (Loveridge et al. 2004; Spiesz et al. 2013; Rolvien, vom Scheidt, et al. 2018). These contradictory data may originate from the fact that Vickers micro-hardness could only partially display heterogeneity of the complex material such as bone tissue (Boivin et al. 2008; Ibrahim et al. 2020; Dall'Ara et al. 2012; Dall'Ara et al. 2007). Namely, previous studies revealed that bone's ability to resist plastic deformation is, at least partially, associated with the bone mineral content (Spiesz et al. 2013; Dall'Ara et al. 2007), calcium and phosphorous ratio in the bone minerals (Rolvien, Schmidt, et al. 2018) and the morphology of the inorganic component of the bone extracellular matrix (Milovanovic et al. 2011). Still, the lack of investigation in CLD individuals, is implying that future studies are required to give a precise estimate of bone mineral content, collagen fibers and other compositional bone disturbances in CLD individuals.

The association between vertebral micro-architectural properties and Knodell's pathohistological scores of liver damage present in individuals with alcoholic and non-alcoholic (cardiac) end-stage CLD was assessed during this doctoral dissertation. Further, we compared findings of altered femoral micro-architecture between individuals with initial (FLD group) and end-stage ALD (ALC group). In our study, deterioration in trabecular micro-architectural integrity was inversely associated with pathohistological scores reflecting the stage of liver damage in individuals with alcoholic and non-alcoholic (cardiac) end-stage CLD. These data suggest that the severity of liver tissue disturbances could be a predictor in CLD-induced bone loss noted in our study. Similar to our data, other studies observed a correlation between bone impairment and clinical staging in patients with various CLD of alcoholic (Culafić et al. 2014) and non-alcoholic origin (Schmidt et al. 2018). Thus, adequate and timely treatment of the liver disease may decelerate the progression of bone impairment in end-

stage CLD patients. However, some other research teams did not find any correlation between bone changes in end-stage CLD patients and their clinical scores of liver disorders (Campbell et al. 2005; Wakolbinger et al. 2019). The main reason for these opposite observations could originate from the applied methodology since subtle and low-scale changes in trabecular micro-architecture can be easily determined by high-resolution micro-CT assessment but not by standard clinical tools (such as pQCT) (Djonić et al. 2013; Cohen et al. 2010). In addition, we should bear in mind that the assessment of the association between clinical scores and bone impairment was not possible to perform in this autopsy study. More so, if we take into consideration that cortical micro-architectural parameters of lumbar vertebrae were not associated with the pathohistological scores developed by Knodell due to significant inter-individual variation in the cortical shell of lumbar vertebrae collected from our individuals. Thus, the clinical utility of our findings requires further confirmation in large, prospective studies performed in controlled clinical settings.

At the same time, a significant decrease in the micro-architectural features of proximal femora was present in the individuals with initial ALD stage when compared to the control group, despite a non-significant decline in DXA findings. Namely, increased cortical porosity, larger pore diameter, and reduced Vickers micro-hardness were noted in the inter-trochanteric region of individuals with alcohol-induced FLD, suggested reduced femoral bone strength among these individuals. These data are following the results of Wang et al. suggesting increased bone fragility in non-alcoholic fatty liver disease patients (Wang et al. 2018), and results of Chen et al. suggesting an increased risk of osteoporosis among individuals suffering from non-alcoholic fatty liver disease (Chen et al. 2018). Our data suggested more pronounced bone deterioration in femoral bone collected from individuals with end-stage ALD (ALC). Namely, decreased BMD in the femoral neck and reduced CSA and CTh of the inter-trochanteric region, accompanied by decreased micro-hardness and altered cortical and trabecular microstructure in all three investigated femoral regions, suggested that advanced stage of ALD could be a significant predictor of bone impairment among these individuals. These data are in line with the results of previous studies suggesting more severe bone loss in individuals with end-stage CLD (liver cirrhosis) when compared to individuals

without end-stage CLD (Montomoli et al. 2018; Díez-Ruiz et al. 2010; Schmidt et al. 2018; Culafić et al. 2014; Jadzic, Milovanovic, et al. 2021).

Nowadays, two morphological types of femoral fracture have been differentiated: intracapsular (inside of hip joint capsule) and extracapsular femoral fracture (outside of the hip joint capsule) (Tanner et al. 2010). In the elderly, intracapsular fractures are usually fractures of the femoral neck, while extracapsular fractures include fractures located in the inter-trochanteric region of the proximal femora (Tanner et al. 2010). Recent studies have shown that inter-trochanteric fractures are more likely associated with osteoporosis (Michaëlsson et al. 1999; Crilly et al. 2016). At the same time, alcohol abuse and CLD occurrence were associated with an increased incidence of unstable inter-trochanteric fractures (Cauley et al. 2009; Montomoli et al. 2018). On the other side, intracapsular fracture incidence is notably increased in men of advanced age (Crilly et al. 2016; Jo et al. 2016). The previous result suggests that inter-site difference in femoral bone microstructure may play a significant role in the occurrence of intracapsular femoral fractures among individuals of advanced age (Djuric et al. 2010; Lundeen et al. 2000; Chen et al. 2013; Stone et al. 2003; Eckstein et al. 2007). With that in mind, we investigated the potential regional microstructural specificities in proximal femora collected from adult cadaveric ALD men. Our data indicate that micro-architectural features of the cortical shell were the most superior in the medial part of the femoral neck when compared to other investigated regions (lateral part of the femoral neck and inter-trochanteric region) in control and ALD group. Still, more severely affected trabecular and cortical micro-architecture in the inter-trochanteric region when compared to femoral neck regions was noted in the ALD group compared to control group. In short, we observed more porous and thinner cortex, along with reduced trabecular thickness and number in the inter-trochanteric region of ALD men, which indicated that impaired mechanical integrity and lower ability to resist mechanical loading could be present in the inter-trochanteric region of our ALD individuals (Djonic et al. 2011; Silva 2007; Djonić et al. 2013; Jadzic, Milovanovic, et al. 2021). In contrast to the evident micro-architectural deterioration in inter-trochanteric region of our ALD group, DXA and HSA measurement did not reveal such site-specific difference. We may speculate that these inconsistent findings

originate from the limitations of osteodensitometry measurements (limited resolution, assumed homogeneity of bone mineral content and axial symmetry of the bone cross-sections) (Beck 2007; Beck et al. 1990). Although most femoral fractures are related to reduced BMD and micro-architectural changes, it should be emphasized that some external factors could contribute to the occurrence of femoral fracture (Sundh et al. 2015; Zimmermann et al. 2021). For example, an increased number of side falls in patients prone to heavy alcohol consumption, combined with magnitude and direction of force (compressive or tension force) during the fall (Sundh et al. 2015; Crilly et al. 2016), could play a significant role in the increased risk of inter-trochanteric fractures among individuals with the alcohol-induced liver disease (Kaukonen et al. 2006; Michaëlsson et al. 1999). Taken together, all these findings suggest that ALD men may have a greater chance to sustain an inter-trochanteric femoral fracture, which is in line with data from previous clinical and epidemiological studies (Kaukonen et al. 2006; Michaëlsson et al. 1999; Cauley et al. 2009).

The etiopathogenetic mechanisms of bone impairment in CLD individuals are multifactorial and still insufficiently clarified. Most often, the pathogenesis of bone impairment is described as a disorder of the bone remodeling process, in which disbalance between bone resorption and bone formation is leading to CLD-induced bone microstructure disruption (Jadzic, Cvetkovic, Tomanovic, et al. 2020; Jadzic, Cvetkovic, Milovanovic, et al. 2020; Wakolbinger et al. 2019) and subsequent CLD-induced decrease in bone mass (López-Larramona et al. 2013; Culafić et al. 2014). It has been known that disturbed RNKL/OPG ratio and hyperproduction of pro-inflammatory cytokines stimulate bone resorption in patients with end-stage CLD (Ehnert et al. 2019; Luo et al. 2017; Guañabens & Parés 2018). In addition, altered activity of a variety of matrix metalloproteinases and cathepsin K could stimulate osteoclasts and bone resorption in patients with CLD (Ehnert et al. 2019; Khalifa et al. 2019; Liang et al. 2016; Hardy & Fernandez-Patron 2020). Osteoblast dysfunction could result from altered IGF-1 or OnfFN production in the liver, or it could be associated with biliary stasis present in the CLD patients (Mitchell et al. 2011; Santori et al. 2008; Sens et al. 2017). Previous results suggested that increased serum concentrations of sclerostin, an osteocyte-derived regulator of bone formation, could be an essential part of mechanisms leading to CLD-

induced bone impairment (González-Reimers et al. 2013; Wakolbinger et al. 2020; Yousry et al. 2016; Ehnert et al. 2019; Rhee et al. 2014). Firstly, in a pilot study including a small number of individuals prone to heavy alcohol intake, increased sclerostin serum concentration was noted (González-Reimers et al. 2013). Then, data about the effect of liver dysfunction on circulating levels of sclerostin were published (Rhee et al. 2014). Finally, recent studies confirmed that increased sclerostin serum concentrations were associated with bone loss in individuals suffering from alcoholic and non-alcoholic forms of CLD (Wakolbinger et al. 2020; Guañabens et al. 2016). At the same time, increased local sclerostin expression was found in the liver tissue biopsy samples taken from patients with primary biliary cirrhosis (Guañabens et al. 2016). Having all that in mind, during our study, the sclerostin expression was analyzed in lumbar vertebrae and proximal femora collected from CLD men. Aligned with previously mentioned results, our finding of increased sclerostin osteocytic expression was confirmed in lumbar vertebrae of men suffering from end-stage alcoholic and nonalcoholic CLD (Figure 20). Thus, we may speculate that our finding of increased sclerostin expression in osteocytes suggests that decreased bone formation could lead to significant bone loss and microstructural disruption noted in the same cadaveric men (Figure 21). More so, if we know that altered sclerostin serum concentrations were previously associated with bone composition changes in human bone samples (Hassler et al. 2014) which could be aligned with our observation of significantly reduced Vickers micro-hardness in individuals with various ALD stages. However, our data did not suggest any significant difference in sclerostin expression between individuals suffering from two etiologically different forms of end-stage CLD (alcoholic liver cirrhosis and cardiac liver fibrosis), suggesting that detrimental effect on bone is more associated with the liver disorder than with the alcoholic origin of the disease. These suggestions are aligned with our results on the non-significant difference in vertebral microstructural impairment noted in the same individuals of our ALC and non-ALC group (Jadzic, Cvetkovic, Tomanovic, et al. 2020) (Figure 22). Thus, increased sclerostin expression may elucidate a potential role of sclerostin in mediating low bone formation associated with CLD. With that in mind, we may speculate that treatment targeting sclerostin may have beneficial effects in attenuating bone changes among CLD patients. However, new prospective

state-of-the-art studies should be conducted in controlled clinical settings to verify these suggestions in years ahead.

Our data also suggested that a certain level of disruption in the osteocyte lacunar network was present in lumbar vertebrae of individuals with end-stage CLD of alcoholic and non-alcoholic origin and proximal femora of ALC individuals. Moreover, we should bear in mind that decreased Cx43 expression in the osteocytic network was noted in lumbar vertebrae and proximal femora samples taken from investigated individuals (Figure 21). These data imply that intercellular communication between osteocytes is compromised in men with end-stage CLD, which was previously suggested by the findings of various animal studies (Davis et al. 2018; Cooreman et al. 2020; Balasubramaniyan et al. 2013). Namely, Davis et al. suggested that increased expression of Cx43 preserves the osteocyte viability and ameliorates age-related changes in the skeleton of a mouse (Davis et al. 2018). Moreover, previous *in vitro* studies using human hepatocyte culture and animal studies using rodent animal models revealed that liver cholestasis could be associated with altered expression of Cx43 (Cooreman et al. 2020; Balasubramaniyan et al. 2013). In various animal heart failure models, deteriorated expression of Cx43 was noted between cardiomyocytes (van Veen et al. 2002; Fernandez-Cobo et al. 1999; Michela et al. 2015). Previous human studies suggested that impaired Cx43 expression and distribution in decompensated cardiac hypertrophy may play a maladaptive role leading to heart failure (Kostin et al. 2004), which was aligned with our finding in bone samples collected from individuals with cardiac end-stage CLD (Figure 23).

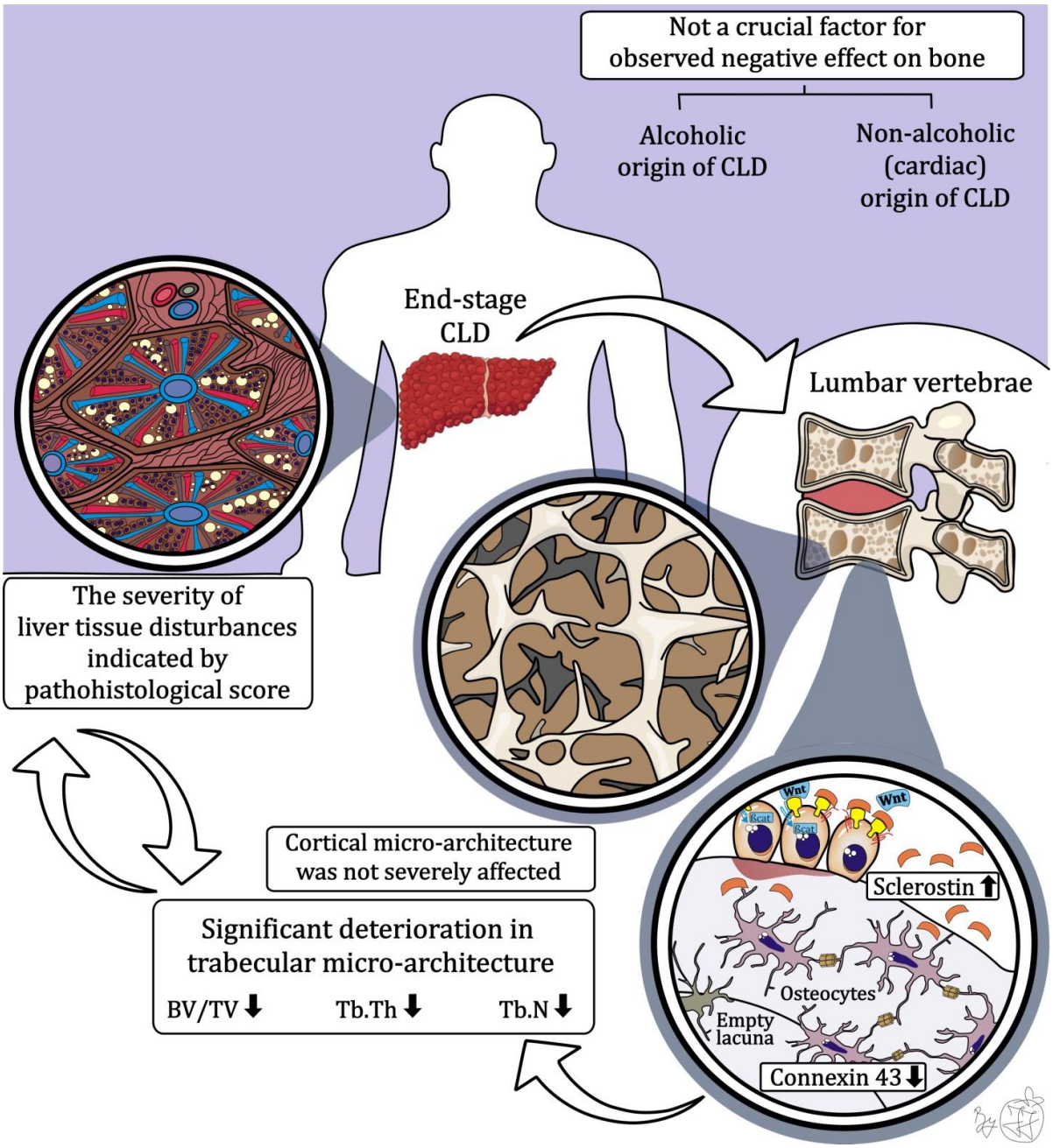


**Figure 22. Schematic representation of our main findings in lumbar vertebrae and hypothetical summary**

Trabecular micro-architecture of lumbar vertebrae was significantly altered in individuals with alcoholic and non-alcoholic (cardiac) end-stage liver disorder, indicating compromised bone strength in these individuals. Our data revealed that pathohistological scoring and the severity of liver tissue disturbances were associated with vertebral micro-architectural impairment of men with alcoholic and non-alcoholic (cardiac) end-stage CLD. However, this study revealed that alcoholic origin of CLD was not a crucial factor for negative effect on lumbar vertebral micro-architecture. The altered intercellular communication between osteocytes was suggested by reduced expression of gap junction forming protein - connexin 43. Thus, signal transduction trough bone could be compromised in men with end-stage CLD of alcoholic and non-alcoholic origin. Our finding of increased sclerostin expression, secreted by osteocytes, indicates that low bone formation plays an important role in bone impairment associated with alcoholic and non-alcoholic (cardiac) CLD.

Considering our and previous data, it may be assumed that signal transduction in the bone tissue triggered by various stimuli may be impaired in lumbar vertebrae of CLD individuals (Plotkin 2011; Stains et al. 2019) (Figure 21). In addition, the mechanosensing

potential and molecular transport could be affected in proximal femora of ALD individuals (Figure 23). However, our data did not reveal significant difference in osteocytic Cx43 expression, as well as in sclerostin osteocytic expression, between two etiologically different forms of end-stage CLD. This observation in men with alcoholic liver cirrhosis and cardiac liver fibrosis, suggesting that altered Cx43 and sclerostin expression were more associated with the CLD-induced negative effect on bone than with the alcohol-induced negative effects on bone.

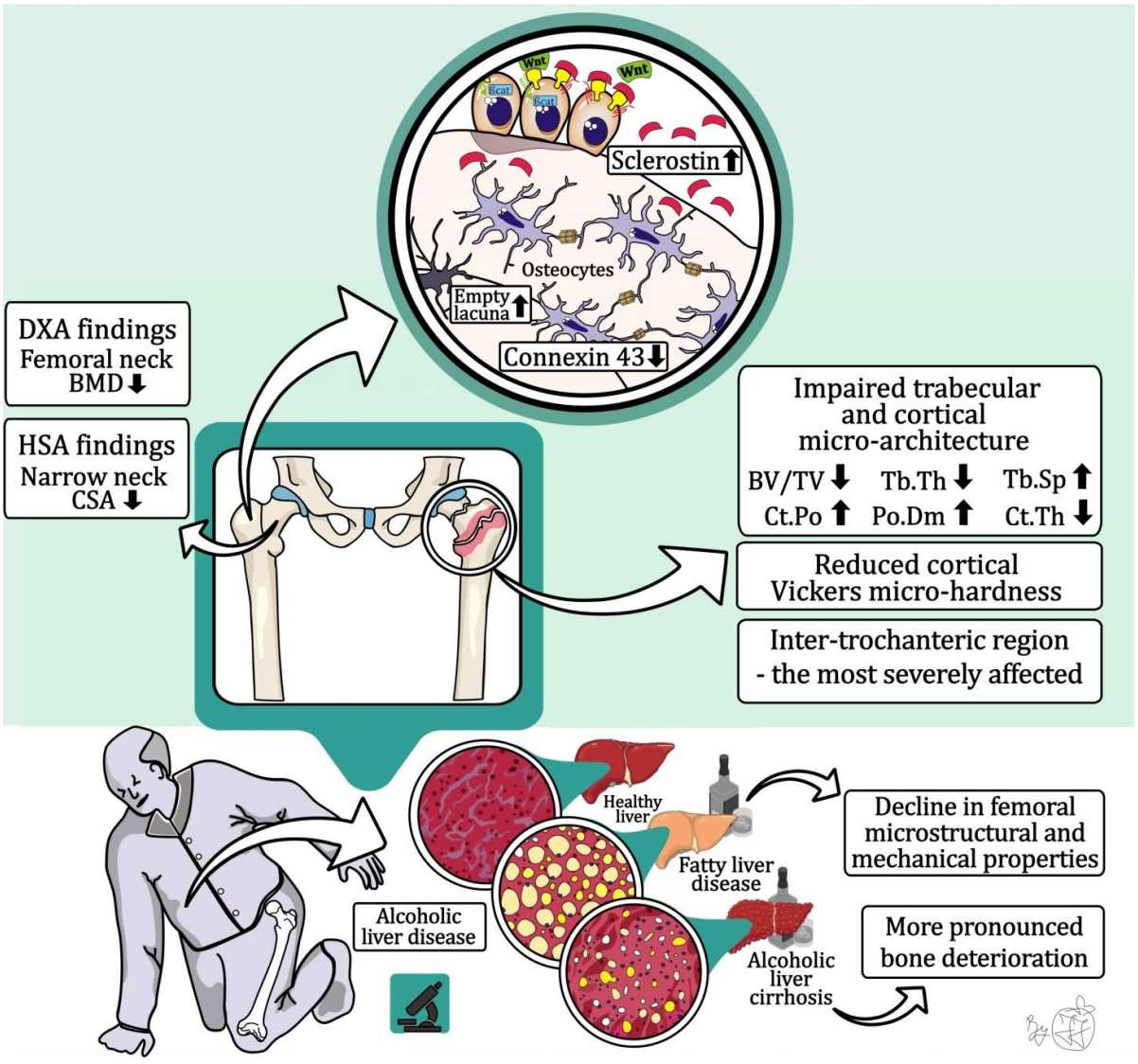


**Figure 23. Schematic representation of our main findings in proximal femora and hypothetical summary**

Our findings suggested that changes in femoral DXA and HAS findings, trabecular and cortical microstructure and Vickers micro-hardness could illuminate the morpho-structural basis for increased femoral fracture risk in patients with alcohol-induced liver disorder. The most prominent micro-architectural differences between ALD and healthy men were noted in inter-trochanteric part of the proximal femora, which may result in increased susceptibility to inter-trochanteric femoral fracture among patients with alcoholic CLD. The more severely affected femoral mechano-structural deterioration was noted in individuals with end stage CLD of alcoholic origin (alcoholic liver cirrhosis). These femoral bone changes could be caused by altered Cx43 and sclerostin expression, coupled with osteocytic network disruption in femoral bone sampled from adult cadaveric men with alcoholic end-stage CLD.

## 6. CONCLUSIONS

Based on the data presented in this thesis, we may conclude the following:

1. This study indicated that trabecular micro-architecture of lumbar vertebrae was significantly deteriorated in individuals with alcoholic and non-alcoholic (cardiac) CLD, suggesting increased vertebral bone fragility in those individuals. On the other side, microstructural parameters of cortical shell in lumbar vertebrae were not influenced by end-stage CLD.
2. Our data revealed that pathohistological scoring and the severity of liver tissue disturbances could be associated with vertebral micro-architectural impairment noted in men with alcoholic and non-alcoholic (cardiac) end-stage CLD.
3. This study revealed that alcoholic origin of CLD was not likely a crucial factor for negative effect on lumbar vertebral micro-architecture.
4. Immunohistochemistry analysis conducted in this study revealed that decreased Cx43 expression in vertebral samples might indicate the deterioration of intercellular communication in the osteocytic network of end-stage CLD individuals. Increased sclerostin expression in bone samples of CLD individuals may elucidate a potential role of sclerostin in mediating low bone formation associated with CLD, which results in bone loss observed in the same individuals.
5. Our findings on proximal femora, suggested that changes in bone densitometry, geometry, microstructure and micro-hardness could illuminate the morpho-structural basis for increased femoral fracture risk in patients with alcohol-induced liver disorder.
6. As our data revealed, micro-architectural properties of inter-trochanteric part of the proximal femora was most severely affected in ALD men, that may result in increased susceptibility to inter-trochanteric femoral fracture.
7. Following our findings in lumbar vertebrae, the more severely affected femoral mechano-structural deterioration was noted in individuals with end-stage CLD of alcoholic origin suggesting that liver disease staging could be significant determinant of ALD-induced bone strength reduction.

8. Our data demonstrate that observed femoral changes in ALC men could be caused by altered Cx43 and sclerostin expression, coupled with osteocytic network disruption in these individuals.

9. Findings of this study indicating that individual vertebral and femoral fracture risk assessment is beneficial in all CLD patients, with a particular accent on patients suffering from end-stage CLD, regardless of the origin of the disease.

## 7. REFERENCES


1. Alcalde Vargas A, Pascasio Acevedo JM, Gutiérrez Domingo I, García Jiménez R, Sousa Martín JM, Ferrer Ríos MT, Sayago Mota M, Giráldez Gallego A & Gómez Bravo MA (2012) Prevalence and characteristics of bone disease in cirrhotic patients under evaluation for liver transplantation. *Transplant. Proc.* 44, 1496–1498. Available at: http://dx.doi.org/10.1016/j.transproceed.2012.05.011

2. Aluoch AO, Jessee R, Habal H, Garcia-Rosell M, Shah R, Reed G & Carbone L (2012) Heart failure as a risk factor for osteoporosis and fractures. *Curr. Osteoporos. Rep.* 10, 258–269. Available at: http://dx.doi.org/10.1007/s11914-012-0115-2

3. Alvisa-Negrín J, González-Reimers E, Santolaria-Fernández F, García-Valdecasas-Campelo E, Valls MRA, Pelazas-González R, Durán-Castellón MC & de los Ángeles Gómez-Rodríguez M (2009) Osteopenia in alcoholics: Effect of alcohol abstinence. *Alcohol Alcohol.* 44, 468–475.
   Available at: http://dx.doi.org/10.1093/alcalc/agp038

4. Ammann P & Rizzoli R (2003) Bone strength and its determinants. *Osteoporos. Int.* 14 Suppl 3, 13–18. Available at: http://dx.doi.org/10.1007/s00198-002-1345-4

5. Arnold M, Zhao S, Ma S, Giuliani F, Hansen U, Cob JP, Abel RL & Boughton O (2017) Microindentation - A tool for measuring cortical bone stiffness? A systematic review. *Bone Jt. Res.* 6, 542–549.
   Available at: http://dx.doi.org/10.1302/2046-3758.69.BJR-2016-0317.R2

6. Asoudeh F, Salari-Moghaddam A, Larijani B & Esmaillzadeh A (2021) A systematic review and meta-analysis of prospective cohort studies on the association between alcohol intake and risk of fracture. *Crit. Rev. Food Sci. Nutr.* 0, 1–23.
   Available at: https://doi.org/10.1080/10408398.2021.1888691.

7. Balasubramaniyan V, Dhar DK, Warner AE, Vivien Li WY, Amiri AF, Bright B, Mookerjee RP, Davies NA, Becker DL & Jalan R (2013) Importance of Connexin-43 based gap junction in cirrhosis and acute-on-chronic liver failure. *J. Hepatol.* 58, 1194–1200. Available at: http://dx.doi.org/10.1016/j.jhep.2013.01.023.

8. Bang CS, Shin IS, Lee SW, Kim JB, Baik GH, Suk KT, Yoon JH, Kim YS & Kim DJ (2015) Osteoporosis and bone fractures in alcoholic liver disease: A meta-analysis. *World J. Gastroenterol.* 21, 4038–4047.
Available at: http://dx.doi.org/10.3748/wjg.v21.i13.4038

9. Bang UC, Benfield T, Bendtsen F, Hyldstrup L & Beck Jensen JE (2014) The risk of fractures among patients with cirrhosis or chronic pancreatitis. *Clin. Gastroenterol. Hepatol.* 12, 320–326. Available at: http://dx.doi.org/10.1016/j.cgh.2013.04.031.

10. Bansal RK, Kumar M, Sachdeva PRM & Kumar A (2016) Prospective study of profile of hepatic osteodystrophy in patients with non-choleastatic liver cirrhosis and impact of bisphosphonate supplementation. *United Eur. Gastroenterol. J.* 4, 77–83. Available at: https://doi.org/10.1177/2050640615584535

11. Beck TJ (2007) Extending DXA beyond bone mineral density: Understanding hip structure analysis. *Curr. Osteoporos. Rep.* 5, 49–55.
Available at: http://dx.doi.org/ 10.1007/s11914-007-0002-4

12. Beck TJ, Ruff CB, Warden KE, Scott WW & Rao GU (1990) Predicting femoral neck strength from bone mineral data. *Invest Radiol* 25, 6–18.
Available at: https://doi.org/10.1097/00004424-199001000-00004

13. Beck TJ, Ruff CB, Warden KE, Scott WW, Rao GU, Guarino M, Loperto I, Camera S, Cossiga V, Di Somma C, Colao A, Caporaso N, Morisco F, Guañabens N & Parés A (2018) Osteoporosis in chronic liver disease. *Liver Int.* 38, 776–785. Available at: https://doi.org/10.1111/liv.1373036

14. Berg KM, Kunins H V., Jackson JL, Nahvi S, Chaudhry A, Harris KA, Malik R & Arnsten JH (2008) Association Between Alcohol Consumption and Both Osteoporotic Fracture and Bone Density. *Am. J. Med.* 121, 406–418. Available at: https://doi.org/ 10.1016/j.amjmed.2007.12.012

15. Bihari C, Lal D, Thakur M, Sukriti S, Mathur D, Patil AG, Anand L, Kumar G, Sharma S, Thapar S, Rajbongshi A, Rastogi A, Kumar A & Sarin SK (2018) Suboptimal Level of Bone-Forming Cells in Advanced Cirrhosis are Associated with Hepatic Osteodystrophy. *Hepatol. Commun.* 2, 1095–1110.
Available at: https://doi.org/10.1002/hep4.1234

16. Blachier M, Leleu H, Peck-Radosavljevic M, Valla DC & Roudot-Thoraval F (2013) The burden of liver disease in Europe: A review of available epidemiological data. *J. Hepatol.* 58, 593–608. Available at: http://dx.doi.org/10.116/j.jhep.2012.12.005

17. Boivin G, Bala Y, Doublier A, Farlay D, Ste-Marie LG, Meunier PJ & Delmas PD (2008) The role of mineralization and organic matrix in the microhardness of bone tissue from controls and osteoporotic patients. *Bone* 43, 532–538. Available at: https://doi.org/10.1016/j.bone.2008.05.024

18. Calis HT, Eryavuz M & Calis M (2004) Comparison of femoral geometry among cases with and without hip fractures. *Yonsei Med. J.* 45, 901–907. Available at: https://doi.org/10.3349/ymj.2004.45.5.901

19. Campbell MS, Lichtenstein GR, Rhim AD, Pazianas M & Faust T (2005) Severity of liver disease does not predict osteopenia or low bone mineral density in primary sclerosing cholangitis. *Liver Int.* 25, 311-316.
Available at: https://doi.org/10.1111/j.1478-3231.2005.01075.x

20. Carey EJ, Balan V, Kremers WK & Hay JE (2003) Osteopenia and osteoporosis in patients with end-stage liver disease caused by hepatitis C and alcoholic liver disease: Not just a cholestatic problem. *Liver Transplant.* 9, 1166–1173. Available at: https://doi.org/ 10.1053/jlts.2003.50242

21. Cauley JA, Lui LY, Genant HK, Salamone L, Browner W, Fink HA, Cohen P, Hillier T, Bauer DC & Cummings SR (2009) Risk factors for severity and type of the hip fracture. *J. Bone Miner. Res.* 24, 943–955.
Available at: https://doi.org/10.1359/jbmr.081246

22. Cawthon PM, Harrison SL, Barrett-Connor E, Fink HA, Cauley JA, Lewis CE, Orwoll ES & Cummings SR (2006) Alcohol intake and its relationship with bone mineral density, falls, and fracture risk in older men. *J. Am. Geriatr. Soc.* 54, 1649–1657. Available at: https://doi.org/10.1111/j.1532-5415.2006.00912.x

23. Chakkalakal DA (2005) Alcohol-induced bone loss and deficient bone repair. *Alcohol. Clin. Exp. Res.* 29, 2077–2090.
Available at: https://doi.org/10.1097/01.alc.0000192039.21305.55

24. Chappard D, Plantard B, Petitjean M, Alexandre C & Riffat G (1991) Alcoholic cirrhosis and osteoporosis in men: A light and scanning electron microscopy study. *J. Stud. Alcohol* 52, 269–274.
Available at: https://doi.org/10.15288/jsa.1991.52.269

25. Chen H, Zhou X, Fujita H, Onozuka M & Kubo K-Y (2013) Age-Related Changes in Trabecular and Cortical Bone Microstructure. *Int. J. Endocrinol.* 2013, 213234. Available at: http://www.hindawi.com/journals/ije/2013/213234

26. Chen HJ, Yang HY, Hsueh KC, Shen CC, Chen RY, Yu HC & Wang TL (2018) Increased risk of osteoporosis in patients with nonalcoholic fatty liver disease A population-based retrospective cohort study. *Med. (United States)* 97, 42(e12835) Available at: https://doi.org/10.1097/MD.0000000000012835

27. Chen TL, Lin CS, Shih CC, Huang YF, Yeh CC, Wu CH, Cherng YG & Liao CC (2017) Risk and adverse outcomes of fractures in patients with liver cirrhosis: Two nationwide retrospective cohort studies. *BMJ Open* 7, 1–10. Available at: https://doi.org/10.1136/bmjopen-2017-017342

28. Cohen A, Dempster DW, Müller R, Guo XE, Nickolas TL, Liu XS, Zhang XH, Wirth AJ, Van Lenthe GH, Kohler T, McMahon DJ, Zhou H, Rubin MR, Bilezikian JP, Lappe JM, Recker RR & Shane E (2010) Assessment of trabecular and cortical architecture and mechanical competence of bone by high-resolution peripheral computed tomography: Comparison with transiliac bone biopsy. *Osteoporos. Int.* 21, 263–273. Available at: https://doi.org/10.1007/s00198-009-0945-7

29. Cooreman A, Campenhout R Van, Yanguas SC, Gijbels E, Leroy K, Pieters A, Brantegem P Van & Annaert P (2020) Cholestasis Differentially Affects Liver Connexins. 21, 6534. Available at: https://doi.org/10.3390/ijms21186534

30. Corazza GR, Trevisani F, Di Stefano M, De Notariis S, Veneto G, Cecchetti L, Minguzzi L, Gasbarrini G & Bernardi M (2000) Early increase of bone resorption in patients with liver cirrhosis secondary to viral hepatitis. *Dig. Dis. Sci.* 45, 1392–1399. Available at: https://doi.org/10.1023/A:1005568406664

31. Crawford BAL, Kam C, Donaghy AJ & McCaughan GW (2003) The heterogeneity of bone disease in cirrhosis: A multivariate analysis. *Osteoporos. Int.* 14, 987–994. Available at: https://doi.org/10.1007/s00198-003-1495-z

32. Crilly RG, Anderson C, Hogan D & Delaquerrière-Richardson L (1988) Bone histomorphometry, bone mass, and related parameters in alcoholic males. *Calcif. Tissue Int.* 43, 269–276. Available at: https://doi.org/10.1007/BF02556634

33. Crilly RG, Kloseck M & Mequanint S (2016) Hip fracture types in Canadian men and women change differently with age: A population-level analysis. *Clin. Med. Insights Arthritis Musculoskelet. Disord.* 9, 75–79.
Available at: https://doi.org/10.4137/CMAMD.S38531

34. Culafić D, Djonic D, Culafic-Vojinovic V, Ignjatovic S, Soldatovic I, Vasic J, Beck TJ & Djuric M (2014) Evidence of degraded BMD and geometry at the proximal femora in male patients with alcoholic liver cirrhosis. *Osteoporos. Int.* 26, 253–259. Available at: https://doi.org/10.4137/CMAMD.S38531

35. Cvetković D, Jadžić J, Milovanović P, Djonić D, Djurić M, Bracanović D, Nikolić S & Živković V (2020) Micro-computed Tomography Study of Frontal Bones in Males and Females with Hyperostosis Frontalis Interna. *Calcif. Tissue Int.* 107, 345–352. Available at: https://doi.org/10.1007/s00223-020-00730-2

36. Cvetkovic D, Jadzic J, Milovanovic P, Djonic D, Djuric M & Ivovic M (2020) Comparative Analysis of Femoral Macro - and Micromorphology in Males and Females With and Without Hyperostosis Frontalis Interna : A Cross - Sectional Cadaveric Study. *Calcif. Tissue Int.* 107, 464-473.
Available at: https://doi.org/10.1007/s00223-020-00740-0

37. Dall'Ara E, Öhman C, Baleani M & Viceconti M (2007) The effect of tissue condition and applied load on Vickers hardness of human trabecular bone. *J. Biomech.* 40, 3267–3270. Available at: https://doi.org/10.1016/j.jbiomech.2007.04.007

38. Dall'Ara E, Schmidt R & Zysset P (2012) Microindentation can discriminate between damaged and intact human bone tissue. *Bone* 50, 925–929. Available at: http://dx.doi.org/10.1016/j.bone.2012.01.002

39. Daneault A, Prawitt J, Fabien Soulé V, Coxam V & Wittrant Y (2017) Biological effect of hydrolyzed collagen on bone metabolism. *Crit. Rev. Food Sci. Nutr.* 57, 1922–1937. Available at: https://doi.org/10.1080/10408398.2015.1038377

40. Danford CJ, Trivedi HD & Bonder A (2019) Bone Health in Patients With Liver Diseases. *J. Clin. Densitom.*
Available at: https://doi.org/10.1016/j.jocd.2019.01.004

41. Davis HM, Aref MW, Aguilar-Perez A, Pacheco-Costa R, Allen K, Valdez S, Herrera C, Atkinson EG, Mohammad A, Lopez D, Harris MA, Harris SE, Allen M, Bellido T & Plotkin LI (2018) Cx43 Overexpression in Osteocytes Prevents Osteocyte Apoptosis and Preserves Cortical Bone Quality in Aging Mice. *JBMR Plus* 2, 206–216. Available at: https://doi.org/10.1002/jbm4.10035

42. Van Diepen S, Majumdar SR, Bakal JA, McAlister FA & Ezekowitz JA (2008) Heart failure is a risk factor for orthopedic fracture: A population-based analysis of 16294 patients. *Circulation* 118, 1946–1952.
Available at: https://doi.org/10.1161/CIRCULATIONAHA.108.784009

43. Díez-Ruiz A, García-Saura PL, García-Ruiz P, González-Calvin JL, Gallego-Rojo F & Fuchs D (2010) Bone mineral density, bone turnover markers and cytokines in alcohol-induced cirrhosis. *Alcohol Alcohol.* 45, 427–430.
Available at: https://doi.org/10.1093/alcalc/agq037

44. Djonić D, Milovanović P & Djurić M (2013) Basis of bone Strength vs. Bone fragility: A review of determinants of age-related hip fracture risk. *Srp. Arh. Celok. Lek.* 141, 548–552. Available at: https://doi.org/10.2298/SARH1308548D

45. Djonic D, Milovanovic P, Nikolic S, Ivovic M, Marinkovic J, Beck T & Djuric M (2011) Inter-sex differences in structural properties of aging femora: Implications on differential bone fragility: A cadaver study. *J. Bone Miner. Metab.* 29, 449–457. Available at: https://doi.org/10.1007/s00774-010-0240-x

46. Djukic K, Milovanovic P, Hahn M, Busse B, Amling M & Djuric M (2015) Bone micorarchitecture at muscle attachement sites: The relationship between macroscopic scores of entheses and their cortical and trabecular microstructural design. *Am. J Phys. Anthopol*. 157, 81-93.
Available at:https://doi.org/10.1016/10.1002/ajpa.22691

47. Djuric M, Djonic D, Milovanovic P, Nikolic S, Marshall R, Marinkovic J & Hahn M (2010) Region-specific sex-dependent pattern of age-related changes of proximal femoral cancellous bone and its implications on differential bone fragility. *Calcif. Tissue Int.* 86, 192–201. Available at: https://doi.org/10.1007/s00223-009-9325-8

48. Eckstein F, Matsuura M, Kuhn V, Priemel M, Müller R, Link TM & Lochmüller EM (2007) Sex differences of human trabecular bone microstructure in aging are site-dependent. *J. Bone Miner. Res.* 22, 817–824.
Available at: https://doi.org/10.1359/jbmr.070301

49. Ehnert S, Aspera-Werz RH, Ruoß M, Dooley S, Hengstler JG, Nadalin S, Relja B, Badke A & Nussler AK (2019) Hepatic Osteodystrophy-Molecular Mechanisms Proposed to Favor Its Development. *Int. J. Mol. Sci.* 20.
Available at: https://doi.org/10.1016/j.lfs.2018.09.044

50. Emkey GR (2018) Secondary osteoporosis. *Encycl. Endocr. Dis.* 39, 253–269. Available at: https://doi.org/10.1016/B978-0-12-801238-3.65820-8

51. Eshraghian A (2017) Bone metabolism in non-alcoholic fatty liver disease: Vitamin D status and bone mineral density. *Minerva Endocrinol.* 42, 164–172. Available at: https://doi.org/10.23736/S0391-1977.16.02587-6

52. Fábrega E, Orive A, Garciá-Suarez C, Gaciá-Unzueta M, Amado JA & Pons-Romero F (2005) Osteoprotegerin and RANKL in alcoholic liver cirrhosis. *Liver Int.* 25, 305–310. Available at: https://doi.org/10.1111/j.1478-3231.2005.01073.x

53. Fernandez-Cobo M, Gingalewski C, Drujan D & De Maio A (1999) Downregulation of connexin 43 gene expression in rat heart during inflammation. The role of tumour necrosis factor. *Cytokine* 11, 216–224.
Available at: https://doi.org/10.1006/cyto.1998.0422

54. Frost RJA, Sonne C, Wehr U & Stempfle HU (2007) Effects of calcium supplementation on bone loss and fractures in congestive heart failure. *Eur. J. Endocrinol.* 156, 309–314. Available at: https://doi.org/10.1530/EJE-06-0614

55. Gallego-Rojo FJ, Gonzalez-Calvin JL, Muñoz-Torres M, Mundi JL, Fernandez-Perez R & Rodrigo-Moreno D (1998) Bone mineral density, serum insulin-like growth factor I, and bone turnover markers in viral cirrhosis. *Hepatology* 28, 695–699. Available at: https://doi.org/10.1002/hep.510280315

56. Giallourakis CC, Rosenberg PM & Friedman LS (2002) The liver in heart failure. *Clin. Liver Dis.* 6, 947–967.
Available at: https://doi.org/10.1016/S1089-3261(02)00056-9

57. Gokcan H (2020) Prevalence and characteristics of bone disease in cirrhotic patients. *Hepatol. Forum* 2, 48-52.
Available at: https://doi.org/10.14744/hf.2020.2020.0007

58. González-Calvin JL, Mundi JL, Casado-Caballero FJ, Abadia AC & Martin-Ibañez JJ (2009) Bone mineral density and serum levels of soluble tumor necrosis factors, estradiol, and osteoprotegerin in postmenopausal women with cirrhosis after viral hepatitis. *J. Clin. Endocrinol. Metab.* 94, 4844–4850.
Available at: https://doi.org/10.1210/jc.2009-0835

59. González-Reimers E, Alvisa-Negrín J, Santolaria-Fernández F, Martín-González MC, Hernández-Betancor I, Fernández-Rodríguez CM, Viña-Rodríguez J & González-Díaz A (2011) Vitamin D and nutritional status are related to bone fractures in alcoholics. *Alcohol Alcohol.* 46, 148–155.
Available at: https://doi.org/10.1093/alcalc/agq098

60. González-Reimers E, Martín-González C, De la vega-Prieto MJ, Pelazas-González R, Fernández-Rodríguez C, López-Prieto J, Alvisa-Negrín J & Santolaria-Fernández F (2013) Serum sclerostin in alcoholics: A pilot study. *Alcohol Alcohol.* 48, 278–282.
Available at: https://doi.org/10.1093/alcalc/ags136

61. Goodman ZD (2007) Grading and staging systems for inflammation and fibrosis in chronic liver diseases. *J. Hepatol.* 47, 598–607.
Available at: https://doi.org/10.1016/j.jhep.2007.07.006

62. Guañabens N & Parés A (2011) Management of osteoporosis in liver disease. *Clin. Res. Hepatol. Gastroenterol.* 35, 438–445.
Available at: https://doi.org/10.1016/j.clinre.2011.03.007

63. Guañabens N & Parés A (2018) Osteoporosis in chronic liver disease. *Liver Int.* 38, 776–785. Available at: https://doi.org/10.1111/liv.13730

64. Guañabens N, Ruiz-Gaspà S, Gifre L, Miquel R, Peris P, Monegal A, Dubrueil M, Arias A & Parés A (2016) Sclerostin Expression in Bile Ducts of Patients With Chronic Cholestasis May Influence the Bone Disease in Primary Biliary Cirrhosis. *J. Bone Miner. Res.* 31, 1725–1733. Available at: https://doi.org/10.1002/jbmr.2845

65. Guarino M, Loperto I, Camera S, Cossiga V, Di Somma C, Colao A, Caporaso N & Morisco F (2016) Osteoporosis across chronic liver disease. *Osteoporos. Int.* 27, 1967–1977. Available at: https://doi.org/10.1007/s00198-016-3512-z

66. Guichelaar MMJ, Malinchoc M, Sibonga J, Clarke BL & Hay JE (2002) Bone metabolism in advanced cholestatic liver disease: Analysis by bone histomorphometry. *Hepatology* 36, 895–903.
Available at: https://doi.org/ 10.1053/jhep.2002.36357

67. Hardy E & Fernandez-Patron C (2020) Destroy to Rebuild: The Connection Between Bone Tissue Remodeling and Matrix Metalloproteinases. *Front. Physiol.* 11, 1–24. Available at: https://doi.org/10.3389/fphys.2020.00047

68. Hassler N, Roschger A, Gamsjaeger S, Kramer I, Lueger S, van Lierop A, Roscher P, Klaushofer K, Paschalis E, Kneissel M & Papapoulos S (2014) Sclerostin Deficiency Is Linked to Altered Bone Composition. *J. Bone Miner. Res.* 29, 2144–2151. Available at: https://doi.org/10.1002/jbmr.2259

69. Havaldar R, Pilli SC & Putti BB (2014) Insights into the effects of tensile and compressive loadings on human femur bone. 3:101, 2–7.
Available at: https://doi.org/10.4103/2277-9175.129375

70. Hegedus D, Ferencz V, Lakatos PL, Meszaros S, Lakatos P, Horvath C & Szalay F (2002) Decreased bone density, elevated serum osteoprotegerin, and β-cross-laps in Wilson disease. *J. Bone Miner. Res.* 17, 1961–1967.
Available at: https://doi.org/10.1359/jbmr.2002.17.11.1961

71. Hernández-Guerra M, Hadjihambi A & Jalan R (2019) Gap junctions in liver disease: Implications for pathogenesis and therapy. *J. Hepatol.* 70, 759–772. Available at: https://doi.org/10.1016/j.jhep.2018.12.023

72. Houghton D, Zalewski P, Hallsworth K, Cassidy S, Thoma C, Avery L, Slomko J, Hardy T, Burt AD, Tiniakos D, Hollingsworth KG, Taylor R, Day CP, Masson S, McPherson S, Anstee QM, Newton JL & Trenell MI (2019) The degree of hepatic steatosis associates with impaired cardiac and autonomic function. *J. Hepatol.* 70, 1203–1213. Available at: https://doi.org/10.1016/j.jhep.2019.01.035

73. Huja SS, Beck FM & Thurman DT (2006) Indentation properties of young and old osteons. *Calcif. Tissue Int.* 78, 392–397.
Available at: https://doi.org/10.1007/s00223-006-0025-3

74. Ibrahim A, Magliulo N, Groben J, Padilla A, Akbik F & Abdel Hamid Z (2020) Hardness, an Important Indicator of Bone Quality, and the Role of Collagen in Bone Hardness. *J. Funct. Biomater.* 11, 85.
Available at: https://doi.org/10.3390/jfb11040085

75. Jadzic J, Cvetkovic D, Milovanovic P, Tomanovic N, Zivkovic V, Nikolic S, Djuric M & Djonic D (2020) The micro-structural analysis of lumbar vertebrae in alcoholic liver cirrhosis. *Osteoporos. Int.*, 31, 2209-2217.
Available at: https://doi.org/10.1007/s00198-020-05509-7

76. Jadzic J, Cvetkovic D, Tomanovic N, Zivkovic V, Nikolic S, Milovanovic P, Djuric M & Djonic D (2020) The severity of hepatic disorder is related to vertebral microstructure deterioration in cadaveric donors with liver cirrhosis. *Microsc. Res. Tech.*, 1–10. Available at: https://doi.org/10. 1002/jemt.23642

77. Jadzic J, Mijucic J, Nikolic S, Djuric M & Djonic D (2021) The comparison of age- and sex-specific alteration in pubic bone microstructure: A cross-sectional cadaveric study. *Exp. Gerontol.* 150, 111375.
Available at: https://doi.org/10.1016/j.exger.2021.111375

78. Jadzic J, Milovanovic P, Cvetkovic D, Ivovic M, Tomanovic N, Bracanovic M, Zivkovic V, Nikolic S, Djuric M & Djonic D (2021) Mechano-structural alteration in proximal femora of individuals with alcoholic liver disease: Implications for increased bone fragility. *Bone* 150, 116020.
Available at: https://doi.org/10.1016/j.bone.2021.116020

79. Jandl NM, Rolvien T, Schmidt T, Mussawy H, Nielsen P, Oheim R, Amling M & Barvencik F (2020) Impaired Bone Microarchitecture in Patients with Hereditary Hemochromatosis and Skeletal Complications. *Calcif. Tissue Int.* 106, 465–475. Available at: https://doi.org/10.1007/s00223-020-00658-7.

80. Jeon YK, Kim BH & Kim IJ (2016) The diagnosis of osteoporosis. *J. Korean Med. Assoc.* 59, 842–846. Available at: https://doi.org/10.5124/jkma.2016.59.11.842

81. Jeong HM & Kim DJ (2019) Bone diseases in patients with chronic liver disease. *Int. J. Mol. Sci.* 20, 4270. Available at: https://doi.org/10.3390/ijms20174270

82. Jo S, Lee SH & Lee HJ (2016) The Correlation between the Fracture Types and the Complications after Internal Fixation of the Femoral Neck Fractures. *Hip Pelvis* 28, 35-42. Available at: https://doi.org/10.5371/hp.2016.28.1.35

83. Jorge-Hernandez JA, Gonzalez-Reimers CE, Torres-Ramirez A, Santolaria-Fernandez F, Gonzalez-Garcia C, Batista-Lopez JN, Pestana-Pestana M & Hernandez-Nieto L (1988) Bone changes in alcoholic liver cirrhosis - A histomorphometrical analysis of 52 cases. *Dig. Dis. Sci.* 33, 1089–1095. Available at: https://doi.org/10.1007/BF01535783

84. Kalmey JK & Lovejoy CO (2002) Collagen fiber orientation in the femoral necks of apes and humans: do their histological structures reflect differences in locomotor loading? *Bone* 31, 327–332. Available at: https://doi.org/10.1016/S8756-3282(02)00828-1

85. Kanis JA, Johansson H, Johnell O, Oden A, De Laet C, Eisman JA, Pols H & Tenenhouse A (2005) Alcohol intake as a risk factor for fracture. *Osteoporos. Int.* 16, 737–742. Available at: https://doi.org/10.1007/s00198-004-1734-y

86. Kaukonen JP, Nurmi-Lüthje I, Lüthje P, Naboulsi H, Tanninen S, Kataja M, Kallio ML & Leppilampi M (2006) Acute alcohol use among patients with acute hip fractures: A descriptive incidence study in Southeastern Finland. *Alcohol Alcohol.* 41, 345–348. Available at: https://doi.org/10.1093/alcalc/agh259

87. Kawazoe Y, Miyauchi M, Nagasaki A, Furusho H, Yanagisawa S, Chanbora C, Inubushi T, Hyogo H, Nakamoto T, Suzuki K, Moriwaki S, Tazuma S, Niida S & Takata T (2015) Osteodystrophy in cholestatic liver diseases is attenuated by anti-γ-glutamyl transpeptidase antibody. *PLoS One* 10, 1–16. Available at: https://doi.org/10.1371/journal.pone.0139620

88. Kawelke N, Bentmann A, Hackl N, Hager HD, Feick P, Geursen A, Singer M V. & Nakchbandi IA (2008) Isoform of fibronectin mediates bone loss in patients with primary biliary cirrhosis by suppressing bone formation. *J. Bone Miner. Res.* 23, 1278–1286. Available at: https://doi.org/10.1359/jbmr.080313

89. Khalifa YH, Mourad GM, Stephanos WM, Omar SA & Mehanna RA (2019) Bone Marrow-Derived Mesenchymal Stem Cell Potential Regression of Dysplasia Associating Experimental Liver Fibrosis in Albino Rats. *Biomed Res. Int.* 2019. Available at: https://doi.org/10.1155/2019/5376165

90. Knodell RG, Ishak KG, Black WC, Chen TS, Craig R, Kaplowitz N, Kiernan TW & Wollman J (1981) Formulation and application of a numerical scoring system for assessing histological activity in asymptomatic chronic active hepatitis. *Hepatology* 1, 431–435. Available at: https://doi.org/10.1002/hep.1840010511

91. Koehne de Gonzalez AK & Lefkowitch JH (2017) Heart Disease and the Liver: Pathologic Evaluation. *Gastroenterol. Clin. North Am.* 46, 421–435. Available at: https://doi.org/10.1016/j.gtc.2017.01.012

92. Kostin S, Dammer S, Hein S, Klovekorn WP, Bauer EP & Schaper J (2004) Connexin 43 expression and distribution in compensated and decompensated cardiac hypertrophy in patients with aortic stenosis. *Cardiovasc. Res.* 62, 426–436. Available at: https://doi.org/10.1016/j.cardiores.2003.12.010

93. LaCroix AZ, Beck TJ, Cauley JA, Lewis CE, Bassford T, Jackson R, Wu G & Chen Z (2010) Hip structural geometry and incidence of hip fracture in postmenopausal women: What does it add to conventional bone mineral density? *Osteoporos. Int.* 21, 919–929. Available at: https://doi.org/10.1007/s00198-009-1056-1

94. Laitinen K, Lamberg-Allardt C, Tunninen R, Harkönen M & Valimaki M (1992) Bone mineral density and abstention-induced changes in bone and mineral metabolism in noncirrhotic male alcoholics. *Am. J. Med.* 93, 642–650. Available at: https://doi.org/10.1016/0002-9343(92)90197-J

95. Liang HPH, Xu J, Xue M & Jackson C (2016) Matrix metalloproteinases in bone development and pathology: current knowledge and potential clinical utility. *Met. Med.* Volume 3, 93–102. Available at: https://doi.org/10.2147/mnm.s92187

96. Liang J, Meng WD, Yang JM, Li SL, Zhong MN, Hou XX, Wang R, Long YY, Bao LX & Bao M (2018) The association between liver cirrhosis and fracture risk: A systematic review and meta-analysis. *Clin. Endocrinol. (Oxf).* 89, 408–413. Available at: https://doi.org/10.1111/cen.13762

97. Lin X, Patil S, Gao YG & Qian A (2020) The Bone Extracellular Matrix in Bone Formation and Regeneration. *Front. Pharmacol.* 11, 1–15. Available at: https://doi.org/10.3389/fphar.2020.00757

98. López-Larramona G, Lucendo AJ, González-Castillo S & Tenias JM (2011) Hepatic osteodystrophy: An important matter for consideration in chronic liver disease. *World J. Hepatol.* 3, 300–307. Available at: https://doi.org/10.4254/wjh.v3.i12.300

99. López-Larramona G, Lucendo AJ & González-Delgado L (2013) Alcoholic liver disease and changes in bone mineral density. *Rev. Española Enfermedades Dig.* 105, 609–621. Available at: https://doi.org/10.4321/s1130-01082013001000006

100. Loveridge N, Power J, Reeve J & Boyde A (2004) Bone mineralization density and femoral neck fragility. *Bone* 35, 929–941. Available at: https://doi.org/10.1016/j.bone.2004.05.025

101. Lundeen GA, Vajda EG & Bloebaum RD (2000) Age-related cancellous bone loss in the proximal femur of Caucasian females. *Osteoporos. Int.* 11, 505–511. Available at: https://doi.org/10.1007/s001980070093

102. Luo Z, Liu Y, Liu Y, Chen H, Shi S & Liu Y (2017) Cellular and molecular mechanisms of alcohol-induced osteopenia. *Cell. Mol. Life Sci.* 74, 4443–4453. Available at: https://doi.org/10.1007/s00018-017-2585-y

103. Lyons KJ, Majumdar SR & Ezekowitz JA (2011) The unrecognized burden of osteoporosis-related vertebral fractures in patients with heart failure. *Circ. Hear. Fail.* 4, 419–424. Available at: https://doi.org/10.1007/s00018-017-2585-y

104. Mahmoudi A, Sellier N, Reboul-Marty J, Chalès G, Lalatonne Y, Bourcier V, Grando V, Barget N, Beaugrand M, Trinchet JC & Ganne-Carrié N (2011) Bone mineral density assessed by dual-energy X-ray absorptiometry in patients with viral or alcoholic compensated cirrhosis. A prospective study. *Clin. Res. Hepatol. Gastroenterol.* 35, 731–737. Available at: https://doi.org/10.1016/j.clinre.2011.07.009

105. Malik P, Gasser RW, Kemmler G, Moncayo R, Finkenstedt G, Kurz M & Fleischhacker WW (2009) Low bone mineral density and impaired bone metabolism in young alcoholic patients without liver cirrhosis: A cross-sectional study. *Alcohol. Clin. Exp. Res.* 33, 375–381. Available at: https://doi.org/10.1111/j.1530-0277.2008.00847.x

106. Michaëlsson K, Weiderpass E, Farahmand BY, Baron JA, Persson PG, Zidén L, Zetterberg C & Ljunghall S (1999) Differences in risk factor patterns between cervical and trochanteric hip fractures. *Osteoporos. Int.* 10, 487–494. Available at: https://doi.org/10.1007/s001980050259

107. Michela P, Velia V, Aldo P & Ada P (2015) Role of connexin 43 in cardiovascular diseases. *Eur. J. Pharmacol.* 768, 71–76. Available at: http://dx.doi.org/10.1016/j.ejphar.2015.10.030.

108. Milovanovic P, Adamu U, Simon MJK, Rolvien T, Djuric M, Amling M & Busse B (2014) Age- and Sex-Specific Bone Structure Patterns Portend Bone Fragility in Radii and Tibiae in Relation to Osteodensitometry: A High-Resolution Peripheral Quantitative Computed Tomography Study in 385 Individuals. *Journals Gerontol. - Ser. A Biol. Sci. Med. Sci.* 70, 1269–1275. Available at: https://doi.org/10.1093/gerona/glv052

109. Milovanovic P & Busse B (2019) Inter-site Variability of the Human Osteocyte Lacunar Network: Implications for Bone Quality. *Curr. Osteoporos. Rep.* 17, 105–115. Available at: https://doi.org/10.1007/s11914-019-00508-y

110. Milovanovic P, Djuric M, Neskovic O, Djonic D, Potocnik J, Nikolic S, Stoiljkovic M, Zivkovic V & Rakocevic Z (2013) Atomic force microscopy characterization of the external cortical bone surface in young and elderly women: Potential nanostructural traces of periosteal bone apposition during aging. *Microsc. Microanal.* 19, 1341–1349.
Available at: https://doi.org/ 10.1017/S1431927613001761

111. Milovanovic P, Potocnik J, Stoiljkovic M, Djonic D, Nikolic S, Neskovic O, Djuric M & Rakocevic Z (2011) Nanostructure and mineral composition of trabecular bone in the lateral femoral neck: Implications for bone fragility in elderly women. *Acta Biomater.* 7, 3446–3451.
Available at: http://dx.doi.org/10.1016/j.actbio.2011.05.028.

112. Milovanovic P, Vukovic Z, Antonijevic D, Djonic D, Zivkovic V, Nikolic S & Djuric M (2017) Porotic paradox: distribution of cortical bone pore sizes at nano- and micro-levels in healthy vs. fragile human bone. *J. Mater. Sci. Mater. Med.* 28, 1–7. Available at: http://dx.doi.org/10.1007/s10856-017-5878-7.

113. Milovanovic P, Zimmermann EA, Riedel C, Scheidt A vom, Herzog L, Krause M, Djonic D, Djuric M, Püschel K, Amling M, Ritchie RO & Busse B (2015) Multi-level characterization of human femoral cortices and their underlying osteocyte network reveal trends in quality of young, aged, osteoporotic and antiresorptive-treated bone. *Biomaterials* 45, 46–55. Available at: https://doi.org/10.1016/j.biomaterials.2014.12.024

114. Mitchell R, McDermid J, Ma MM & Chik CL (2011) MELD score, insulin-like growth factor 1 and cytokines on bone density in end-stage liver disease. *World J. Hepatol.* 3, 157–163. Available at: https://doi.org/10.4254/wjh.v3.i6.157

115. Montomoli J, Erichsen R, Gammelager H & Pedersen AB (2018) Liver disease and mortality among patients with hip fracture: A population-based cohort study. *Clin. Epidemiol.* 10, 991–1000. Available at: https://doi.org/10.2147/CLEP.S168237

116. Moschen AR, Kaser A, Stadlmann S, Millonig G, Kaser S, Mühllechner P, Habior A, Graziadei I, Vogel W & Tilg H (2005) The RANKL/OPG system and bone mineral density in patients with chronic liver disease. *J. Hepatol.* 43, 973–983. Available at: https://doi.org/10.1016/j.jhep.2005.05.034

117. Mounach A, Ouzzif Z, Wariaghli G, Achemlal L, Benbaghdadi I, Aouragh A, Bezza A & El Maghraoui A (2008) Primary biliary cirrhosis and osteoporosis: A case-control study. *J. Bone Miner. Metab.* 26, 379–384. Available at: https://doi.org/10.1007/s00296-009-1071-8

118. Myers RP, Cerini R, Sayegh R, Moreau R, Degott C, Lebrec D & Lee SS (2003) Cardiac hepatopathy: Clinical, hemodynamic, and histologic characteristics and correlations. *Hepatology* 37, 393–400. Available at: https://doi.org/ 10.1053/jhep.2003.50062

119. Nakchbandi I (2014) Osteoporosis and fractures in liver disease: Relevance, pathogenesis and therapeutic implications. *World J. Gastroenterol.* 20, 9427–9438. Available at: https://doi.org/10.3748/wjg.v20.i28.9427

120. Nakchbandi IA & van der Merwe SW (2009) Current understanding of osteoporosis associated with liver disease. *Nat. Rev. Gastroenterol. Hepatol.* 6, 660–670. Available at: http://dx.doi.org/10.1038/nrgastro.2009.166.

121. Ninkovic M, Love SA, Tom B, Alexander GJM & Compston JE (2001) High prevalence of osteoporosis in patients with chronic liver disease prior to liver transplantation. *Calcif. Tissue Int.* 69, 321–326. Available at: https://doi.org/ 10.1007/s00223-001-2028-4

122. O'Shea RS, Dasarathy S, McCullough AJ, Shuhart MC, Davis GL, Franco J, Harrison SA, Howell CD, Ling SC, Liu LU, Martin P, Reau N, Runyon BA, Talwalkar JA, Wong JB, Yim C, Inadomi J, Baroni D, Bernstein D, Brugge W, Chang L, Cunningham J, Dendrinos KG, Edmundowicz S, Ginsburg PM, Hornbuckle K, Kefalas C, Koch T, Lehrer J, Lembo A, Mullick T, O'Brien J, Papp J, Parkman H, Perumalsamy KS, Prasad GA, Qureshi WA, Roach A, Sampliner R, Sonnenberg A, Vargo J, Vege SS, Vela M, Zein N & Zuckerman MJ (2010) Alcoholic liver disease. *Hepatology* 51, 307–328. Available at: https://doi.org/10.1002/hep.23258

123. Ormarsdóttir S, Ljunggren Ö, Mallmin H, Michaëlsson K & Lööf L (2002) Increased rate of bone loss at the femoral neck in patients with chronic liver disease. *Eur. J. Gastroenterol. Hepatol.* 14, 43–48.
Available at: https://doi.org/10.1097/00042737-200201000-00008

124. Osterhoff G, Morgan EF, Shefelbine SJ, Karim L, McNamara LM & Augat P (2016) Bone mechanical properties and changes with osteoporosis. *Injury* 47, S11–S20. Available at: http://dx.doi.org/10.1016/S0020-1383(16)47003-8.

125. Otete H, Deleuran T, Fleming KM, Card T, Aithal GP, Jepsen P & West J (2018) Hip fracture risk in patients with alcoholic cirrhosis: A population-based study using English and Danish data. *J. Hepatol.* 69, 697–704. Available at: https://doi.org/10.1016/j.jhep.2018.04.002

126. Ott SM (2016) Bone strength: More than just bone density. *Kidney Int.* 89, 16–19. Available at: http://dx.doi.org/10.1016/j.kint.2015.11.004.

127. Parés A & Guañabens N (2018) Primary biliary cholangitis and bone disease. *Best Pract. Res. Clin. Gastroenterol.* 34–35, 63–70. Available at: https://doi.org/ 10.1016/j.bpg.2018.06.005

128. Peris P, Guañabens N, Parés A, Pons F, del Rio L, Monegal A, Surís X, Caballería J, Rodés J & Muñoz-Gómez J (1995) Vertebral fractures and osteopenia in chronic alcoholic patients. *Calcif. Tissue Int.* 57, 111–114. Available at: https://doi.org/ 10.1007/BF00298430

129. Pimpin L, Cortez-Pinto H, Negro F, Corbould E, Lazarus J V., Webber L & Sheron N (2018) Burden of liver disease in Europe: Epidemiology and analysis of risk factors to identify prevention policies. *J. Hepatol.* 69, 718–735. Available at: https://doi.org/10.1016/j.jhep.2018.05.011

130. Plotkin LI (2011) Connexin 43 and Bone: Not Just a Gap Junction Protein. *Actual. osteol.* 7, 79–90.
Available at: http://www.ncbi.nlm.nih.gov/pubmed/22679450%0A

131. Popovic DD, Kovacevic N V., Tepavcevic DBK, Trajkovic GZ, Alempijevic TM, Spuran MM, Krstic MN, Jesic RS, Younossi ZM & Pekmezovic TD (2013) Validation of the chronic liver disease questionnaire in Serbian patients. *World J. Gastroenterol.* 19, 4950–4957. Available at: https://doi.org/10.3748/wjg.v19.i30.4950

132. Ranjan R, Rampal S, Jaiman A, Ali Tokgöz M, Kit Koong J, Ramayah K & Rajaram R (2021) Common musculoskeletal disorders in chronic liver disease patients. *Jt. Dis. Relat. Surg.* 32, 1-6. Available at: https://doi.org/10.52312/jdrs.2021.25

133. Rhee Y, Kim WJ, Han KJ, Lim SK & Kim SH (2014) Effect of liver dysfunction on circulating sclerostin. *J. Bone Miner. Metab.* 32, 545–549. Available at: https://doi.org/10.1007/s00774-013-0524-z

134. Richardson CT & Singal AK (2018) Epidemiology of alcoholic liver disease. *Clin. Epidemiol. Chronic Liver Dis.*, 75–98. Available at: https://doi.org/10.1007/978-3-319-94355-8_7

135. Rolvien T, vom Scheidt A, Stockhausen KE, Milovanovic P, Djonic D, Hubert J, Hawellek T, Wacker A, Jebens V, Püschel K, Zimmermann EA, Djuric M, Amling M & Busse B (2018) Inter-site variability of the osteocyte lacunar network in the cortical bone underpins fracture susceptibility of the superolateral femoral neck. *Bone* 112, 187–193. Available at: https://doi.org/10.1016/j.bone.2018.04.018.

136. Santori C, Ceccanti M, Diacinti D, Attilia ML, Toppo L, D'Erasmo E, Romagnoli E, Mascia ML, Cipriani C, Prastaro A, Carnevale V & Minisola S (2008) Skeletal turnover, bone mineral density, and fractures in male chronic abusers of alcohol. *J. Endocrinol. Invest.* 31, 321–326.
Available at: https://doi.org/10.1007/BF03346365

137. Schmidt C, Stürznickel J, Strahl A, Oheim R, Weiler-Normann C, Sebode M, Barvencik F, Lohse AW, Schinke T, Amling M, Schramm C & Rolvien T (2021) Bone microarchitecture in patients with autoimmune hepatitis. *J. Bone Miner. Res.* 36, 1316–1325. Available at: : https://doi.org/10.1002/jbmr.4289

138. Schmidt T, Schmidt C, Schmidt FN, Butscheidt S, Mussawy H, Hubert J, Hawellek T, Oehler N, Barvencik F, Lohse AW, Schinke T, Schramm C, Amling M & Rolvien T (2018) Disease Duration and Stage Influence Bone Microstructure in Patients With Primary Biliary Cholangitis. *J. Bone Miner. Res.* 33, 1011–1019. Available at: https://doi.org/10.1002/jbmr.3410

139. Schnitzler CM, Mesquita JM & Shires R (2010) Cortical and trabecular bone microarchitecture and turnover in alcohol-induced chronic pancreatitis: A histomorphometric study. *J. Bone Miner. Metab.* 28, 456–467. Available at: https://doi.org/10.1007/s00774-009-0151-x

140. Seeman E (2003) The structural and biomechanical basis of the gain and loss of bone strength in women and men. *Endocrinol. Metab. Clin. North Am.* 32, 25–38. Available at: https://doi.org/10.1016/S0889-8529(02)00078-6

141. Seitz HK, Bataller R, Cortez-Pinto H, Gao B, Gual A, Lackner C, Mathurin P, Mueller S, Szabo G & Tsukamoto H (2018) Alcoholic liver disease. *Nat. Rev. Dis. Prim.* 4. Available at: http://dx.doi.org/10.1038/s41572-018-0014-7

142. Sens C, Altrock E, Rau K, Klemis V, von Au A, Pettera S, Uebel S, Damm T, Tiwari S, Moser M & Nakchbandi IA (2017) An O-Glycosylation of Fibronectin Mediates Hepatic Osteodystrophy Through α4β1 Integrin. *J. Bone Miner. Res.* 32, 70–81. Available at: https://doi.org/10.1002/jbmr.2916

143. Silva MJ (2007) Biomechanics of osteoporotic fractures. *Injury* 38, 69–76. Available at: https://doi.org/10.1016/j.injury.2007.08.014

144. Spiesz EM, Reisinger AG, Kaminsky W, Roschger P, Pahr DH & Zysset PK (2013) Computational and experimental methodology for site-matched investigations of the influence of mineral mass fraction and collagen orientation on the axial indentation modulus of lamellar bone. *J. Mech. Behav. Biomed. Mater.* 28, 195–205. Available at: http://dx.doi.org/10.1016/j.jmbbm.2013.07.004.

145. Stains JP, Fontana F & Civitelli R (2019) Intercellular junctions and cell-cell communication in the skeletal system, *Elsevier Inc.* Chapter 18 in the: Cell-cell interaction in the skeleton
Available at: http://dx.doi.org/10.1016/B978-0-12-814841-9.00018-X

146. Stains JP, Watkins MP, Grimston SK, Hebert C & Civitelli R (2014) Molecular mechanisms of osteoblast/osteocyte regulation by connexin43. *Calcif. Tissue Int.* 94, 55–67. Available at: https://doi.org/10.1007/s00223-013-9742-6

147. Stone KL, Seeley DG, Lui LY, Cauley JA, Ensrud K, Browner WS, Nevitt MC & Cummings SR (2003) BMD at Multiple Sites and Risk of Fracture of Multiple Types: Long-Term Results From the Study of Osteoporotic Fractures. *J. Bone Miner. Res.* 18, 1947–1954. Available at: https://doi.org/10.1359/jbmr.2003.18.11.1947

148. Streba LAM, Vere CC, Streba CT & Ciurea ME (2014) Focus on alcoholic liver disease: From nosography to treatment. *World J. Gastroenterol.* 20, 8040–8047. Available at: https://doi.org/10.3748/wjg.v20.i25.8040

149. Sundh D, Mellström D, Nilsson M, Karlsson M, Ohlsson C & Lorentzon M (2015) Increased cortical porosity in older men with fracture. *J. Bone Miner. Res.* 30, 1692–1700. Available at: https://doi.org/10.1002/jbmr.2509

150. Tanner DA, Kloseck M, Crilly RG, Chesworth B & Gilliland J (2010) Hip fracture types in men and women change differently with age. *BMC Geriatr.* 10, 2007–2010. Available at: https://doi.org/10.1186/1471-2318-10-12

151. Ulhøi MP, Meldgaard K, Steiniche T, Odgaard A & Vesterby A (2017) Chronic Alcohol Abuse Leads to Low Bone Mass with No General Loss of Bone Structure or Bone Mechanical Strength. *J. Forensic Sci.* 62, 131–136. Available at: https://doi.org/10.1111/1556-4029.13256

152. Valenti L, Varenna M, Fracanzani AL, Rossi V, Fargion S & Sinigaglia L (2009) Association between iron overload and osteoporosis in patients with hereditary hemochromatosis. *Osteoporos. Int.* 20, 549–555. Available at: https://doi.org/10.1007/s00198-008-0701-4

153. van Veen TAB, van Rijen HVM, Wiegerinck RF, Opthof T, Colbert MC, Clement S, de Bakker JMT & Jongsma HJ (2002) Remodeling of Gap Junctions in Mouse Hearts Hypertrophied by Forced Retinoic Acid Signaling. *J. Mol. Cell. Cardiol.* 34, 1411–1423. Available at: https://doi.org/10.1006/jmcc.2002.2102

154. Viguet-Carrin S, Garnero P & Delmas PD (2006) The role of collagen in bone strength. *Osteoporos. Int.* 17, 319–336.
Available at: https://doi.org/10.1007/s00198-005-2035-9

155. Wakolbinger R, Muschitz C, Scheriau G, Bodlaj G, Kocijan R, Feichtinger X, Schanda JE, Haschka J, Resch H & Pietschmann P (2019) Bone microarchitecture and bone turnover in hepatic cirrhosis. *Osteoporos. Int.* 30, 1195–1204. Available at: https://doi.org/10.1007/s00198-019-04870-6

156. Wakolbinger R, Muschitz C, Wallwitz J, Bodlaj G, Feichtinger X, Schanda JE, Resch H, Baierl A & Pietschmann P (2020) Serum levels of sclerostin reflect altered bone microarchitecture in patients with hepatic cirrhosis. *Wien. Klin. Wochenschr.* 132, 19–26. Available at: https://dx.doi.org/10.1007%2Fs00508-019-01595-8

157. Wang J, Yin B, Liu G, Li S, Zhang X, Hu Z, Wu W & Zhang Y (2019) Microhardness distribution of the tibial diaphysis and test site selection for reference point indentation technique. *Medicine (Baltimore).* 98, e16523. Available at: https://doi.org/10.1097/MD.0000000000016523

158. Wang Y, Wen G, Zhou R, Zhong W, Lu S, Hu C & Chai Y (2018) Association of nonalcoholic fatty liver disease with osteoporotic fractures: A cross-sectional retrospective study of Chinese individuals. *Front. Endocrinol. (Lausanne).* 9, 1–9. Available at: https://doi.org/10.3389/fendo.2018.00408

159. Weiner S & Wagner HD (1998) The material bone: Structure-mechanical function relations. *Annu. Rev. Mater. Sci.* 28, 271–298. Available at: https://doi.org/10.1146/annurev.matsci.28.1.271

160. Wells ML & Venkatesh SK (2018) Congestive hepatopathy. *Abdom. Radiol.* 43, 2037–2051. Available at: https://doi.org/ 10.1007/s00261-017-1387-x

161. Wibaux C, Legroux-Gerot I, Dharancy S, Boleslawski E, Declerck N, Canva V, Mathurin P, Pruvot FR & Cortet B (2011) Assessing bone status in patients awaiting liver transplantation. *Jt. Bone Spine* 78, 387–391. Available at: https://doi.org/10.1016/j.jbspin.2011.03.001

162. Wölfel EM, Jähn-rickert K, Schmidt FN, Wulff B, Mushumba H, Sroga GE, Püschel K, Milovanovic P, Amling M & Campbell GM (2020) Individuals with type 2 diabetes mellitus show dimorphic and heterogeneous patterns of loss in femoral bone quality. *Bone* 140, 115556. Availble at: https://doi.org/10.1016/j.bone.2020.115556.

163. Wu W wei, Zhu Y bin, Chen W, Li S, Yin B, Wang J zhao, Zhang X juan, Liu G bin, Hu Z sheng & Zhang Y ze (2019) Bone Hardness of Different Anatomical Regions of Human Radius and its Impact on the Pullout Strength of Screws. *Orthop. Surg.* 11, 270–276. Available at: https://doi.org/10.1111/os.12436

164. Xanthopoulos A, Starling RC, Kitai T & Triposkiadis F (2019) Heart Failure and Liver Disease: Cardiohepatic Interactions. *JACC Hear. Fail.* 7, 87–97. Available at: https://doi.org/10.1016/j.jchf.2018.10.007

165. Yadav A & Carey EJ (2013) Osteoporosis in chronic liver disease. *Nutr. Clin. Pract.* 28, 52–64. Available at: https://doi.org/10.1177/0884533612470145

166. Yanguas SC, Willebrords J, Maes M, da Silva TC, Pereira IVA, Cogliati B, Dagli MLZ & Vinken M (2016) Connexins and Pannexins in liver damage. *EXCLI J.* 15, 177–186. Available at: https://doi.org/10.17179/excli2016-119

167. Yin B, Guo J liang, Wang J zhao, Li S, Liu Y ke & Zhang Y ze (2019) Bone Material Properties of Human Phalanges Using Vickers Indentation. *Orthop. Surg.* 11, 487–492. Available at: https://doi.org/10.1111/os.12455

168. Yousry WA, Hussein MM, Mohse MM, W S & El-EZZ MA (2016) Value of Serum Sclerostin in Osteopenia and Osteoporosis Associated with Liver Cirrhosis and Post Liver Transplantation. *IOSR J. Dent. Med. Sci.* 15, 59–64. Available at: https://doi.org/10.9790/0853-1508065964

169. Zimmermann EA, Fiedler IAK & Busse B (2021) Breaking new ground in mineralized tissue: Assessing tissue quality in clinical and laboratory studies. *J. Mech. Behav. Biomed. Mater.* 113. Available at: https://doi.org/10.1016/j.jmbbm.2020.104138

170. Zwierzak I, Baleani M & Viceconti M (2009) Microindentation on cortical human bone: Effects of tissue condition and indentation location on hardness values. *Proc. Inst. Mech. Eng. Part H J. Eng. Med.* 223, 913–918. Available at: https://doi.org/10.1243/09544119JEIM634

**Author's short biography**

Dr. Jelena Jadžić was born on 25th of December 1992, in Čačak, where she finished elementary school and Gymnasium. In 2017, she graduated from the Faculty of Medicine, University of Belgrade, with an average grade of 9.79 (out of 10.00). Dr. Jadžić was chosen as the winner of several student awards and scholarships during the integrated academic studies of medicine. Also, Dr. Jadžić was the winner of the European Union ERAWEB scholarship for student mobility, so during the 2016/2017 school year, she attended postgraduate training in public health and clinical epidemiology at the Netherlands Institute for Health Sciences (NIHES) and the Erasmus Medical Center (Erasmus MC) in Rotterdam, the Netherlands.

Dr. Jadžić was enrolled in doctoral studies (course: Skeletal Biology) at the Faculty of Medicine, University of Belgrade, in the 2018/2019 academic year. Dr. Jadžić was appointed to the teaching associate position in 2018, while in 2020, she was appointed to the position of teaching assistant at the Institute of Anatomy, Faculty of Medicine, University of Belgrade. Since 2018, Jelena Jadžić has actively participated in the multidisciplinary scientific research project at the Laboratory of Bone biology and Bioanthropology in Belgrade, Serbia. Since year of 2019, she has been a participant in the international project *"Osteocyte's viability as a marker of bone health in human bone"* in collaboration with University Medical Center Hamburg-Eppendorf, while since year of 2020 she has been actively participating in the PROMIS project funded by the Science Fund of the Republic of Serbia, entitled *"Effects of diabetes mellitus on osteocytic, neural and vascular networks in bone: implications for increased fracture susceptibility at the proximal femur" DiaBoNet"*. So far, Dr. Jadzic has been the author or co-author of a total of 33 scientific publications, seven of which have been published *in extenso* in journals indexed in the Journal Citation Reports list, and two papers have been published *in extenso* in journals not referenced in the said list.

**Кратка биографија аутора**

Др Јелена Јаџић је рођена 25. децембра 1992. године у Чачку, где је завршила основну школу и природно-математички смер Гимназије у Чачку. На Медицинском факултету Универзитета у Београду је дипломирала 2017. године са просечном оценом 9,79. Током интегрисаних академских студија медицине, др Јаџић је за постигнут успех и просечну оцену током студија изабрана као добитница награде и стипендије Задужбине др Милош Смиљковић, Задужбине Раде и Милана Вукићевића и Фонда за младе таленте Републике Србије. Такође, др Јаџић је била добитница *ERAWEB* стипендије Европске Уније за мобилност студената, па је током школске 2016/2017. године боравила на постдипломском усавршавању из области јавног здравља и клиничке епидемиологије на Холандском институту за јавно здравље (енгл. *Netherlands Institute for Health Sciences - NIHES*) и Медицинском центру *Erasmus* (енгл. *Erasmus MC*) у Ротердаму, Холандија.

Докторске студије на енглеском језику, на модулу Биологија скелета, уписала је на Медицинском факултету у Београду школске 2018/2019 године. У звање сарадника у настави, др Јаџић је изабрана 2018. године, док је 2020. изабрана у звање асистента на катедри за анатомију Медицинског факултета у Београду. Од 2018. године, др Јелена Јаџић активно учествује на мултидисциплинарном научно-истраживачком пројекту Лабораторије за коштану биологију и биоантропологију у Београду, од 2019. године је и истраживач на интернационалном пројекту „*Osteocyte's viability as a marker of bone health in human bone*“, док од 2020. године активно учествује на пројекту Фонда за науку Републике Србије, под називом „*Effects of diabetes mellitus on osteocytic, neural and vascular networks in bone: implications for increased fracture susceptibility at the proximal femur - DiaBoNet*”. До сада, др Јаџић је била аутор или коаутор укупно 33 научне публикације, међу којима је седам штампано у целини у часописима индексираним у *Journal Citation Reports* листи, а два рада су објављена у целини у часописима који нису реферисани у наведеној листи.

**Prilog 1**

*образац изјаве о ауторству*

# Изјава о ауторству

Име и презиме аутора **Јелена Јацић**
Број индекса **5012/2017**

**Изјављујем**

да је докторска дисертација под насловом

**Промене у коштаном ткиву код особа са хроничним обољењима јетре алкохолне и неалкохолне етиологије (енгл. *The bone tissue changes in individuals with alcoholic and non-alcoholic chronic liver disease)***

- резултат сопственог истраживачког рада;
- да дисертација у целини ни у деловима није била предложена за стицање друге дипломе према студијским програмима других високошколских установа;
- да су резултати коректно наведени и
- да нисам кршио/ла ауторска права и користио/ла интелектуалну својину других лица.

У Београду, 05.10.2021. године

**Потпис аутора**

Јелена Јацић

**Prilog 2**

*образац изјаве о истоветности штампане и електронске верзије докторског рада*

# Изјава о истоветности штампане и електронске верзије докторског рада

Име и презиме аутора Јелена Јаџић
Број индекса 5012/2017
Студијски програм Биологија скелета
Наслов рада Промене у коштаном ткиву код особа са хроничним обољењима јетре алкохолне и неалкохолне етиологије
(енгл. *The bone tissue changes in individuals with alcoholic and non-alcoholic chronic liver disease)*

Ментор проф. др Данијела Ђонић

Изјављујем да је штампана верзија мог докторског рада истоветна електронској верзији коју сам предао/ла ради похрањивања у **Дигиталном репозиторијуму Универзитета у Београду.**

Дозвољавам да се објаве моји лични подаци везани за добијање академског назива доктора наука, као што су име и презиме, година и место рођења и датум одбране рада.

Ови лични подаци могу се објавити на мрежним страницама дигиталне библиотеке, у електронском каталогу и у публикацијама Универзитета у Београду.

**Потпис аутора**

У Београду, 05.10.2021. године

Јелена Јаџић

**Prilog 3**

*образац изјаве о коришћењу*

# Изјава о коришћењу

Овлашћујем Универзитетску библиотеку „Светозар Марковић“ да у Дигитални репозиторијум Универзитета у Београду унесе моју докторску дисертацију под насловом:

Промене у коштаном ткиву код особа са хроничним обољењима јетре алкохолне и неалкохолне етиологије (енгл. *The bone tissue changes in individuals with alcoholic and non-alcoholic chronic liver disease)*

која је моје ауторско дело.

Дисертацију са свим прилозима предао/ла сам у електронском формату погодном за трајно архивирање.

Моју докторску дисертацију похрањену у Дигиталном репозиторијуму Универзитета у Београду и доступну у отвореном приступу могу да користе сви који поштују одредбе садржане у одабраном типу лиценце Креативне заједнице (Creative Commons) за коју сам се одлучио/ла.

1. Ауторство (CC BY)
2. Ауторство – некомерцијално (CC BY-NC)
3. Ауторство – некомерцијално – без прерада (CC BY-NC-ND)
4. Ауторство – некомерцијално – делити под истим условима (CC BY-NC-SA)
5. Ауторство – без прерада (CC BY-ND)
6. Ауторство – делити под истим условима (CC BY-SA)

(Молимо да заокружите само једну од шест понуђених лиценци. Кратак опис лиценци је саставни део ове изјаве).

**Потпис аутора**

У Београду, 05.10.2021. године

Јелена Јакшић